

TOWARDS THE SYNTHESIS OF PHOTOBACTIN: METHODOLOGY AND METAL BINDING ASPECTS

by

Michelle Shuoprasad

Bachelor of Science, Chemistry

Ryerson University, Toronto, Ontario, Canada, 2011

A thesis presented to Ryerson University

In partial fulfillment of the requirements for the degree of

Master of Science in the Program of Molecular Science

Toronto, Ontario, Canada, 2014

© Michelle Shuoprasad 2014

Author's Declaration

I hereby declare that I am the sole author of this thesis. This is a true copy of the thesis, including any required final revisions, as accepted by my examiners.

I authorize Ryerson University to lend this thesis to other institutions or individuals for the purpose of scholarly research.

I further authorize Ryerson University to reproduce this thesis by photocopying or by other means, in total or in part, at the request of other institutions or individuals for the purpose of scholarly research.

I understand that my thesis may be made electronically available to the public.

X *M. Shuoprasad*

Michelle Shuoprasad

Abstract

TOWARDS THE SYNTHESIS OF PHOTOBACTIN: METHODOLOGY AND METAL BINDING ASPECTS

by Michelle Shuoprasad

Molecular Science

Master of Science, Ryerson University, 2014

Siderophores are metal-typically iron-chelating compounds that have received countless attention in research, as they can play a role in medicine intended for drug delivery and iron overload treatment. The synthesis of Photobactin has been of interest as it has been previously isolated (<10 mg) from *Photorhabdus luminescence* and has not once been synthesized. This thesis examined the preparation of Photobactin using a multi-step approach: synthesizing two building blocks individually and coupling them together with an amide coupling reagent. Both building blocks were synthesized successfully. However, the deprotection of the ester group on one of the building blocks has been uncooperative, and therefore the total synthesis of Photobactin was not achieved. Moreover, DFT computation calculations were performed to study Photobactin binding properties with Fe^{3+} . According to the results, iron (Fe^{3+}) is likely to form a hexadentate (6-coordinate ligand) or a tetradentate (4-coordinate ligand) complex with Photobactin.

Each of the compounds leading to Photobactin was characterized using ^1H and ^{13}C -NMR. Some compounds were characterized using elemental analysis and performing 2D-NMR (COSY, HMBC, and HSQC) to make final assignments.

Acknowledgements

It is a pleasure to thank the many people who made this thesis possible.

I would first like to express my special gratitude and thanks to my supervisor, Dr. Robert Gossage, for taking me in as his student. Throughout this thesis research he has provided support, patience, guidance, and assistance. Thank you Dr. Gossage.

I would like to thank my committee members Dr. Russell Viirre and Dr. Daniel Foucher for their assistance and sharing their knowledge with me. I would also like to thank Dr. Andrew McWilliams for taking the time to read my thesis.

My sincere thanks to Dr. Bryan Koivisto for challenging me, since the day he came to Ryerson University. I am more critical in my writing because of him, and he has given me advice when I needed it, even though I was not his student. So I thank him for his kind assistance.

Khrystyna Herasymchuk, thank you for putting up with me for three years, I bet it was not that easy. You have been an amazing friend and you were always there when I needed you. I will miss working with you in the lab. All the best.

Gossage Group and my lab mates (from KHN 202, KHN 209, KHE 322C) thanks for your assistance in the lab, I appreciated it. Lab would be lonely and not entertaining without you guys (Aman, Lucas, Grace, Shane, Maryam, and Krmo).

I would also love to thank my friends for helping me get through these couple of years, for all the emotional support, and valuable advice. I genuinely appreciate your belief in me. Love you all—Carolyn Khalil, Dulce Banegas, Sossina Gezahegn, Katie Lyashkevich, Pegah Baratzadeh, and Nick Tulsiram (cousin).

Finally, I wish to thank my parents Minawatie and Moonilal, my brother Kevin, and my sister Christina. Thank you for your support, patience, and love throughout this thesis project.

To my immediate family

“The Shuoprasads”

Table of Contents

<u>CHAPTER</u>	<u>PAGE</u>
AUTHOR'S DECLARATION.....	ii
ABSTRACT	iii
ACKNOWLEDGMENTS	iv
DEDICATION.....	v
LIST OF TABLES	viii
LIST OF FIGURES	ix
LIST OF SCHEMES.....	xi
LIST OF ABBREVIATIONS.....	xiii
CHAPTERS	
CHAPTER 1 – Introduction.....	1
1.1 Synthesis of Oxazolines and Oxazoles.....	1
1.2 Natural Occurring Oxazolines and Their Biological Roles.....	3
1.3 Siderophore Binding to Iron.....	5
1.4 Applications.....	7
1.5 Objective.....	9
1.6 Synthetic Strategy.....	11
CHAPTER 2 – Results and Discussion.....	15
2.1 Synthesis of L-Threonine Methyl and Benzyl Ester.....	15
2.1.1 L-Threonine Methyl Ester Hydrochloride (1).....	16
2.1.2 L-Threonine Benzyl Ester (2).....	17
2.2 Synthesis of an Amide.....	18
2.2.1 <i>N</i> -(<i>o</i> , <i>m</i>)-Dimethoxybenzoyl-L-threonine methyl ester (3).....	18
2.2.2 <i>N</i> -(<i>o</i> , <i>m</i>)-Dimethoxybenzoyl-L-threonine benzyl ester (4).....	19
2.3 Synthesis of an Oxazoline.....	20

2.3.1 ((4 <i>S</i> , 5 <i>R</i>)-2-(<i>o</i> , <i>m</i>)-Dimethoxyphenyl)-5-methyl-4-oxazolinecarboxylic acid methyl ester (5).....	22
2.3.2 ((4 <i>S</i> , 5 <i>R</i>)-2-(<i>o</i> , <i>m</i>)-Dimethoxyphenyl)-5-methyl-4-oxazolinecarboxylic acid benzyl ester (6)	23
2.4 Deprotection of the Ester protecting group.....	24
2.5 Synthesis of the Benzamide: Part I.....	27
2.5.1 Boc-1, 4-diaminobutane (8).....	28
2.5.2 <i>N</i> -Boc (1, 4-aminobutyl)-2, 3-(dimethoxyphenyl) benzamide (9).....	28
2.5.3 <i>N</i> -Boc (1, 4-aminobutyl)-[2, 3-bis (benzyloxy) phenyl] benzamide (10).....	29
2.6 Deprotection of Boc Protecting Group.....	30
2.6.1 1, 4-aminobutyl)-[2, 3-bis (benzyloxy) phenyl] benzamide (11).....	32
2.7 Synthesis of the Benzamide: Part II.....	33
2.7.1 <i>N</i> -(2,3-dimethoxybenzoyl)-1,4-diaminobutane) (12).....	36
2.7.2 <i>N,N</i> -Bis(2,3 –bis(methoxy)benzoyl) diaminobutane (13).....	37
2.8 Demethylation Using BBr ₃	38
2.8.1 <i>N,N</i> - Bis(2,3-dihydroxybenzoyl)diaminobutane (15).....	38
2.9 Alternative Route.....	39
2.10 Analogue of Photobactin.....	42
2.10.1 <i>N</i> -[2-(benzyloxy)benzoyl]-L-serine methyl ester (20).....	44
2.10.2 (<i>S</i>)-Methyl 2-[2-Benzyloxy)phenyl]-1,3-oxazoline-4-carboxylate (21).....	45
2.11 Binding Studies with Fe ³⁺	45
CHAPTER 3 – Conclusion and Future Work.....	49
CHAPTER 4 – Experimental.....	51
CHAPTER 5 – Appendix.....	77
A1 –NMR SPECTRA	77
A2 – UV/VIS SPECTRA	109
CHAPTER 6 – References	112

List of Tables

Table 1	Different Methods Used to Synthesize Oxazoline	21
Table 2	Attempts of Deprotection of Methyl Ester using Different Methods	26
Table 3	Attempts of Deprotection of Benzyl Ester using Different Methods	26
Table 4	Different Methods used to cleave Boc	30
Table 5	Reaction conditions for <i>N</i> -(2,3-dimethoxybenzoyl)-1,4-diaminobutane synthesis	34

List of Figures

Figure 1.1.1	Oxazoline (i), Oxazole (ii), Hydroxyphenyl oxazoline (Hphox) (iii)	1
Figure 1.2.1	Siderophore mediated iron availability	3
Figure 1.2.2a	Structures of siderophores that contain the Hphox Unit	4
Figure 1.2.2b	Structures of siderophores that contain the Hphox Unit	5
Figure 1.3.1	Binding constant reaction/ equation	5
Figure 1.3.2	Other ligand motifs common in siderophores	5
Figure 1.3.3	Ferric Agrobactin (R=OH) and Ferric Parabactin (R=H)	6
Figure 1.3.4	The structure of Serratiochelin	7
Figure 1.3.5	Resonance structure of an oxazoline	7
Figure 1.4.1:	The structure of Transvalencin Z	9
Figure 1.4.2:	The structure of Photobactin	9
Figure 2.2.1	The structure of EDC·HCl	18
Figure 2.4.1	Deprotection of Bn ester using a balloon filled with H ₂	25
Figure 2.5.1	Common protecting groups for amines	27
Figure 2.6.1:	Comparing ¹ H-NMR spectra of Boc (10) and No Boc (11)	33
Figure 2.7.1:	Structures of CDI and HBTU	33

Figure 2.7.2:	Compound 13 is formed when using HBTU or SOCl_2	35
Figure 2.7.3:	Compound 13 (top spectrum - using HBTU) Vs. N-(2,3-dimethoxybenzoyl)diaminobutane) (12) (bottom spectrum-using DMTMM) in CDCl_3	36
Figure 2.10.1	Structure of Photobactin and the analogue of Photobactin	42
Figure 2.11.1	Orbital energy of compound (15) calculated using DFT (B3LYP/6-31G*)	46
Figure 2.11.2:	Possible Fe-Photobactin complexes calculated using DFT (B3LYP/6-31G*)	47

List of Schemes

Scheme 1	Typical synthesis of oxazolines	1
Scheme 2	Robinson-Gabriel synthesis	2
Scheme 3	Fischer oxazole synthesis	2
Scheme 4	Cornforth rearrangement	2
Scheme 5	Synthesis of Acinetobactin	12
Scheme 6	Synthesis of Mycobactin S from two building blocks	13
Scheme 7	Proposed synthesis of Photobactin-a two building block approach	14
Scheme 8	Synthesis of L-Threonine methyl ester (1)	15
Scheme 9	Synthesis of L-Threonine benzyl ester (2)	16
Scheme 10	Synthesis of an amide (3 and 4)	18
Scheme 11	The synthesis of an oxazoline	20
Scheme 12	The mechanism of an amide to a nitrile by an E2 elimination	20
Scheme 13	Cyclodehydration of β -hydroxy amide to oxazoline	22
Scheme 14	Mo(VI)=O catalyst used to synthesize an oxazoline	22
Scheme 15	Deprotection of methyl and benzyl ester from the 1 st building block	25
Scheme 16	Synthesis of Boc-1,4-diaminobutane	28

Scheme 17	Synthesis of compound (9) and (10)	28
Scheme 18	General mechanism of deprotection of Boc	32
Scheme 19	Synthesis of <i>N</i> -(2,3-dimethoxybenzoyl)diaminobutane (12) using a coupling reagent	34
Scheme 20	Synthesis of DMTMM (14)	35
Scheme 21	Mechanism of demethylation using BBr ₃	38
Scheme 22	Demethylation of compound 13	38
Scheme 23	An alternative approach to synthesize Photobactin	40
Scheme 24	Synthesis of ethyl 2,3-dihydroxybenzimidate (19)	41
Scheme 25	Synthesis of compound 21 via Burgess reagent	43
Scheme 26	Using Burgess reagent to yield an oxazoline	44
Scheme 27	The results from proposed synthesis of Photobactin	50

List of Abbreviations

ACN	Acetonitrile
atm	Atmosphere
BBr₃	Boron tribromide
BnOH	Benzyl alcohol
Boc	<i>tert</i> -Butyloxycarbonyl
Boc₂O	Di- <i>tert</i> -butyl dicarbonate
Bu₄NF	Tetra- <i>n</i> -butylammonium fluoride
C₆H₆	Benzene
Cbz	Carboxybenzyl
CDI	Carbonyldiimidazole
CD₃OD	Deuterated methanol
CDCl₃	Deuterated chloroform
CDMT	2-chloro-4,6-dimethoxy-1,3,5-triazine
CHCl₃	Chloroform
CN	Coordination number
DCM	Dichloromethane
DEAD	Diethyl azodicarboxylate
DFT	Density Functional Theory
DMTMM	4-(4,6-Dimethoxy-1,3,5-triazin-2-yl)-4-methylmorpholinium chloride
D₂O	Deuterium oxide
EDC·HCl	<i>N</i> -(3-Dimethylaminopropyl)- <i>N</i> -ethylcarbodiimide hydrochloride

Et₂O	Diethyl ether
Et₃N	Triethylamine
EtOAc	Ethyl acetate
EtOH	Ethanol
FeCl₃	Iron (III) chloride
F-moc	9-Fluorenylmethyloxycarbonyl
H₂	Hydrogen (gas)
HBTU	<i>N,N,N',N'</i> -Tetramethyl- <i>O</i> -(<i>1H</i> -benzotriazol-1-yl)uronium hexafluorophosphate
HCl	Hydrochloric acid, Hydrogen chloride
HOBt	Hydroxybenzotriazole
HOMO	Highest Occupied Molecular Orbital
hrs	hours
K₂CO₃	Potassium carbonate
LG	Leaving group
LiOH	Lithium hydroxide
LMCT	Ligand-Metal Charge Transfer
LUMO	Lowest Unoccupied Molecular Orbital
MeOH	Methanol
Methyl DAST	(Dimethylamino)sulfur trifluoride
Min	Minute(s)
MgSO₄	Magnesium sulfate
N₂	Nitrogen (gas)
Na₂CO₃	Sodium carbonate
NaHCO₃	Sodium bicarbonate

NaOH	Sodium hydroxide
NH₄OH	Ammonium hydroxide
NMM	<i>N</i> -Methylmorpholine
NMR	Nuclear Magnetic Resonance
O/N	Overnight
PPh₃	Triphenylphosphine
RT	Room temperature
SEM	2-(Trimethylsilyl)ethoxymethyl
SO₂	Sulfur dioxide
SOCl₂	Thionyl chloride
TBDPS	<i>tert</i> -Butyldiphenylsilyl
TFA	Trifluoroacetic acid
TLC	Thin Layer Chromatography
TMSCI	Trimethylsilyl chloride
UV-Vis	Ultraviolet-Visible Spectroscopy
ε_{max}	Molar absorptivity
λ_{max}	Absorbance peak (maximum)

1. Introduction

1.1 Synthesis of Oxazolines and Oxazoles

Oxazolines and Oxazoles (i & ii respectively: **Figure**

1.1.1) belong to a class of heterocyclic compounds which continue to be of great interest in all aspects of synthetic chemistry. This is supported by a continuous growth in the

number of research publications and reviews that focus on the chemical and biological importance of oxazolines and

oxazoles, since the early 1980's. The continued interest in these compounds are mainly due to their simple synthetic preparation. There are several known synthetic routes to oxazolines, but

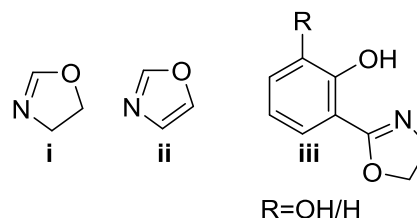
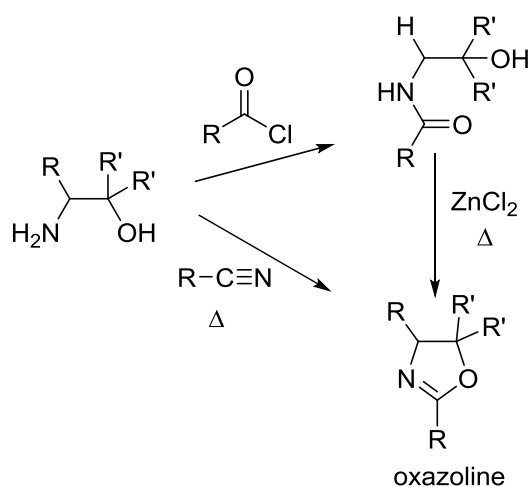


Figure 1.1.1: Oxazoline (i), Oxazole (ii), Hydroxyphenyl oxazoline (Hphox) (iii)

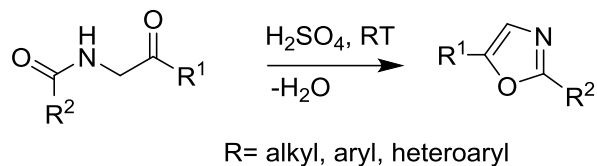


Scheme 1: Typical synthesis of oxazolines

the two most common approaches are summarized in

Scheme 1. Readily available β -amino alcohols can be coupled with an acid chloride to yield an amide, which is then cyclized to the oxazoline in the presence of a Lewis acid catalyst.¹ This method requires two steps. Alternatively, the one step synthesis of oxazoline can be achieved by reacting a β -amino alcohol with a nitrile, also under Lewis acid catalysis.¹ There are various other procedures that have been developed for the

preparation of 2-substituted oxazolines using carboxylic acid, carboxylic ester, aldehydes, and olefins as starting materials. However, most of the methods have numerous disadvantages which includes strongly acidic conditions, toxic solvents, long reaction times, use of complex reagents, and low yield of products.

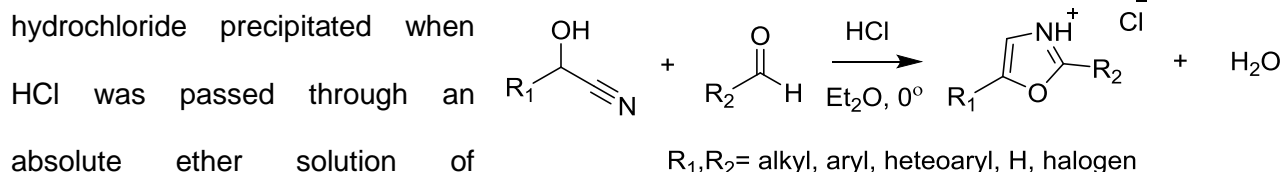


Scheme 2: Robinson-Gabriel synthesis

Oxazoles can also be prepared by reducing oxazoles. There are three common synthetic routes to oxazoles. The primary synthetic route is the dehydration of 2-acylamino-ketones, also known as Robinson-Gabriel synthesis (**Scheme**

2).² In this reaction, concentrated sulphuric acid or phosphorus pentachloride is used as the dehydration agent; typically sulphuric acid gives better yields and produces fewer by-products.²

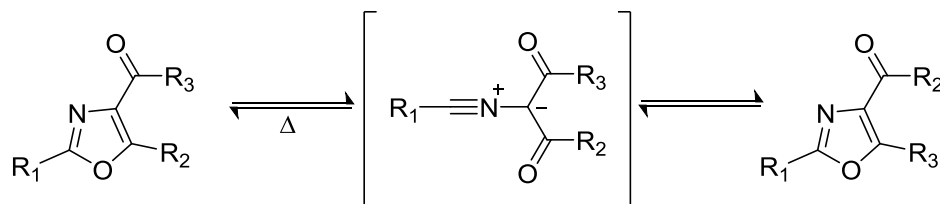
Another route to oxazoles is the Fischer synthesis (**Scheme 3**). This reaction involves the acidified condensation of equimolar amounts of cyanohydrins and aromatic aldehyde in dry ether.³ This synthesis was discovered by Hermann Emil Fischer in 1896, who found that 2,5-diphenyloxazole hydrochloride precipitated when



Scheme 3: Fischer oxazole synthesis

cyanohydrins.³ This synthetic route is typically high yielding (~80%).

Another common reaction generating substituted oxazole is the Cornforth Rearrangement which is shown in **Scheme 4**. Cornforth rearrangement is a thermal interconversion of 4-carbonyl substitute oxazoles with exchange between the C-C=O side chains and C=C-O fragment of the oxazole ring.⁴



Scheme 4: Cornforth Rearrangement

1.2 Natural Occurring Oxazolines and Their Biological Roles

The discovery of natural occurring oxazolines and oxazoles have stimulated significant interest in the chemistry and biology of these heterocycles. Naturally occurring oxazolines (*i.e.*, 4, 5-dihydro-2-oxazoles) which contain a secondary phenolic functionality are also known as hydroxyphenyl oxazolines (**iii**: **Figure 1.1.1**). Photobactin is a naturally occurring oxazoline compound and it is the main focus of this thesis project. The 2-(2'-hydroxyphenyl)-2-oxazoline (Hphox: **iii**) moiety is a common constituent found in many microbial siderophores. Siderophores are low molecular weight compounds (500-1000 Daltons) with a very high and specific binding affinity for iron (*vide infra*).⁵

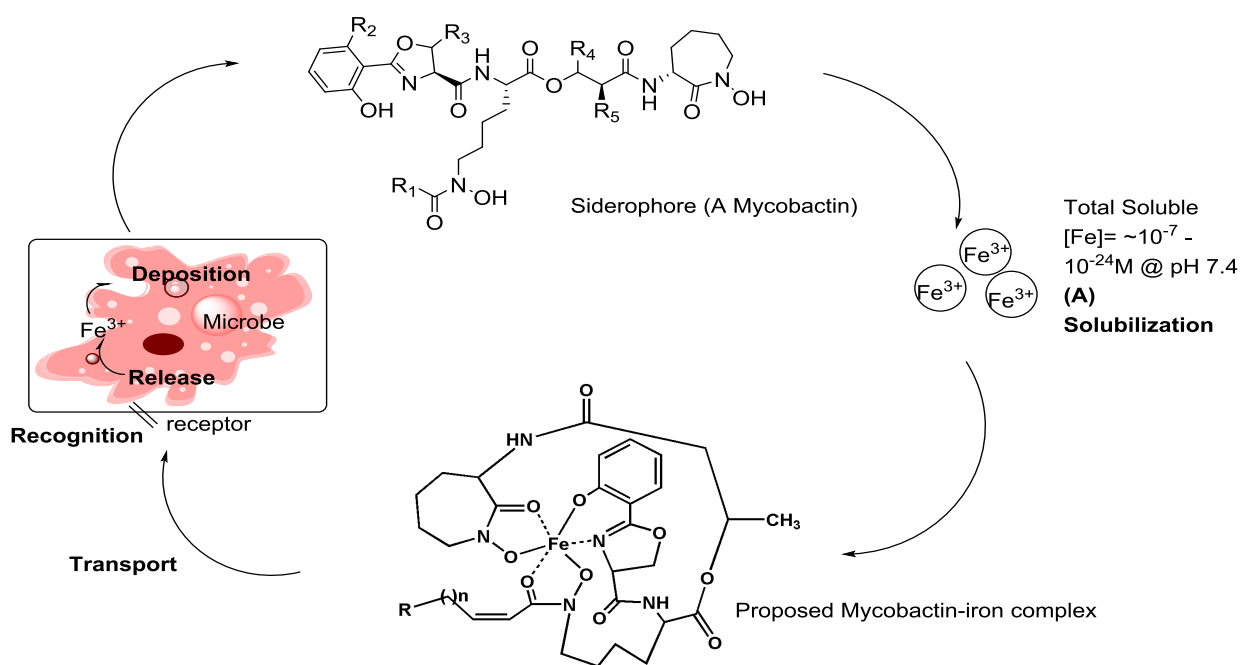


Figure 1.2.1: Siderophore mediated iron availability

Siderophores are found in microorganisms and in some plants. Microorganisms, such as bacteria, biosynthesize these compounds to selectively sequester iron from the environment. This decreases its availability for competitors while scavenging and regulating iron concentration in

the cell (**Figure 1.2.1**). In addition, ferric ion at physiological pH is extremely insoluble, thus, siderophores have been evolved by microorganisms to solubilize it. Therefore, outside the cell, siderophores can sequester iron in its different natural forms in aqueous-aerobic conditions at pH 7.4: **(A)** $\text{Fe}^{3+}(\text{aq})$ ($K_{sp} = 2.60 \times 10^{-39}$), $[\text{Fe}(\text{OH})]^{2+}(\text{aq})$, and $[\text{Fe}(\text{OH})_2]^+(\text{aq})$ ($K_{sp} = 4.90 \times 10^{-7}$). Donor atoms with a high affinity for Fe (III) include negatively charged oxygen atoms. Siderophores contain these hard O-donor atoms as ligands and form thermodynamically very stable complexes with Fe^{3+} . The concentration of iron in the environment of a microorganism is extremely low (between 10^{-7} and 10^{-24} M).⁶ Once the iron is chelated, it forms a soluble iron complex. The siderophores transport the iron to the bacteria using a specific outer-membrane receptor, a periplasmic protein, and several inner-membrane associated proteins (**Figure 1.2.1**).⁶ Once the iron is in the cell, it is removed from the siderophore, and the cycle repeats itself. Moreover, the oxidation state of iron has major influence on the stability of iron siderophore complexes. Fe^{2+} siderophore complexes are more liable than Fe^{3+} siderophore complexes. Fe^{2+} is a softer cation than Fe^{3+} . The interaction to a hard oxygen of the binding ligand is therefore not as favourable. Some examples of siderophores that have a 2-hydroxyphenyl-2-oxazoline unit are: Parabactin, Agrobactin, Mycobactin S, and Transvalencin Z (**Figure 1.2.2a**). Siderophores that have 2,3-dihydroxyphenyl-2-oxazoline unit are: Photobactin, Vibriobactin, and Acetobactin (**Figure 1.2.2b**). All of the siderophores mentioned come from a different type of bacterium.

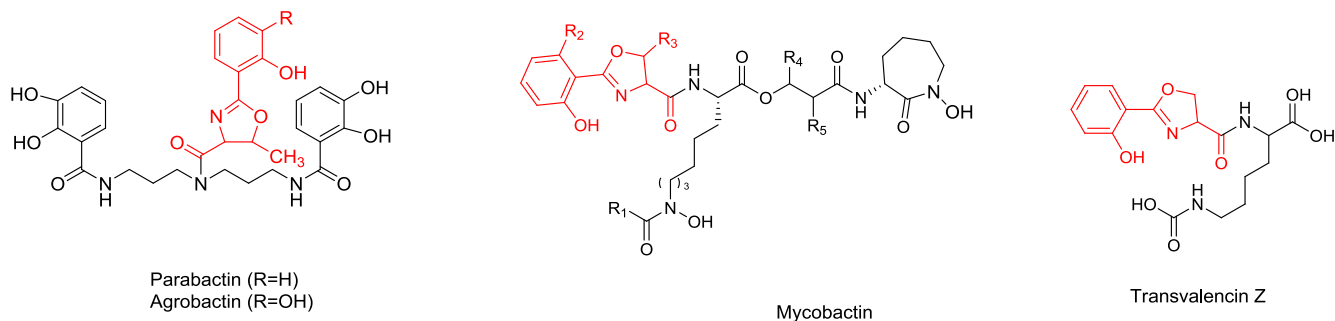


Figure 1.2.2a: Structures of siderophores that contain the Hphox Unit

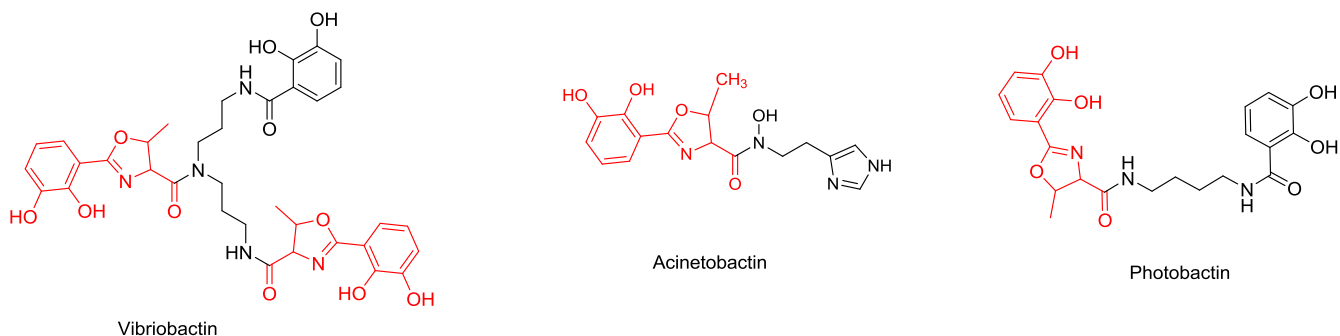


Figure 1.2.2b: Structures of siderophores that contain the Hphox Unit

1.3 Siderophore Binding to Iron

Siderophores are chelators with exceptionally strong affinity for iron and best known for their capacity to feed microorganism with ferrous and ferric ions. The binding constant (K_{Binding}) of

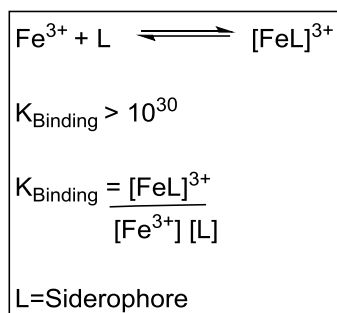
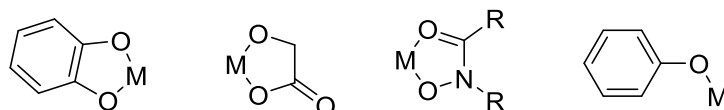


Figure 1.3.1: Binding Constant Reaction/Equation

Fe^{3+} complex is 10^{30} or higher (**Figure 1.3.1**), that means upon deprotonation of the hydroxyl groups on the Hphox moiety (iii) siderophore ligands bind strongly to the metal.⁷ The siderophore ligands are usually catecholate and hydroxamate or, less frequently, Hphox residues. For instance, with the Mycobactin S, the two hydroxamate residues and Hphox residues act in concert to form an extremely stable iron (III) complex (**Figure 1.2.2a**). Moreover, the hydroxyphenyl oxazoline moiety can also behave as a bidentate

ligand with a metal centre coordination.⁷

Catecholate, carboxylate, hydroxamate, and phenolate which are incorporated into the siderophores as major groups are the most efficient Fe-binding ligands found in nature (**Figure**



M=Transition Metal

Figure 1.3.2: Other ligand motifs common in siderophores

1.3.2).⁵ The catecholate, carboxylate, and hydroxamate each occupy two sites of the iron centre. Iron coordinates to a lone pair of electrons

on an oxygen atom from the siderophore ligand. As oxygen is a very hard donor atom it shows high affinity for hard Fe (III) cations. Siderophore ligands are weak acids, therefore the greater the basicity of the chelator, the greater its affinity for Fe^{3+} .⁵ In aqueous solution, the formation of iron siderophore complexes is affected by the pH. The free protons and the iron compete for the free siderophore ligand. The higher the pK_a value, the stronger competition by protons. Therefore, siderophore ligands show high affinity for high oxidation state iron.

Majority of siderophores display octahedral coordination to Fe^{3+} where six ligands coordinate to the iron ($\text{CN}=6$), and that is because three of the oxygen donor ligands are usually incorporated into the siderophore.^{6,8} In Parabactin and Agrobactin, the tertiary nitrogen atom of the oxazoline contains a binding site for the six coordinate ferric ion (**Figure 1.3.3**). Ferric ion is known as a hard acid, so it prefers to coordinate to oxygen rather than a softer base like nitrogen. However, binding to nitrogen in Agrobactin or Parabactin places the ferric ion in a six membered ring and the environment is known to favour its stability. In addition, the stability of iron siderophore complexes is not only affected by the number and type of ligand binding sites but also by their relative arrangements to each other. A preorganization of the binding sites is what keeps them in order and allows an octahedral configuration which affects the stability of the complex. However, siderophores like Photobactin and Serratiochelin (**Figure 1.3.4**) have only two catechol ligands. Researchers hypothesize that

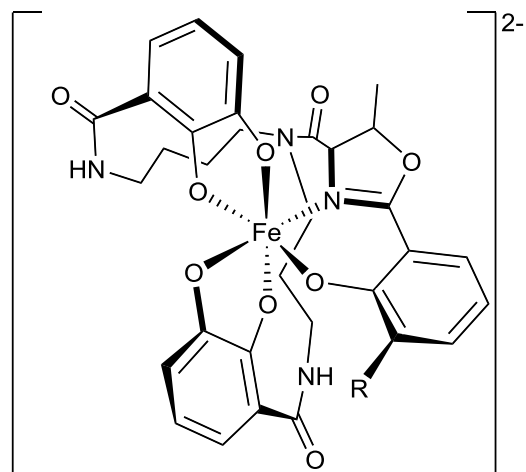


Figure 1.3.3: Ferric Agrobactin ($\text{R}=\text{OH}$) and Ferric Parabactin ($\text{R}=\text{H}$)

Serratiochelin may be a hexadentate (*6-coordinate*) or tetradentate (*4-coordinate*) ligand.⁹ For it to form an octahedral, there has to be two catechols, which would give it four binding sites. Also, the nitrogen on the oxazoline, and the oxygen on the L-Threonine moiety would give two extra binding sites.⁹ Alternatively, it might be a tetrahedral complex with only one of the catechol (both

–OH) coordinating to the iron, which would give it two binding sites. The nitrogen on the oxazoline, and one hydroxyl group from the catecholate gives it the two additional binding sites.⁹ The reason why tertiary nitrogen on the oxazoline will be favoured over the second hydroxyl on the catechol can probably be explained by the corresponding pK_a values of around 7 and 11 respectively.^{6,8,9}

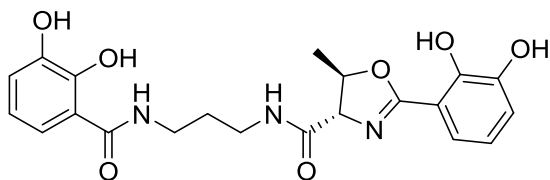


Figure 1.3.4: The Structure of Serratiochelin

Due to the resonance effect (*the partial charge*) on the nitrogen atom (**Figure 1.3.5**), Fe-N (oxazoline) bond formation would be preferred, since oxygen is relatively electron deficient. Moreover, the type of iron coordination with Vibriobactin is debatable according

to researchers, since it contains three catechol ligands and two oxazolines. Griffiths *et.al*,^{7, 10} suggested that nitrogen atom of the oxazoline / oxazole can partake in iron coordination while Miethke *et.al*,^{6, 10} suggested that six oxygens from the catechol ligands would coordinate to the iron atom. Based on the holo-ViuP structure,¹⁰ it discloses that Ferric-Vibriobactin complex has six binding sites from five hydroxyl groups of the catechol ligands and the last binding site comes from the nitrogen on the oxazoline.¹⁰ ViuP is a periplasmic transport protein which moves Fe-Vibriobactin complex from outer membrane to inner membrane of *Vibrio cholerae*.¹⁰ Holo is a protein with ligands, while Apo is a protein without ligands.

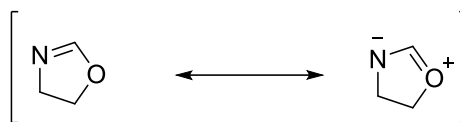


Figure 1.3.5: Resonance structure of an oxazoline

Furthermore, a potential Fe-Photobactin complex

could be a distorted tetrahedral or octahedral where nitrogen from the oxazoline participates as a coordinating ligand.

1.4 Applications

The extraordinary ability of siderophores to chelate and mobilize iron, allow there to be potential applications for siderophores in medical sciences. Iron is an important element involved in proper functioning of various physiological activities among living systems such as plants, animals, and

human beings. Its excess and deficiency lead to numerous diseased situations, which makes siderophores suitable for applications in medicine such as, selective drug delivery, treatment of iron overload, and cancer therapy.

Siderophores can be used for selective delivery of antibiotics. This new antimicrobial approach to defeat drug resistant bacteria, uses the iron transport abilities of siderophores to take drugs into cells by means of conjugates formed between siderophores and antimicrobial agents.⁶ Siderophores are used as mediators to facilitate the cellular uptake of antibiotics.⁶ This interaction of antibiotics with siderophores results in formation of siderophore-conjugate known as siderocymins.⁶ The siderophore part of this conjugate is capable of hunting for iron, while the other part of the conjugate bears an antibiotic activity, which uses the siderophore as a Trojan horse and mediates iron transport mediated drug delivery into the cell.⁶ Additionally, the antimicrobial agents covalently linked to the siderophore are actively transported across the outer membrane of gram-negative bacteria. Generally the drug conjugate consist of a linker for attaching the drug to the siderophore. Once getting into the bacterial cell, the siderophore–drug conjugate kills the cell by releasing the drug, acting as a complete antibacterial agent, or by blocking further iron acquisition. Natural and synthetic are the two types of conjugates.⁶

Natural siderophore-antibiotic conjugates are ferrimycin, danomycin, and salmycin. Ferrimycin prevent gram positive bacteria by changing protein biosynthesis.⁶ Danomycin and salmycin prevent protein synthesis in gram positive bacteria. These are isolated from streptomycetes and actinomycetes. They apply antibacterial activity to prevent protein synthesis. Synthetic siderophore-antibiotic conjugates are prepared using antibiotics with cell permeability and reduced susceptibility to resistance mechanism (*for instance secretion*).⁶ The siderophore is bound to a powerful antibiotic such as erythromycin or a beta-lactam.

Several siderophores are used in treatment of acute iron intoxication and chronic iron overload disease such as hemochromatosis and sickle disease. Siderophores (*i.e.*, deferoxamine/desferrioxamine) can be used as chelating agents which bind to iron to produce complexes that lead to formation of ferrioxamine. Ferrioxamine is a stable complex, which is eliminated through the kidney. Deferoxamine is a chelating agent used to remove excess iron from the body. This bacterial siderophore acts by binding free iron in the bloodstream and enhances its removal through urine and feces.⁶ Therefore, it can be used to decrease iron overload in the body.

Microbial ferric siderophore complexes may also be useful for cancer therapy. Siderophores such as dexrazoxane and desferrithiocin are used in cancer therapy.⁶

1.5 Objective

The total synthesis of Transvalencin Z (**Figure 1.4.1**) was the original objective for this thesis project. This siderophore is produced by a rare *Nocardia* species and has simply been isolated from a bacterium called *Nocardia transvalensis*, which was sequestered from a Japanese patient in 2006.¹¹

Actinomycotic mycetoma are caused by *Nocardia* species. Actinomycotic mycetoma is a slow growing bacterium that occurs

in one area of the body, usually the hands or feet.¹¹ However, the total synthesis of Transvalencin Z was published shortly after and this thesis project was thus revised. The intention is to focus on

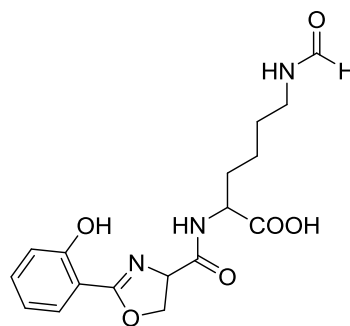


Figure 1.4.1: The structure of Transvalencin Z

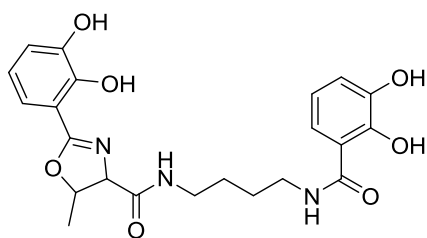


Figure 1.4.2: The structure of Photobactin

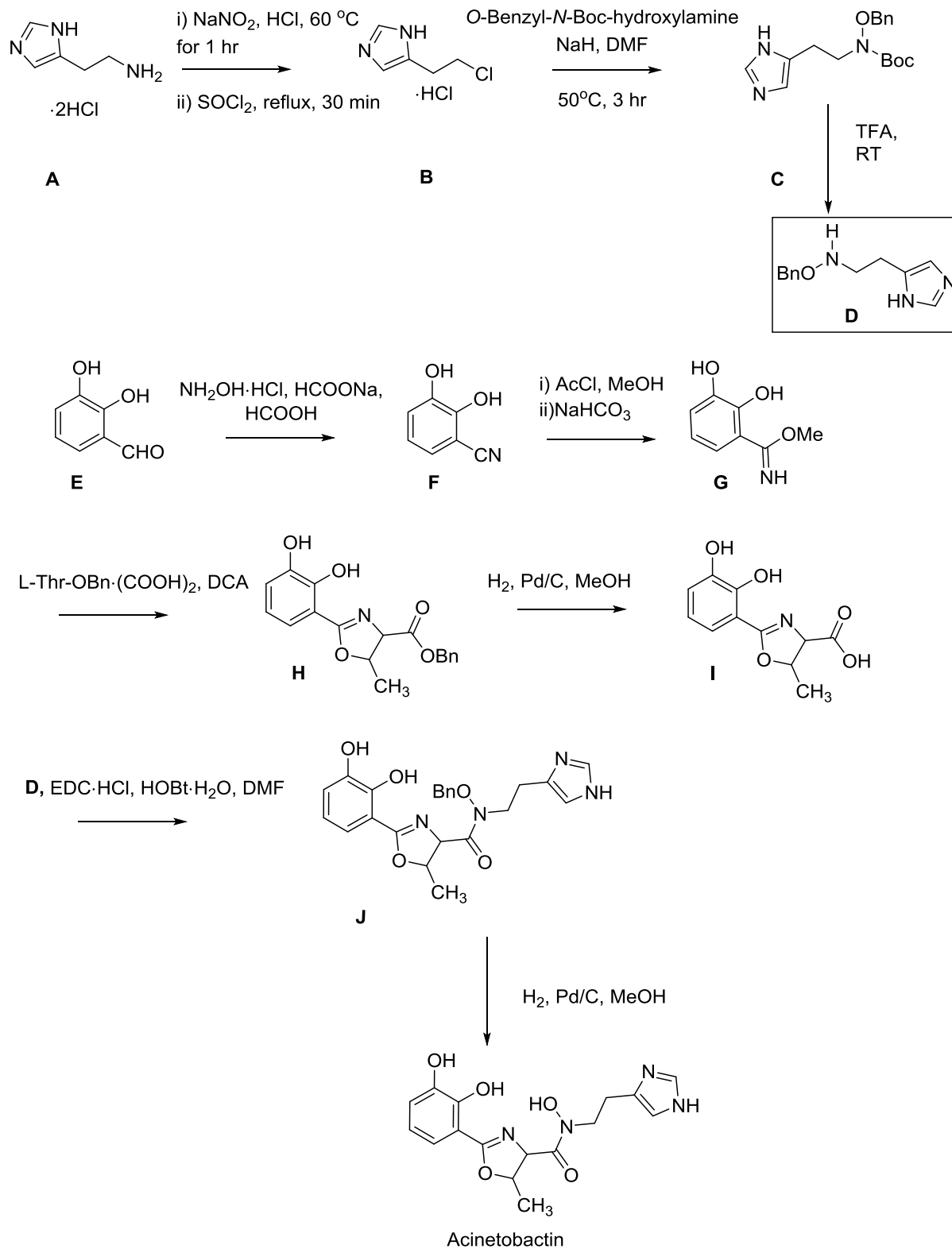
the total synthesis of a different siderophore named Photobactin (**Figure 1.4.2**), and to study its binding properties with iron through Ultraviolet–visible (UV-Vis) spectroscopy and density functional theory (DFT) calculations. Photobactin is a related catechol siderophore that comes from an insect killing bacterium, *Photorhabdus luminescens* (*Enterobacteriaceae*).¹²

Members of the family *Enterobacteriaceae* (*gram-negative bacteria*) commonly produce catechol and hydroxamate siderophores such as Enterobactin and Aerobactin. Photobactin is found in the gut (innards) of roundworms also known as nematodes. This siderophore has been previously isolated (< 10 mg) and purified in order to determine if the siderophore activity is required for *Photorhabdus luminescens* to support the growth and reproduction of its nematode host. It has been characterized by UV-Vis, mass spectrometry, and nuclear magnetic resonance (NMR). The proposed Photobactin molecule was related to Vibriobactin and Agrobactin. Vibriobactin (**Figure 1.2.2b**) comes from *Vibrio Cholera*⁷ and Agrobactin (**Figure 1.2.2a**) comes from *Agrobacterium tumefaciens*.^{13,14} Agrobactin has a spermidine backbone and vibriobactin has a norspermidine backbone, while photobactin has a putrescine backbone. Agrobactin and Vibriobactin have one more 2,3-dihydroxybenzoic acid moiety compared to Photobactin. Upon characterization of Photobactin the IUPAC name was assigned as 2-(2,3-dihydroxyphenyl)-5-methyl-4,5-dihydro-oxazole-4-carboxylic acid [4-(2,3-dihydroxybenzoylamino)butyl]amide.¹² Photobactin is the generic or trivial name and will be used hereafter.

1.6 Synthetic Strategy

The synthetic strategy to produce useful quantities of the title material, Photobactin, involves the coupling of two key building blocks. This method was inspired by Miller *et al.* who synthesized Mycobactin S, and Takeuchi *et al.* who synthesized Acinetobactin. Mycobactin S and Acinetobactin come from bacteria called *Mycobacterium smegmatis* and *Acinetobacter baumannii*, respectively.^{15,16}

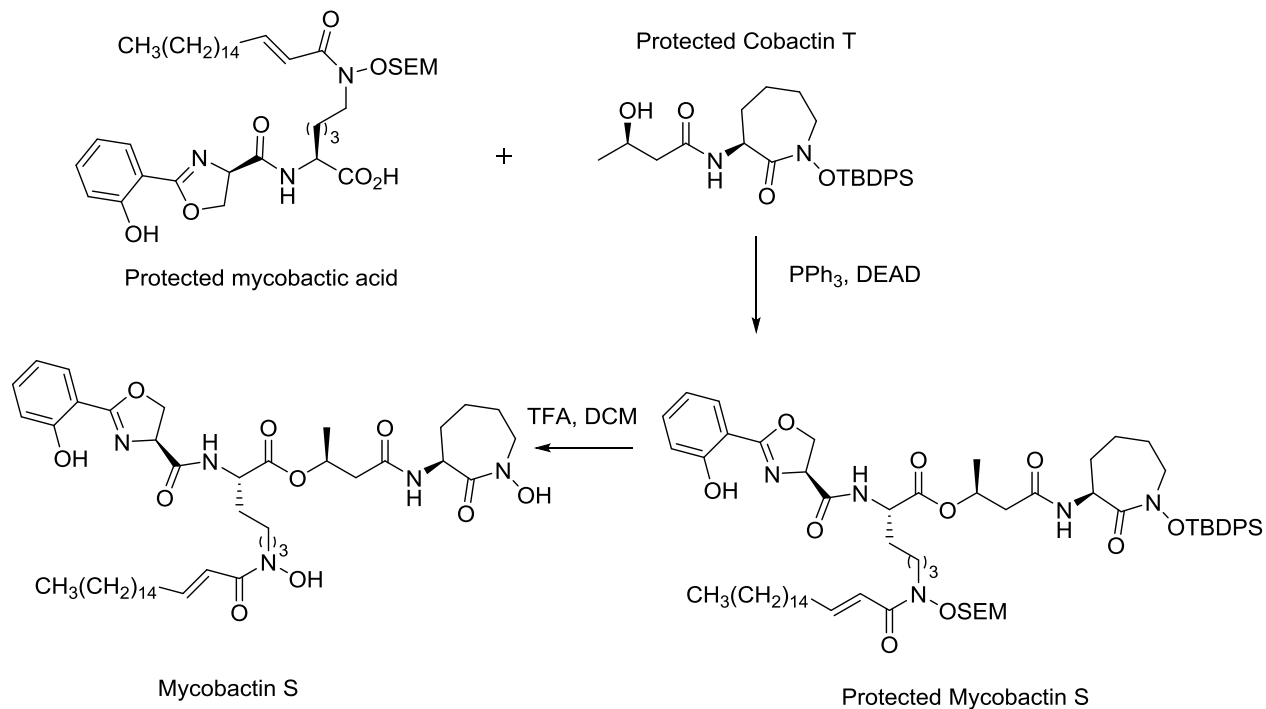
Scheme 5 shows the synthesis of Acinetobactin. Reaction of compound **A** with sodium nitrite, following with a substitution reaction with thionyl chloride yielded compound **B**, which was then coupled to O-benzyl-N-Boc-hydroxylamine in the presence of NaH.¹⁶ The protecting group (Boc) on compound **C** was then removed with TFA to afford **D**. 2,3-Dihydroxybenzaldehyde (**E**) was combined with hydroxylamine hydrochloride, sodium formate, and formic acid to yield compound **F**.¹⁶ Reacting compound **F** with acyl chloride, methanol, and sodium carbonate produced compound **G**, which was in turn mixed with L-Threonine derivative resulting in an oxazolidine (**H**). Compound **I** was synthesized by the hydrogenolysis of **H**, which cleaved the Bn protecting group.¹⁶ Product **D** was coupled with **I** to give the desired compound **J** (55%). Compound **J** underwent hydrogenolysis and yielded the title material, Acinetobactin.¹⁶



Scheme 5: Synthesis of Acinetobactin¹⁶

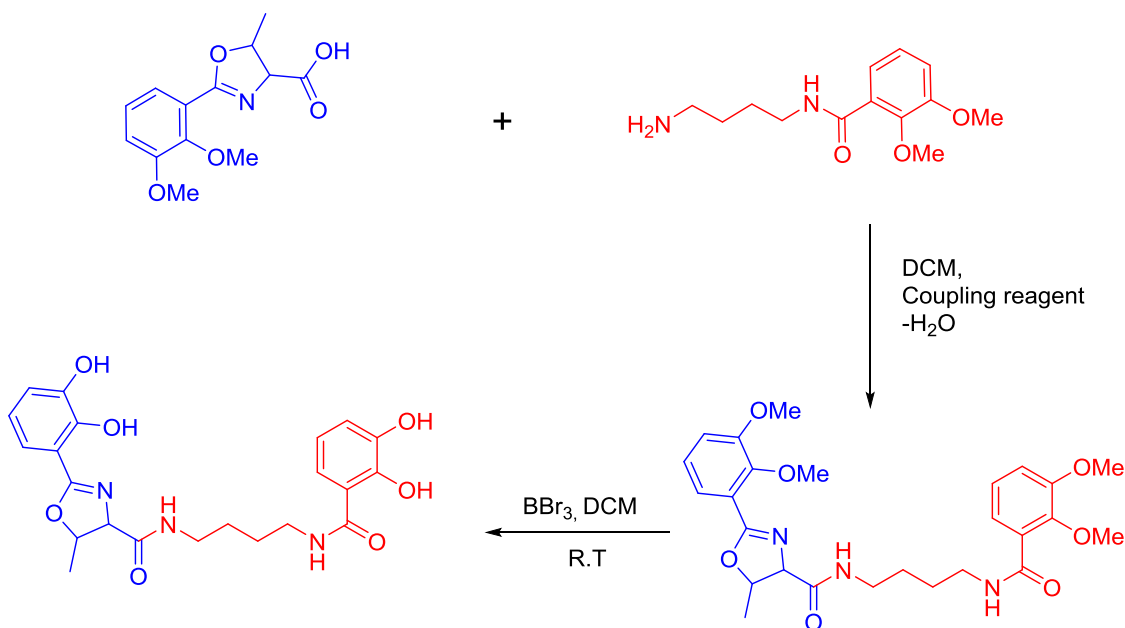
Scheme 5 also outlines a general approach to siderophore synthesis, which results in synthesizing two building blocks individually. Therefore, a multi-step procedure is required to yield the product (*siderophore*). As one can see in **Scheme 5**, nine steps are involved in order to produce Acinetobactin.

Moreover, Miller also synthesized two building blocks separately which were the protected Mycobactin acid and Cobactin T (**Scheme 6**). Protected Mycobactin S was obtained under Mitsunobu conditions (PPh_3 , DEAD).¹⁵ The step-by-step synthesis is not presented since it was comprised of more steps than Acinetobactin.



Scheme 6: Synthesis of Mycobactin S from two building blocks¹⁵

Based on the two syntheses mentioned (*Acinetobactin* and *Mycobactin S*), the same approach is being followed to synthesize Photobactin. The oxazoline acid and the putrescine-containing building block are synthesized separately which involved Boc, methyl ester, methyl ether, benzyl ester, and benzyl ether protecting groups. Protecting groups are required for this total synthesis since certain functional groups can interfere with other reactions. The two building blocks can be combined together with a coupling reagent, following with the removal of the protecting groups (*deprotection*), to produce the title material, Photobactin (**Scheme 7**).



Scheme 7: Proposed synthesis of Photobactin-a two building block approach

2. Results and Discussion

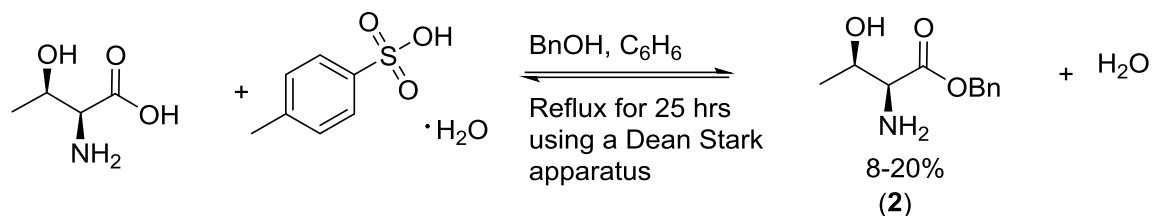
The total synthesis of Photobactin was attempted by synthesizing two building blocks separately as proposed in **Scheme 7**. The first building block mentioned is the oxazoline acid, while the second building block is the putrescine containing or derivative moiety. A variety of reactions were performed and certain ones were troublesome, especially the deprotection of an ester. The purification of selected compounds was sometimes tricky due to solubility issues (*e.g. liquid-liquid extraction*). Furthermore, the fundamental chemical reactions are introduced, and the results of the reaction outcomes, as well as the iron binding studies are discussed in this chapter.

2.1 Synthesis of *L*-Threonine Methyl and Benzyl Ester

The carboxylic acid group in the amino acids is usually protected during synthetic modifications of these starting materials. The reason for that, is because amino acids have multiple reactive groups therefore, the peptide synthesis must be carefully performed. An ester can serve as a protecting group of carboxylic acids to prevent the carboxyl group from reacting in some undesired manner during peptide (*amide*) synthesis. Hence, the carboxylic functional group on *L*-Threonine and *L*-Serine is protected with either a benzyl or methyl ester group, so that peptide (*amide*) synthesis undergoes smoothly in the next step.



Scheme 8: The synthesis of *L*-Threonine methyl ester (1)



Scheme 9: The synthesis of L-Threonine benzyl ester (**2**)

An esterification reaction was performed in order to form an ester protecting group. Esterification using a carboxylic acid (*in this case: amino acid*) and an alcohol, requires an acid catalyst (e.g., *trimethylsilyl chloride* or *p-toluenesulfonic acid monohydrate*). Esterification is an equilibrium reaction, which is therefore reversible. The reaction must be shifted to the right by using excess of one reagent (*methanol / benzyl alcohol*) or removing one of the products (*water*), in order to favour the formation of the ester (*Le Chatelier's Principle*).¹⁷ In the esterification (**Scheme 9**), the mixture was heated under reflux, and the benzene-water azeotrope (bp 69 °C) was distilled out of the flask *via* a Dean Stark apparatus. Water distills out of the reaction into the burette and benzene condenses back into the flask. The azeotrope, however, has to have lower boiling than the alcohol used. In methyl esterification (**Scheme 8**), however, methanol has a lower boiling point (65 °C) than the benzene-water azeotrope (69 °C), which means methanol would distill out of the reaction first and that would be ineffective. Therefore, a different procedure was used in **Scheme 8**, where it did not require a Dean Stark apparatus and/or reflux temperatures.¹⁷

2.1.1 L-Threonine Methyl Ester Hydrochloride (**1**)

L-Threonine methyl ester hydrochloride (**1**) was synthesized following **Scheme 8**. The ¹H-NMR spectrum (**Figure A1.1**) showed a doublet with a chemical shift (δ) at 1.34 ppm integrating for three protons. This was assigned to the methyl group of the L-Threonine moiety. The signal at δ = 3.87 ppm corresponds to the methyl protons of the ester functional group integrating for three protons as well. The signal at δ = 4.09 ppm was assigned to the methine proton that is bound to the amine. It integrates for one proton. The resonance signal for the methine proton adjacent to

the methyl and hydroxyl group was observed at $\delta = 4.43$ ppm which integrates for one proton as well. The ^{13}C -NMR spectrum (**Figure A1.2**) matches perfectly with the molecule having four carbon signals. The carbonyl carbon signal is very weak and downfield to observe, due to sp^2 -hybridization and no protons attached (*ipso carbon*). This is typical for carbonyl carbons.¹⁷

2.1.2 *L*-Threonine Benzyl Ester (**2**)

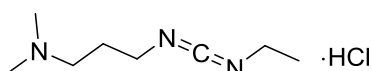
Compound **2** was synthesized following **Scheme 9**, which was based on the literature reported by S. Pétursson and J. Baldwin.¹⁸ However, purification of the crude product was done by flash chromatography and not recrystallized as reported in the literature.¹⁸

^1H -NMR data (**Figure A1.3**) was consistent with that previously reported by Pétursson and Baldwin.¹⁸ The ^{13}C -NMR spectrum (**Figure A1.4**) showed a signal at $\delta = 19.79$ ppm which was assigned to the methyl carbon of the *L*-Threonine-derived moiety. The signal at $\delta = 59.93$ ppm corresponds to the carbon atom attached to the amine. The $-\text{CH}_2$ from the benzyl functional group was observed at $\delta = 65.42$ ppm. The signal at $\delta = 68.11$ ppm was assigned to the carbon atom of the *L*-Threonine moiety bound to the hydroxyl group and the methyl group. The aromatic carbons of the benzyl functional group were observed at $\delta_{\text{C}} = 127.00, 127.65, 127.69, \text{ and } 128.59$ ppm. The resonance at $\delta = 140.87$ ppm was assigned to the carbonyl carbon of the molecule.

The percent yield was low. The loss of product was probably due to the liquid-liquid extraction, the reaction did not go to completion, and/or not all of the water was collected in the Dean Stark apparatus. Aqueous layer may need to be washed an additional time to recover more of the *L*-Threonine benzyl ester.

2.2 Synthesis of an Amide

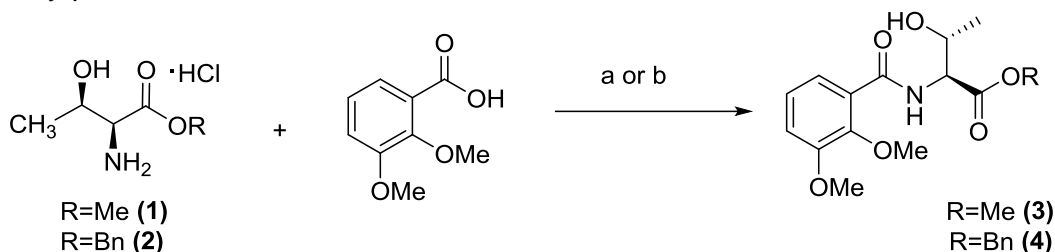
Amide is a derivative of a carboxylic acid in which the hydroxyl group has been replaced by an amine group. Amide bond (peptide bond) formation was prepared in two ways (**Scheme 10**): *via* an acyl chloride and using a carbodiimides coupling reagent (EDC·HCl). Acyl chlorides¹⁹ are usually produced from the corresponding acids that require either thionyl chloride, oxalyl chloride, phosphorus pentachloride or phosphorous trichloride. *N*-(3-dimethylaminopropyl)-*N*-



ethylcarbodiimide hydrochloride (EDC·HCl; **Figure 2.2.1**)

is a coupling reagent that is commonly used for amide formation since it is a one-pot procedure.¹⁹ Nonetheless,

urea is the by-product whereas using thionyl chloride has SO₂(g) and triethylamine hydrochloride as the by-products.



Scheme 10: a. (i) Et₃N, DCM, SOCl₂, 0°C, N₂, 30 min (ii) L-Threonine benzyl/methyl ester, overnight (O/N), RT, N₂
b. DCM, HOBT, Et₃N, EDC·HCl, RT, O/N, N₂

Based on these two methods, the amide was isolated easily through the use of the acyl chloride which gave a better yield than when using the EDC·HCl coupling reagent.

2.2.1 *N*-(*o,m*)-Dimethoxybenzoyl-L-Threonine methyl ester (**3**)

Method (a), shown in **Scheme 10**, depicts an approach taken to synthesize the methyl ester amide from the compound (**1**).¹H and ¹³C-NMR chemical shift values were consistent with data reported by Sakakura *et al.* (**Figure A1.5 and A1.6**).²⁰ The percent yield was low (29%) and the loss of product is presumably during the purification step (*flash column chromatography*).

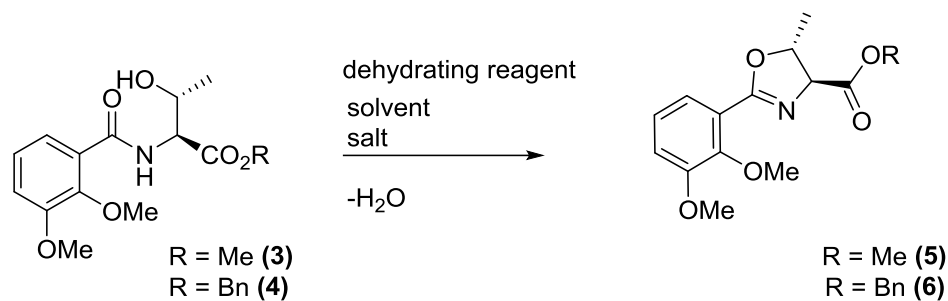
2.2.2 *N*-(*o*, *m*)-Dimethoxybenzoyl-*L*-Threonine benzyl ester (**4**)

N-(*o*,*m*)-Dimethoxybenzoyl-*L*-threonine benzyl ester (**4**) was synthesized using two different approaches: acyl chloride and by EDC·HCl coupling reagent (**Scheme 10** (a) and (b)) which was based on the literature reported by Miller.¹⁵ The impurities and by-products were removed by extraction and flash column chromatography. The acyl chloride method afforded the amide product as yellowish-brown coloured solid in a 55% yield, while EDC·HCl method gave only a 33% isolated yield.

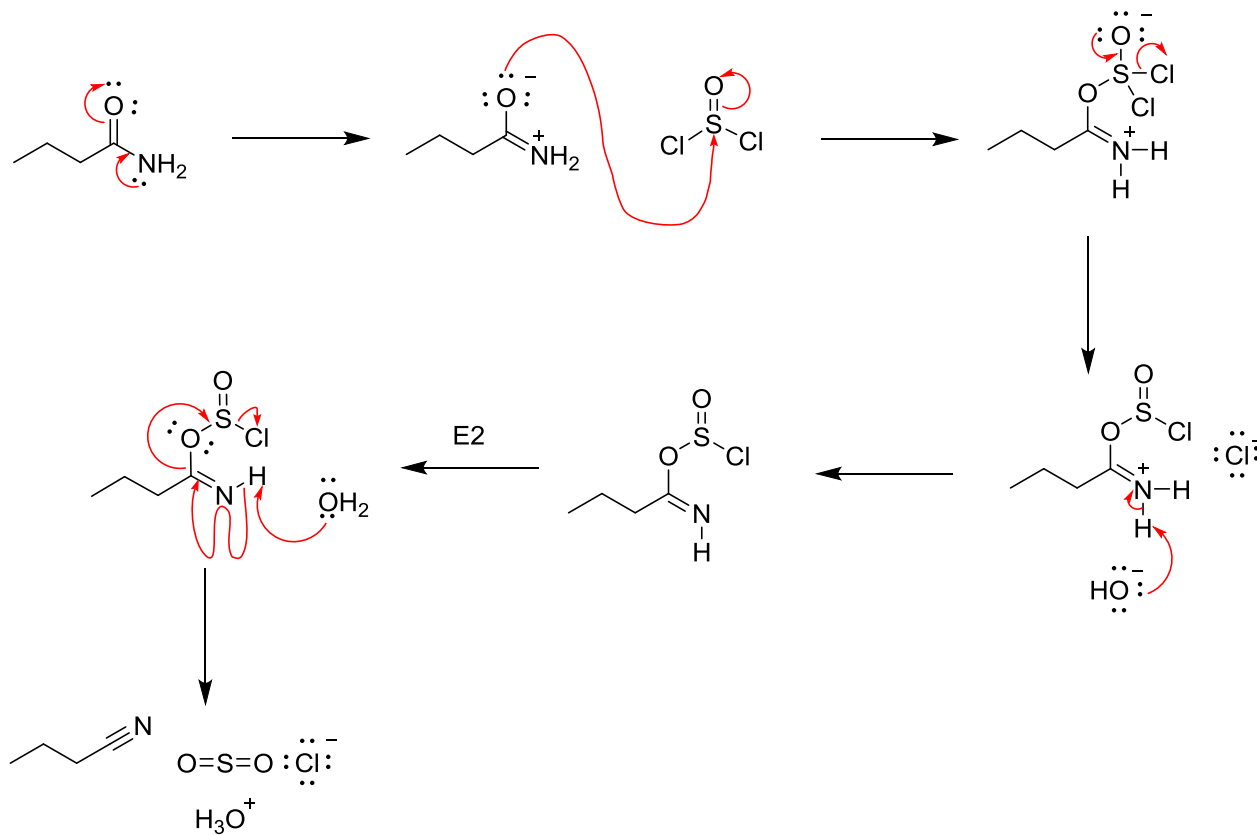
The ¹H-NMR spectrum of compound **4** (**Figure A1.7**) showed a singlet with a chemical shift (δ) at 3.91 ppm integrating for six protons. This was assigned to the methyl protons of the methoxy group. A quartet of doublets was seen at δ = 4.43 ppm and doublet of doublets was seen at δ = 4.88 ppm both integrating for one proton each. These were assigned to the protons of the methine adjacent to the amide nitrogen. The singlet observed at δ = 5.23 ppm corresponds to the protons on the -CH₂ on the benzyl moiety, which integrates for two protons. The two doublet of doublets observed at δ = 7.07 ppm, 7.71 ppm, the triplet and multiplet observed at δ = 7.18 ppm and 7.32-7.35 ppm corresponds to the aromatic protons of the benzyl and 2,3-dimethoxy benzoic acid moiety. The ¹³C-NMR (**Figure A1.8**) showed signal at δ = 20.11 ppm which was assigned to the carbon atom of the methyl group. The signals at δ = 56.14 and 57.90 ppm were assigned to the carbon atoms of the methoxy groups. The peaks observed δ = 61.64 and 68.27 ppm corresponds to the -CH groups on the amide. The -CH₂ from the benzyl functional group was observed at δ = 67.26 ppm. Six unsubstituted aromatic carbons were observed. The signal at δ = 128.62 ppm was assigned to the ipso carbon of the aromatic ring attached to the carbonyl group. The signal at δ = 135.36 ppm was assigned to the ipso carbon of the aromatic ring from the benzyl functional group (Bn). The signals at δ = 148.06 and 152.75 ppm were assigned to the aromatic carbons that were bound to the carbon atoms of the methoxy groups. The signals at δ = 165.70 and 171.01 ppm were assigned to the carbonyl carbons of the molecule. These appear less intense than the

other carbon signals in the molecule, which was expected for carbonyl carbons. In addition, the $^1\text{H-NMR}$ for the EDC·HCl method was consistent with the data recorded for the acyl chloride method.

2.3 Synthesis of an Oxazoline



Scheme 11: The synthesis of an oxazoline

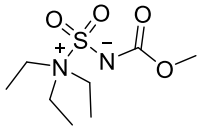
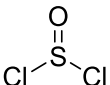
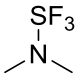


Scheme 12 : The mechanism of an amide to a nitrile by an E2 elimination

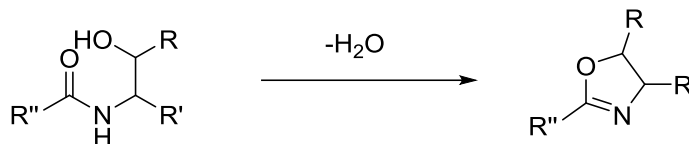
Methyl *N*-(triethylammoniumsulfonyl) carbamate, also known as the *Burgess reagent*, was discovered in 1968 by E. M. Burgess. It is a mild and selective dehydrating reagent often used in organic chemistry.²¹ This reagent is used in the dehydration of alcohols, preparation of nitriles from primary amides, and in the synthesis of heterocyclic compounds.

Thionyl chloride is an inorganic compound which is highly reactive. This reagent is used in chlorination reaction and can ease various chemical transformations. It converts alcohols to alkyl chlorides and can produce nitriles from amides through *E2* elimination mechanism.²² The base (e.g. H₂O) attacks the hydrogen (from the N-H amide bond). The N-H bond breaks and a new π bond is formed on the double bond (π , σ) making it form a triple bond (2π , 1σ). However, this can only occur, when the leaving group (LG) leaves. The LG in this case in order to form the nitrile is O=S=O-Cl, that leaves as sulfur dioxide gas (SO₂) which drives the reaction forward. This all takes place in one step, just like S_N2 reactions (**Scheme 12**).

Table 1: Different methods used to synthesize oxazoline

	Method #1	Method #2	Method #3
Dehydrating reagent	Burgess reagent 	SOCl ₂ 	Methyl DAST 
Solvent	THF	Neat \ DCM	DCM
Salt	-	-	K ₂ CO ₃
Conditions	Refluxed for 30 min, 12hrs, 24 hrs	Heated for 30 min at 45° C	Stirred for 1 hr at -78 °C
Yield	0%	12-14%	46%-99%

Methyl DAST (dimethylamino)sulfur trifluoride is a dehydrating reagent which has been used for the cyclodehydration of β -hydroxy amides to yield oxazolines (**Scheme 13**).²³

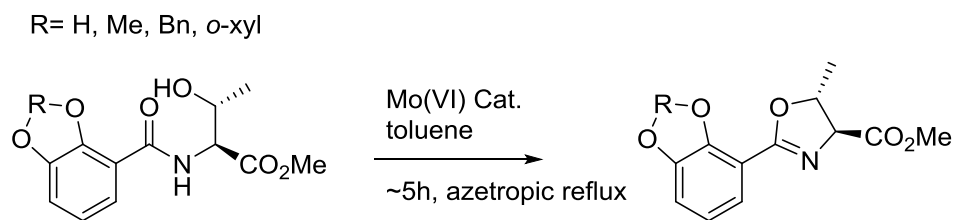


Scheme 13: Cyclodehydration of β -hydroxy amide to oxazoline

Out of the three dehydrating reagents, Methyl DAST gave the best yield of the product (**Table 1**). The Burgess reagent only gave the starting material (**3**), (**4**) after extended reaction times (up to 24 hours). This method failed, but worked well when *L*-Serine methyl/benzyl ester hydrochlorides were used. The reason for that could be the Burgess reagent is milder than the other two reagents. The thionyl chloride worked, but provided a low yield of the desired oxazoline. This is due to racemization that takes place on the oxazoline ring. Therefore, Methyl DAST was the main reagent used for preparing oxazolines from amides (**Scheme 11: Table 1: method 3**).

2.3.1 ((4*S*, 5*R*)-2-(*o*, *m*)-Dimethoxyphenyl)-5-methyl-4-oxazolinecarboxylic acid methyl ester (**5**)

Compound **5** was a colourless solid with a 46% yield after extraction and purification using flash column chromatography. ¹H and ¹³C-NMR chemical shift values were identical to the reported values stated by Sakakura *et al.* (**Figure A1.9 and A1.10**).²⁰



Scheme 14: Mo(VI)=O catalyst used to synthesize an oxazoline.²⁰

The method they used required Molybdenum (VI) oxide as a dehydrative cyclization catalyst which is shown in **Scheme 14**²⁰, whereas **Method 3** from **Table 1** was used instead. The molybdenum (VI) oxide was attempted twice but failed both times. This could be due to the fact

the Soxhlet extractor, as well as dry solvents and inert atmosphere were required. Methyl DAST however, was easier to use, the method was simple, and gave higher yields.

2.3.2 ((4*S*,5*R*)-2-(*o,m*)-Dimethoxyphenyl)-5-methyl-4-oxazolinecarboxylic acid benzyl ester (**6**)

Method 3 (Table 1) was used to synthesize (4*S*,5*R*)-2-(*o,m*)-Dimethoxyphenyl)-5-methyl-4-oxazolinecarboxylic acid benzyl ester (**6**). The by-products were removed by liquid-liquid extractions and the product was purified by flash column chromatography. This afforded the title product as a colourless oil in yields between 84% and 100%.

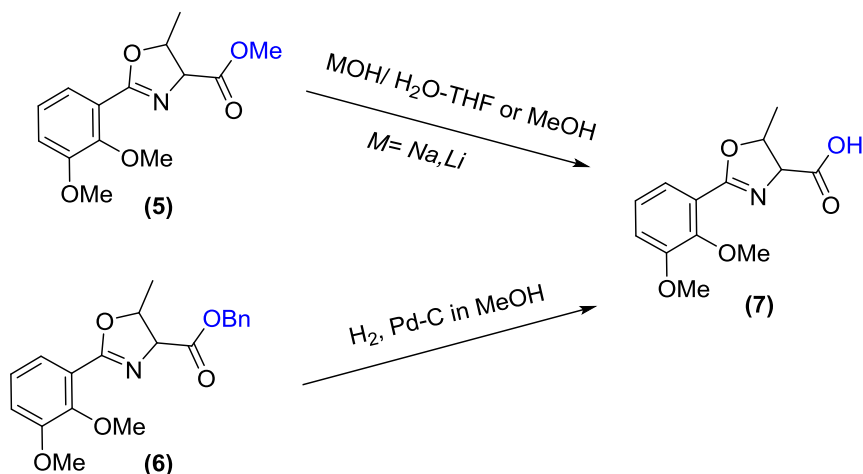
The ¹H-NMR spectrum (**Figure A1.11**) showed a doublet with a chemical shift (δ) 1.33 ppm integrating for three protons. This chemical shift was assigned to the methyl group on the oxazoline. The two singlets at δ = 3.86 and 3.87 ppm integrating for three protons each were assigned to the methyl protons of the methoxy group. The signal at δ = 4.99-5.04 ppm integrated for two protons, this was assigned to the protons on the oxazoline ring (the -CHs). The singlet at δ = 5.22 ppm was assigned to the -CH₂ of the benzyl functional group which integrated for two protons. The peaks observed at δ = 7.02 to 7.09 and 7.32 to 7.37 ppm were aromatic protons since they appeared in the aromatic region of the spectrum. The ¹³C-NMR (**Figure A1.12**) showed signal at δ = 16.10 ppm corresponding to the carbon atom of the methyl group that was bound to the oxazoline ring. The resonance signals observed at δ = 56.18 and 61.50 ppm were assigned to the methoxy carbons. The signal of the benzyl -CH₂ carbon was seen at δ = 66.94 ppm. The signals at δ = 71.67 and 77.55 ppm were assigned to the carbon atoms of the -CHs on the oxazoline ring. The signals at δ_c = 115.58, 122.44, 122.68, 123.87, 128.50, and 128.59 ppm were assigned to the aromatic carbons. The signals at δ = 128.73 ppm was assigned to the aromatic carbon that was bound to the carbon atom of the oxazoline moiety. The signal at δ = 135.33 ppm corresponds to the aromatic carbon of the benzyl functional group that was attached to the -CH₂. The peaks observed at δ = 148.92 and 153.42 ppm are assigned to the aromatic carbons that are bound to the methoxy functional groups. The signal at δ = 165.41 ppm correspond to the carbon

atom on the oxazoline attached to the nitrogen atom. Double bond and triple bond carbon atoms generally appear more downfield than single bonded carbon atoms. The last signal was at $\delta = 169.79$ ppm and that appeared as a carbonyl carbon of the ester functional group.

On the other hand, the compounds **5** and **6** were not stable for extended periods, they tend to ring open after two weeks in air. They are therefore usually sealed and stored in the fridge (-10°C to -20°C).

2.4 Deprotection of the Ester protecting group

Deprotection of the carboxylic acid usually involves saponification (under basic conditions). Bulky esters like benzyl esters may or may not be able to cleave under basic conditions, so they are generally removed by catalytic hydrogenation. That being said, simple methyl esters are regularly cleaved by base catalyzed hydrolysis using alkali metal hydroxides (e.g. NaOH, LiOH) in aqueous methanol or THF. In more complex compounds, it is suggested to use LiOH in a mixture of THF- H_2O or MeOH. Benzyl esters on the other hand are regularly cleaved under reductive conditions using anhydrous methanol with activated palladium on carbon and $\text{H}_2(\text{g})$. Therefore, deprotections are simple reactions, but the reason why deprotection is challenging is because some substrates and compounds are not compatible with the deprotection methods used. **Scheme 15** displays the reaction of the deprotection of compounds **5** and **6** from the first building blocks; **Table 2** and **Table 3** show the various methods and conditions taken to attempt the deprotection.¹⁷



Scheme 15 : Deprotection of methyl and benzyl ester from the 1st building block

From the series of attempts, the deprotection was unsuccessful for both **5** and **6**. Methyl ester compounds are stable compounds and are trouble-free protecting groups. Vigorous treatment is required in deprotection due to their high stability. Saponification is sometimes satisfactory but even when it is carried out under carefully controlled optimized conditions as the methods shown in **Table 2**, the alkali metals can cause side reactions or racemization. This is why when ¹H-NMR was performed for those reactions, each one resulted



Figure 2.4.1: Deprotection of Bn Ester using a balloon filled with H₂

in an unsuitable spectrum. The peaks were not resolved properly, it was difficult to say if a peak was a doublet or triplet because they all appeared as broad singlets. The aqueous layer of (**7**) from (**5**) was also checked because if the deprotection was successful, the compound becomes more polar which means more soluble in water than ethyl acetate. However, when spotted on TLC plate, no spot was shown under the UV lamp. Compound **7** would be UV active because there is an aromatic ring. The conditions were then altered by using different concentrations of HCl, where it was used to acidify the aqueous layer in order to protonate the oxygen. Additionally, the reactions for both **Methods 1** and **2** went for a longer period of time and were monitored by

TLC (**Table 2**). **Method 2**²⁴ was followed by a literature procedure by S. Banala *et al.* but the method was ineffective. Both methods were unsuccessful even when the conditions were modified.

Table 2: Attempts of deprotection of methyl ester using different methods

Method	Attempts	Solvent	Condition	Time	Product
1	4	MeOH	Methyl ester (5) in 1 mL MeOH and 1 mL of 0.5 N NaOH. This was stirred (<i>monitored by TLC</i>). Then add 1 mL of water and extract with Et ₂ O. Aqueous layer was acidified to pH=2 with HCl (6N, 1 M, 0.5 N) and extracted with EtOAc.	5 min – 2 hrs.	NO
2	2	THF- H ₂ O	1 eq of methyl ester (5) in 10 mL THF and H ₂ O (5 mL) and 2 eq LiOH•H ₂ O were added. Reaction stirred at RT. Then THF was removed. Aqueous layer was acidified to pH 2 with 5% HCl and extracted with EtOAc. Then the organic layer concentrated <i>in vacuo</i> .	1 hr – 2 hrs.	NO

Table 3: Attempts of deprotection of benzyl ester using different methods

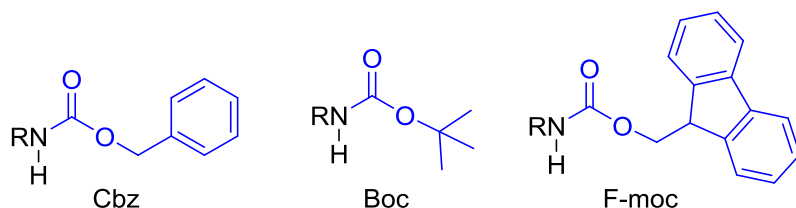
Method	Attempt	Solvent	Condition	Time	Product
1	8	MeOH	For every 0.1 mmol of Bn ester (6) add 10 mg of Pd/C and 1mL of MeOH with H ₂ bubbling through the solution (<i>balloon/directly from tank</i>). Once it was complete (<i>monitored by TLC</i>). The mixture was filtered through celite and concentrated <i>in vacuo</i> .	1 – 6 hrs.	NO
2	3	ACN	0.5 mL of ACN in 10 mg of Bn ester (6). Add 1 mL of 1 M LiOH and stir at RT (<i>monitoring by TLC</i>). Add 1 mL of water and extract with Et ₂ O. To the aqueous solution add buffer 4 solution till the reaction is pH 4. Then extract with EtOAc, and the organic layer is left to evaporate.	30 min – 2 hrs.	NO

Removing the benzyl ester from (**6**) was challenging. It was expected that the benzyl ester could be easily cleaved by catalytic hydrogenolysis. However, the reaction failed more than once, as can be shown in **Table 3**. The reason for that could be due to short reaction time at 1 atm, the reaction needed to be under a higher pressure (>1 atm), and/ or the slight impurities in compound **6** can interfere with the deprotection.

A balloon was first filled with $H_2(g)$ since there was less than 200 milligrams of the compound (**Figure 2.4.1**). After a couple of trials, $H_2(g)$ was then bubbled directly through the mixture. However, the regulator on the hydrogen tank was not functioning properly since $H_2(g)$ was constantly bubbling on and off throughout the reaction. From 1H -NMR, the benzyl group did not cleave. As this method was causing difficulties, it was decided to do it under basic conditions analogous to the deprotection of the methyl ester but instead a buffer (pH 4) is used (**Table 3: Method 2**). The buffer is used to allow the aqueous layer to not reach a pH 2, as it can be too acidic; oxazolines are sensitive to acid. Therefore, the phosphate buffer (pH 4) was prepared with 1M trisodium phosphate and phosphoric acid. Therefore, the deprotection of the ester from the first building block has been unsuccessful, which has prevented the synthesis of Photobactin.

2.5 Synthesis of the Benzamide: Part I

The most common protecting groups for amines are carbamates such as Cbz, Boc, and F-moc (**Figure 2.5.1**). Boc (*i.e.*, *tert*-butoxycarbonyl) is widely used in synthetic organic chemistry for

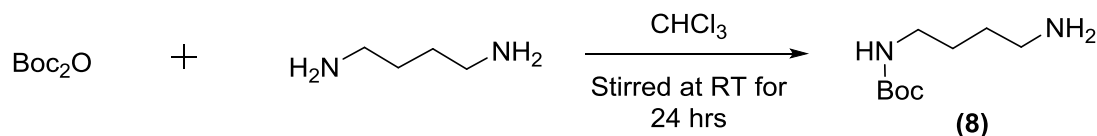


protecting NH_2 groups and it is unreactive to most bases and nucleophiles. This protecting group is used in this thesis

Figure 2.5.1: Common protecting groups for amines

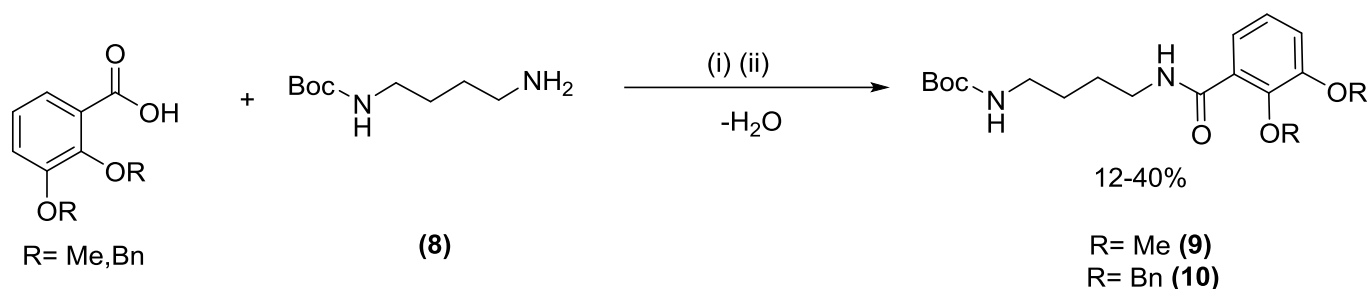
as one of the ways to synthesize the second building block. If Boc group was not used, side reactions, such as forming dimers can happen. *N,N'*-Bis(2,3-bis(methoxy)benzoyl)-1,4-diaminobutane can be formed because 1,4-diaminobutane is a symmetrical compound as a result

the amine group is identical on both sides of the molecule. This means both amines on the compound will attack the electrophile, which is why Boc protecting group are generally added to the amine (on one side) using di-tert-butyl dicarbonate (Boc_2O), shown in **Scheme 16**.



Scheme 16: Synthesis of Boc-1,4-diaminobutane (**8**)

The reaction in **Scheme 17** is straightforward and is a one pot synthesis. This reaction forms a benzamide compound as the product by using carbodiimide coupling reagent - EDC·HCl.



Scheme 17: (i) DCM, HOBt, Et_3N , EDC·HCl (ii) stirred O/N, under N_2 , RT, 12-40%

2.5.1 Boc-1,4-diaminobutane (**8**)

The compound was a pale yellow coloured thick liquid isolated after gravity filtration similar to the commercially available one bought from Sigma Aldrich. ^1H -NMR chemical shift values were analogous to the reported values stated in the Spectral Database of Organic (**Figure A1.13**).²⁵

2.5.2 N-Boc (1,4-aminobutyl)-2,3-(dimethoxyphenyl) benzamide (**9**)

N-Boc (1,4-aminobutyl)-2,3-(dimethoxyphenyl) benzamide (**9**) was synthesized by an amide coupling reagent EDC·HCl (**Scheme 17**). The impurities and by-products were removed by extraction and flash column chromatography. This method gave a 25% yield of the target compound after purification as a yellow coloured solid. The ^1H -NMR spectrum (**Figure A1.14**)

showed a singlet at $\delta = 1.42$ ppm integrating for nine protons. This was assigned to the methyl of the Boc group. Overlapping signals at $\delta = 1.62$ ppm was assigned to two of the $-\text{CH}_2$ of the compound, because the broad signal integrates for four protons. The multiplet at $\delta = 3.15 - 3.18$ ppm and the doublet of doublets at $\delta = 3.47$ ppm was assigned to the remaining $-\text{CH}_2$ units, each integrating for two protons each. The singlet at $\delta = 3.89$ ppm integrated for six protons corresponding to the protons of the methoxy group. The peak at $\delta = 4.61$ ppm corresponded to the amine proton which integrated for one. The signal at $\delta = 7.03, 7.14, \text{ and } 7.67$ ppm were doublet of doublets. These signals corresponded to the aromatic protons and each integrating for one proton. The broad signal at $\delta = 7.99$ ppm was assigned to the other amine proton, integrating for one. The ^{13}C -NMR (**Figure A1.15**) showed signal at $\delta_{\text{C}} = 27.00, 27.62, 33.71, \text{ and } 39.27$ ppm which were assigned to the carbon atoms of the four methylene units in the chain. Signal at $\delta = 29.68$ ppm corresponded to the methyl carbons of the Boc group. The methoxy carbons were observed at $\delta = 56.19$ ppm and 61.28 ppm. The signals at $\delta = 115.26, 122.79, \text{ and } 124.44$ ppm were assigned to the unsubstituted aromatic carbons. The signal at $\delta = 126.84$ ppm corresponded to the ipso carbon of the aromatic ring bound to the carbonyl group. The aromatic carbons (*ipso carbons*) that were bound to the methoxy group were seen at $\delta = 147.39$ and 152.55 ppm. Last but not least, the two carbonyl carbons were both shown at $\delta = 162.55$ and 165.21 ppm.

Elemental analysis is in agreement with the expected structure, where the “found” values were analogous within experimental error to the “calculated” values (see Experimental Section)

2.5.3 *N*-Boc(1,4-aminobutyl)-[2,3-bis(benzyloxy)phenyl]benzamide (**10**)

N-Boc(1,4-aminobutyl)-[2,3-bis (benzyloxy)phenyl]benzamide (**10**) was synthesized following the procedure shown in **Scheme 17**. The urea byproduct that is formed during the reaction is soluble in water and can be removed by extraction. The product was purified by flash chromatography which gave the title material as a yellow coloured solid with a 40% yield.

The ^1H -NMR (**Figure A1.16**) was analogous to the product *N*-Boc(1,4-aminobutyl)-2,3-(dimethoxyphenyl)benzamide except that there were no methoxy groups. The signals at $\delta = 5.09$ and 5.16 ppm integrated for two protons each, were assigned to the protons of $-\text{CH}_2$ of the two benzyl groups. The signals at $\delta = 7.15$ ppm to 7.75 ppm were the aromatic protons from the benzyl groups and the benzamide. This region integrated for a total of 13 protons. The last signal at $\delta = 7.95$ ppm was assigned to the amine proton that integrated for one proton.

Elemental analysis is in agreement with the expected structure (see Experimental Section).

2.6 Deprotection of Boc Protecting Group

Boc protecting groups are generally removed by using mild acidic conditions such as TFA, either neat or in DCM, and HCl in either MeOH or EtOAc. From different scientific journals and organic chemistry textbooks,^{26,27,28} many different attempts have been made to cleave Boc protecting group from compound **10**.

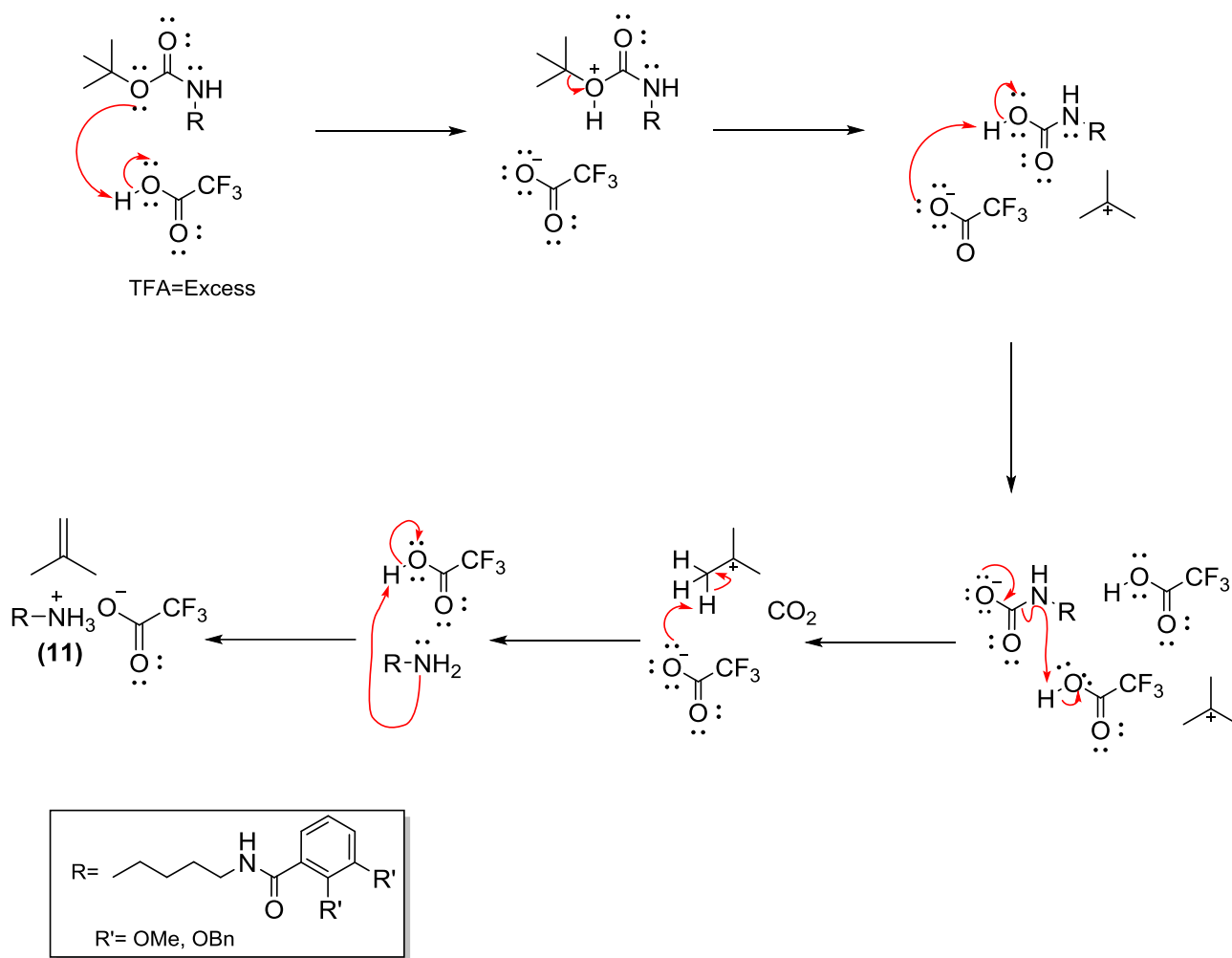
Table 4: Different methods used to cleave Boc

Deprotecting Agent	Solvent	Time	Condition	Product
Water ²⁶	DCM	8hrs	Air, Reflux	NO
	1,4-dioxane	O/N	N ₂ , Reflux	NO
Bu ₄ NF ²⁷	Dry THF	8hrs	Air, Reflux	NO
HCl (conc.)	MeOH	1-3 min	Air, RT	NO
TFA (1 eq)	DCM	10,30 min	Air, RT	NO
	DCM (1eq)	1-3 min	Air, 0°C	YES 60%

Table 4 displays the different methods used to remove the Boc group. Boc removal was conveniently carried out by the dissolution in TFA.²⁸ Therefore, the only method that was successful was using one equivalent of TFA in one equivalent of DCM.²⁸ The mechanism of the deprotection of Boc using TFA is shown in **Scheme 18**, where the by-products were carbon

dioxide and isobutene. ^1H -NMR displayed that the t-butyl from Boc was not there at $\delta = 1.44$ ppm (**Figure 2.6.1**). This concluded that the Boc protecting group was cleaved from the benzamide compound. Initial attempts at dilute TFA concentration were unsuccessful as having an excess of DCM prevented Boc cleavage.

When HCl and Bu_4NF (*i.e.*, tetrabutylammonium fluoride) were used, starting material was retrieved and the Boc group was still present. As the “green method” alternative water was used as a deprotecting agent. At elevated temperatures of $150 - 275\text{ }^\circ\text{C}$, water can be used as a catalyst and reaction solvent in the removal of Boc protecting group.²⁶ However, the method was unsuccessful after several of attempts and ^1H -NMR analysis did not support the formation of the target compound. The chemical shifts and the integrals did not match with the proposed compound.



Scheme 18: General mechanism of deprotection of Boc

2.6.1 1,4-aminobutyl)-[2,3-bis (benzyloxy)phenyl]benzamide (**11**)

One equivalent of TFA with one equivalent of DCM was used to successfully deprotect the Boc group. This gave a white solid with a 60% yield. $^1\text{H-NMR}$ analysis of the product indicated the presences of impurities, as one can see in **Figure 2.6.1**. Comparing the two $^1\text{H-NMR}$ spectra (**Figure 2.6.1**), the peak at $\delta = 1.45$ ppm integrated for nine protons was assigned to the $-\text{CH}_3$ of the *t*-butyl group was not present in **Figure 2.6.1** (top), that indicated the Boc group was removed from the compound. The slight shifts in $^1\text{H-NMR}$ also shows that it was not identical to the starting

material (**10**). The reactive nature of TFA made it hard for purification to be successful. Hence, the spectrum (**Figure 2.6.1: top**) was quite chaotic. This made it extremely complicated to assign peaks and integrate due to the fact that very little product was obtained to run $^1\text{H-NMR}$, and product may have been lost during extraction.

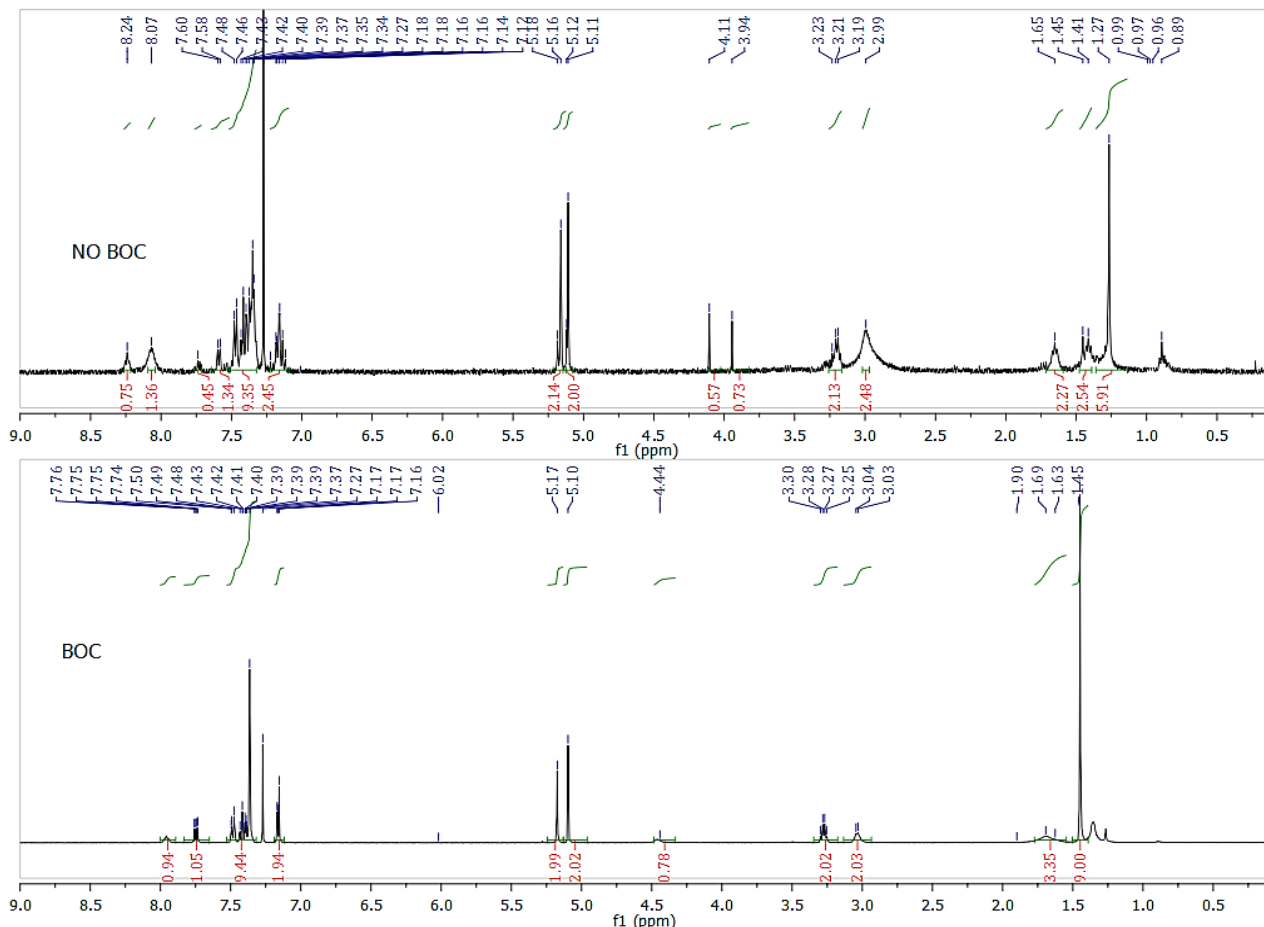


Figure 2.6.1: Comparing $^1\text{H-NMR}$ of Boc (**10**) and No Boc (**11**)

2.7 Synthesis of the Benzamide: Part II

The starting material Boc-1,4-diaminobutane (**8**) was expensive to purchase, synthesizing was time consuming, and having to deprotect it was problematic. It was decided to synthesize the second building block without needing to protect the NH_2 group with Boc. Since it is an amide synthesis, amide bond formation was prepared in several

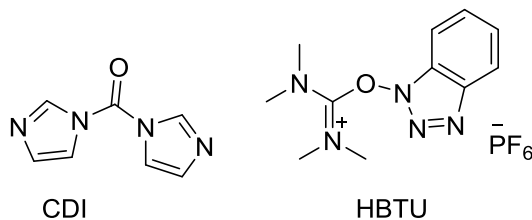
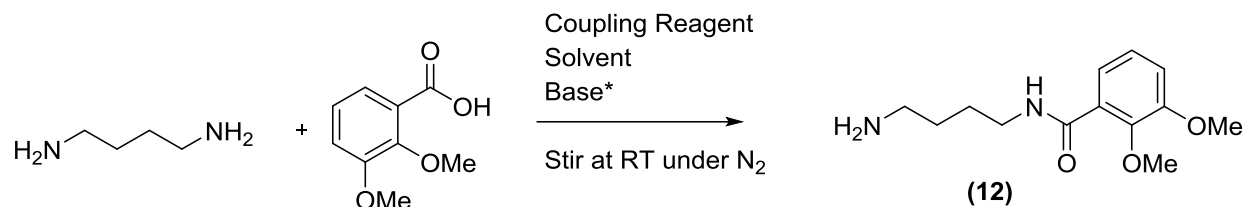


Figure 2.7.1: Structure of CDI and HBTU

ways using coupling reagent or acid chloride (using SOCl₂). Different types of coupling reagents were used such as CDI, EDC·HCl, HBTU, and DMTMM (**Scheme 19** and **Table 5**).



*not always added

Scheme 19: Synthesis of *N*-(2,3-dimethoxybenzoyl)diaminobutane (**12**) using a coupling reagent

CDI (*i.e.* *N,N'*-carbonyldiimidazole) (**Figure 2.7.1**) and DMTMM (*i.e.*, 4-(4,6-Dimethoxy-1,3,5-triazin-2-yl)-4-methylmorpholinium chloride) (**14**) is a one pot coupling procedure. These two coupling agents do not require additional base.¹⁹ CDI reagent is usually used on a large scale and DMTMM is effective coupling agent for ester, amide, and peptide synthesis. HBTU (*N,N,N',N'*-Tetramethyl-*O*-(1*H*-benzotriazol-1-yl)uronium hexafluorophosphate) (**Figure 2.7.1**) and EDC·HCl (*N*-(3-dimethylaminopropyl)-*N'*-ethylcarbodiimide hydrochloride) are also a one-pot synthesis but require base (triethylamine: Et₃N). The driving force is the making of the by-product – urea derivative.¹⁹

Table 5: Reaction conditions for *N*-(2,3-dimethoxybenzoyl)-1,4-diaminobutane synthesis

Coupling Reagent	Base	Solvent	Mole ratio	Condition	Product
CDI	-	DCM, THF, MeOH	1:1, 2:1	Stirred O/N at RT under N ₂	NO
EDC·HCl	Et ₃ N	DCM	1:1	Stirred O/N at RT under N ₂	NO
HBTU	Et ₃ N	DCM	1:1.1, 2.5:1, 5:1	Stirred 19 hrs at RT under N ₂	NO
DMTMM	-	MeOH, THF, DCM	1.1:1, 2.5:1	Stirred 19 hrs at RT under N ₂	YES (9%)

*1,4-diaminobutane usually in excess

CDI did not work as a good coupling reagent to synthesize the second building block. The solvent MeOH and THF did not dissolve the starting materials fully. DCM was a good solvent since both starting materials (1,4-diaminobutane and 2,3-dimethoxy benzoic acid) dissolved. However, after the liquid-liquid extraction, the organic layer did not have the product. There was nothing shown in the aromatic region in $^1\text{H-NMR}$ spectrum. There was also a lot of by-product (*imidazole*) in the organic layer which was difficult to remove.

EDC·HCl worked well to synthesize the amide for the first building block but did not succeed in synthesizing the second building block. $^1\text{H-NMR}$ spectrum was very messy, and came to a conclusion that the two starting materials never coupled together. Carbodiimides are mild amide coupling reagents, which is the reason why EDC·HCl did not work this time. An even more efficient, expensive, and exotic coupling reagent is HBTU.

HBTU coupling reagent gave a clean $^1\text{H-NMR}$ spectrum, however the product formed *N,N'*-Bis(2,3-bis(methoxy)benzoyl)-1,4-diaminobutane (**13**, **Figure 2.7.2**) and not the title compound. Similar result happened when the acid chloride reaction took place following the same reaction as **Scheme 19** with the same conditions from **Scheme 10** (a).

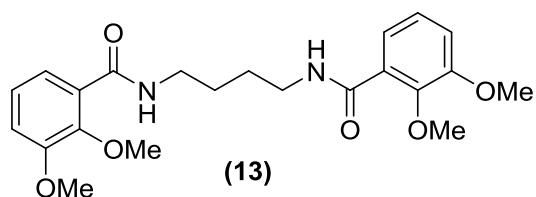
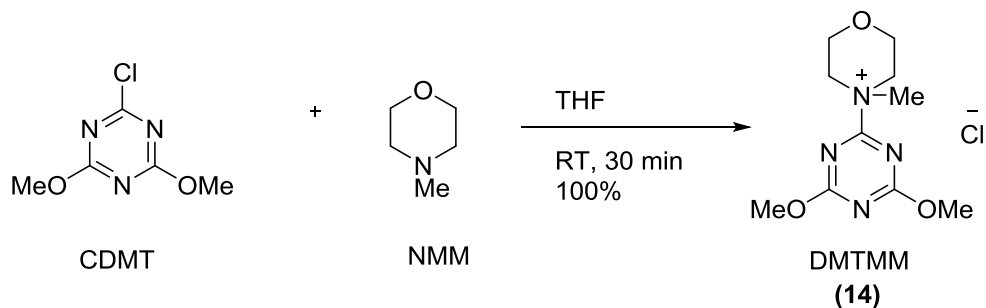


Figure 2.7.2: Compound **13** is formed when using HBTU or SOCl_2



Scheme 20: Synthesis of DMTMM (**14**)

DMTMM (**14**) (**Figure A1.22**) was first synthesized (**Scheme 20**) and then used as a coupling reagent. Compound **14** is stable in MeOH and THF, and that is why those were the solvents used first in the reaction (**Scheme 19**). DMTMM has been reported to decompose in DCM after three hours.²⁹

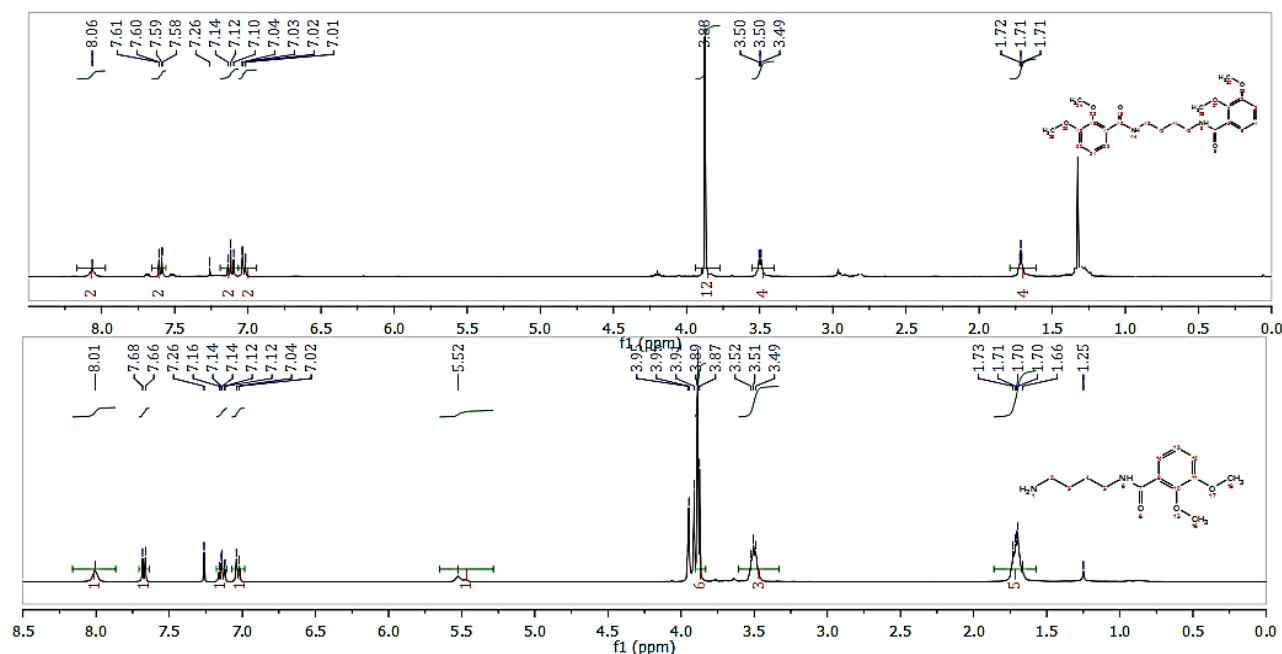


Figure 2.7.3: Compound **13** (top spectrum - using HBTU) Vs Compound **12** (bottom spectrum-using DMTMM) in CDCl_3

However, the synthesis failed when the solvent THF or MeOH were used, due to the poor solubility of the starting materials. DCM was then used and the product was successfully synthesized with only few impurities (**Figure A1.17**). The comparison between the actual compound **12** and compound **13** is shown in **Figure 2.7.3**.

2.7.1 *N*-(2,3-dimethoxybenzoyl)-1,4-diaminobutane) (**12**)

The triazinone (4,6-dimethoxy-1,3,5-triazin-2(1*H*)-one) by-product was separated from the product by flash chromatography (eluting with only ethyl acetate) and preparative TLC. This gave a white solid with a 9% yield as the title product using DMTMM. ^1H -NMR (**Figure A1.17**) analysis of *N*-(2,3-dimethoxybenzoyl)-1,4-diaminobutane) in CDCl_3 showed a signal at $\delta = 1.73$ to 1.66 ppm which integrated for five protons. The multiplet at $\delta = 3.52$ -3.49 ppm integrated for three

protons. Both peaks were assigned to the -CH₂ of the 1,4-diaminobutane moiety. The broad peak at δ = 5.52 ppm was assigned to the amine proton. The doublet at δ = 7.03 ppm and 7.67 ppm integrated for one proton each. The doublet of doublets at δ = 7.14 ppm integrated for one proton. These were assigned to the aromatic protons of the product. The broad peak at δ = 8.01 ppm was assigned to the amine proton integrating for one proton. 2D-NMR was performed (COSY, HSQC, HMBC) and this confirmed the title product was synthesized successfully (**Figure A1.18, A1.19, A1.20**). However, ¹H-NMR indicated there was still some triazinone even after the purification step. The peak at δ = 3.95 ppm was assigned to the protons of the methoxy groups in the by-product. The percent yield was very low because the product may be lost during the purification step (*flash chromatography and prep TLC*). Also, two compounds were produced in this reaction using DMTMM, which were compounds **12** and **13** that was why the desired product obtained was very small.

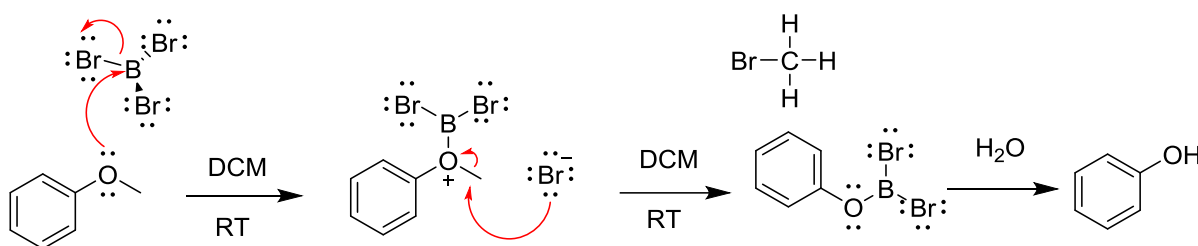
2.7.2 *N,N'*-Bis(2,3-bis(methoxy)benzoyl)-1,4-diaminobutane (**13**)

Unfortunately, (**12**) was unable to be synthesized using thionyl chloride and/or HBTU. However, the reaction produced a byproduct instead (**Figure 2.7.1**). Compound **13** was isolated in poor yields but was useful for further study. The two studies that were completed with compound **13** were: (i) the demethylation of the methyl aryl ether and (ii) its binding properties with Fe (III). The binding studies were performed using UV-Vis, and computational calculations (*e.g. DFT*) were performed using Spartan 10' (Shown in **Section 2.11**). The reason these studies were conducted is because the compound **13** is a catechol compound and catechol derivatives have been a great interest to many scientists, since they act as a chelating ligand in siderophores (*e.g. Photobactin, Enterbactin, etc*).

N,N'-Bis(2,3-bis(methoxy)benzoyl)-1,4-diaminobutane (**13**) is a white crystal line compound with a 27% yield. ¹H-NMR (**Figure A1.21**) chemical shift values were identical to the reported values stated by K. Winstanely and D. Smith.³⁰

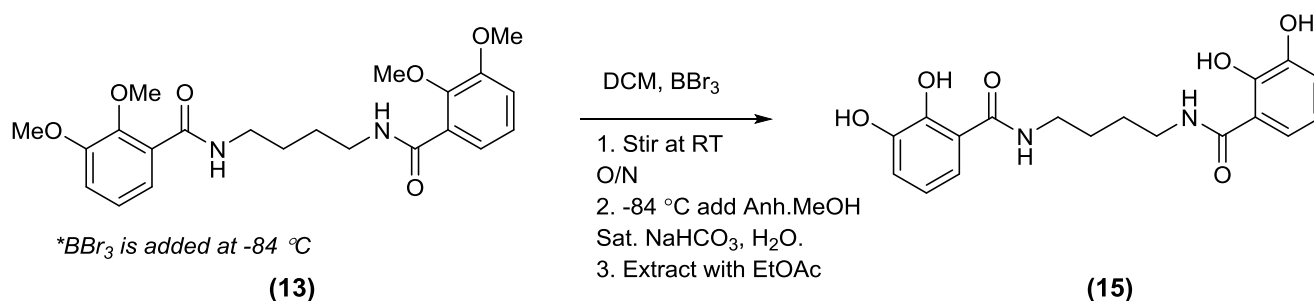
2.8 Demethylation Using BBr₃

Demethylation is the removal of a methyl group from a molecule. Boron tribromide (BBr₃) is the most effective reagent used for cleaving methyl aryl ethers. This reagent was used to demethylate the methoxy groups on compound **13** shown in **Scheme 22** as a test trial. The mechanism of methyl aryl ether demethylation (**Scheme 21**) continues through the formation of a complex between the boron and the ether oxygen followed by the removal of bromomethane to yield dibromophenoxyborane. The dibromophenoxyborane undergoes hydrolysis to produce phenol, boric acid, and hydrogen bromide as the products.³¹



Byproducts : bromomethane, boric acid, and hydrogen bromide

Scheme 21: Mechanism of demethylation using BBr₃



Scheme 22: Demethylation of compound **13**

2.8.1 *N,N'*-Bis(2,3-dihydroxybenzoyl)-1,4-diaminobutane (**15**)

N,N'-Bis(2,3-dihydroxybenzoyl)-1,4-diaminobutane was synthesized by deprotecting the methoxy groups using boron tribromide shown in **Scheme 22**. Water was added to the reaction flask after the reaction was complete at -84 °C until addition no longer caused the evolution of HBr. Methanol

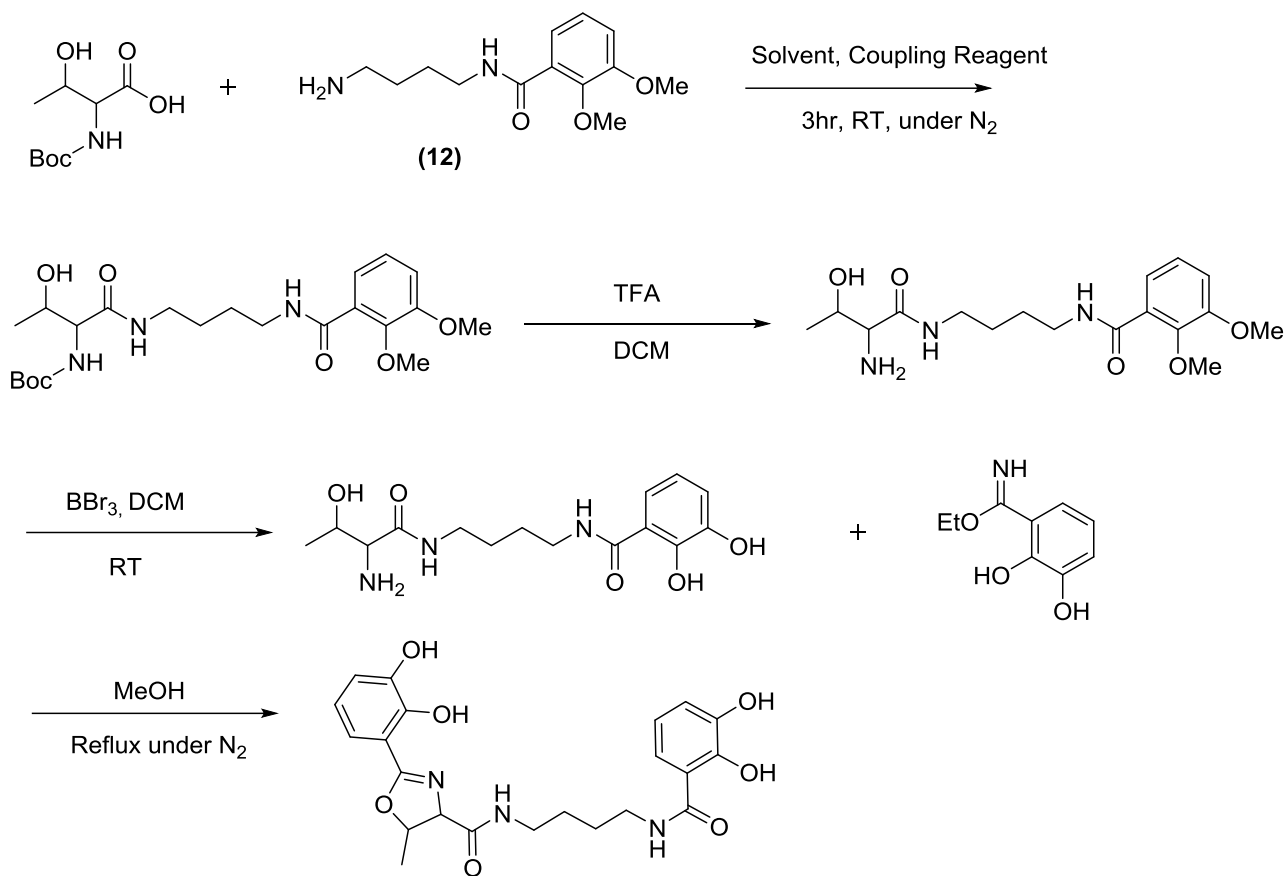
was then added to remove boron impurities such as boric acid and bromomethane. No purification was needed and gave a whitish-grey solid with a 77% yield.

$^1\text{H-NMR}$ (**Figure A1.23**) is consistent with data previously reported by K. Winstanley and D. Smith.³⁰ The NMR chemical shift are shifted slightly (*downfield*) because CD_3OD was used while the reported $^1\text{H-NMR}$ was in $\text{DMSO-}d_6$. Since CD_3OD was used, the hydroxyl ($-\text{OH}$) and amine protons ($-\text{NH}$) were not observed on the spectrum. $\text{MeOH-}d_4$ exchanges out the exchangeable protons from hydroxyl, amine, or amide protons with deuterium. This compound was only soluble in CD_3OD and insoluble in CDCl_3 and acetone- d_6 .

N,N'-Bis(2,3-dihydroxybenzoyl)-1,4-diaminobutane (**15**) displayed a UV-Vis spectrum typical for catechol ligands with an absorbance peak (λ_{max}) at 318 nm resulting from the π - π^* transition (**Figure A2.1**). The catechol ligand absorb near Ultraviolet light ($\lambda = 300\text{-}400\text{ nm}$)¹⁷ and the molar absorptivity at 318 nm was calculated to be $677\text{ M}^{-1}\text{cm}^{-1}$.

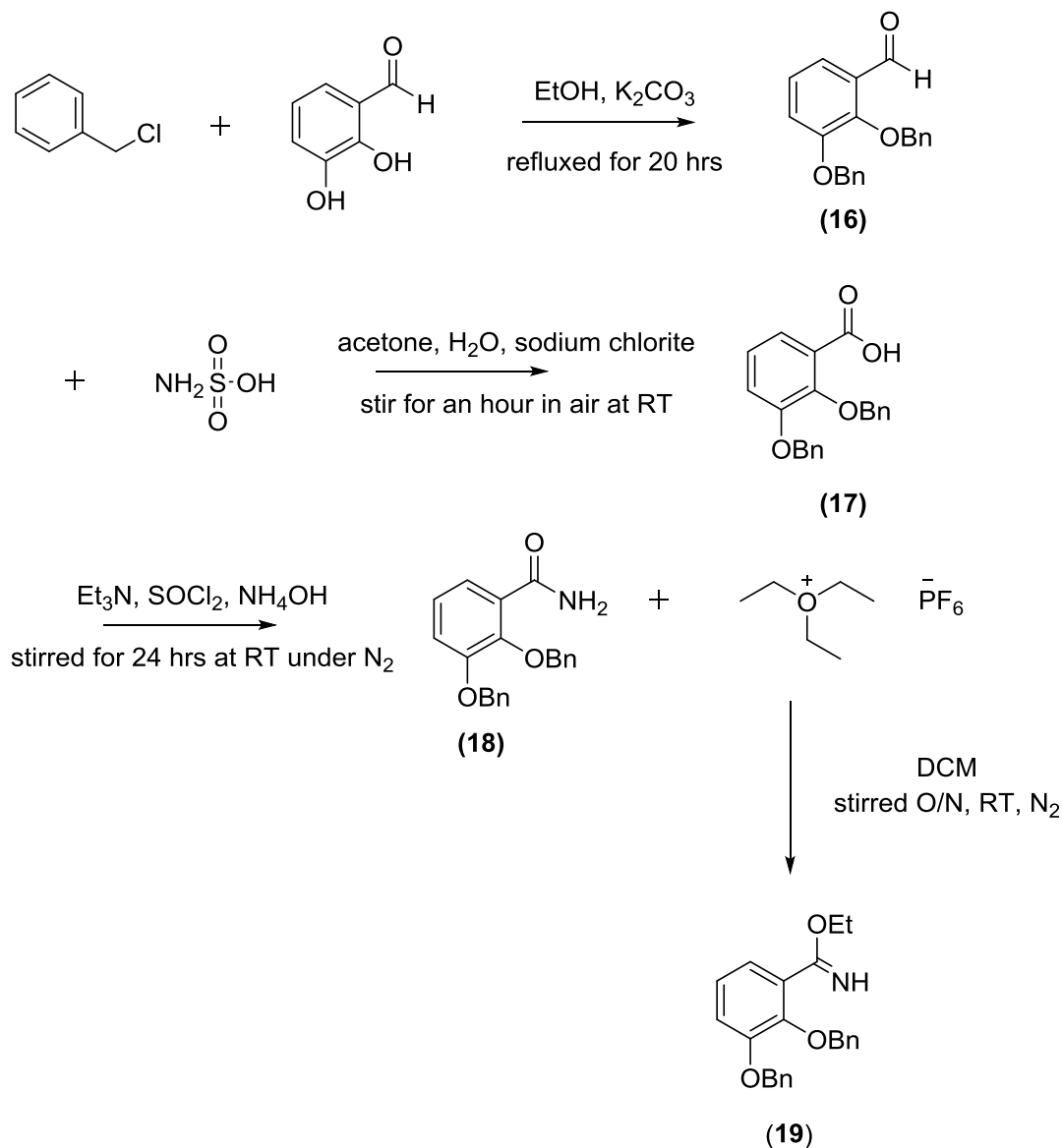
2.9 Alternative Route

The main method taken to attempt to synthesize Photobactin is presented in **Scheme 7**, while this was being done, an alternative approach was also taken. This required synthesizing the oxazoline in the final step rather than in the beginning steps. The alternative procedure is shown in **Scheme 23**, and was inspired by the work of R. Bergeron, J. Garlich, and J. McManis.³²



Scheme 23: An alternative approach to synthesize Photobactin

Boc-*L*-Threonine couples to compound **12** using a coupling reagent such as DMTMM, HBTU, or EDC·HCl. The Boc is then cleaved using TFA and the methyl aryl ethers are deprotected using BBr₃. The final step is the cyclization to produce the oxazoline, which occurs by adding ethyl 2, 3-dihydroxybenzimidate in the reaction flask with methanol and refluxing under nitrogen for approximately 24 hours, is intended to afford Photobactin (**Scheme 23**).



Scheme 24: The synthesis of ethyl 2,3-dihydroxybenzimidate (**19**)

The ethyl-2,3-bis(benzyloxy) benzimidate (**19**) was synthesized followed by a literature procedure, which is shown in **Scheme 24**.³³ In the last step of **Scheme 24**, compound **18** with triethyloxonium hexafluorophosphate which acts as a catalyst activating agent afforded an imine compound (**19**). ¹H-NMR chemical shifts for compounds **16** to **19** were consistent with data reported (**Figure A1.24-A1.27**).^{33,34} The final step is then removing the benzyl group by catalytic

hydrogenation using activated Palladium on carbon with H₂ to afford ethyl-2,3-dihydroxybenzimidate, which would be used in **Scheme 23** for the cyclization step.

The attempt to couple the Boc-*L*-Threonine with compound **12** was not successful. The coupling reagent used was DMTMM. However, ¹H-NMR spectrum showed only starting materials. This could be due to the fact that DMTMM is not a good coupling reagent for this type of reaction or the by-product of the compound **12**, triazinone, could have interfered with the reaction. Either way, another coupling reagent can be used such as HBTU or EDC·HCl, since they are both one pot synthesis, and may work more effectively than DMTMM.

2.10 Analogue of Photobactin

The analogue of Photobactin is mainly different from the first building block (*oxazoline acid*). Compound **21** was prepared using strategy equivalent to that employed for the total synthesis of Mycobactin S (**Scheme 25**).¹⁵ Compound **21** is incorporated in Mycobactin S, Transvalencin Z, and Parabactin. **Figure 2.10.1** displays the difference between the two Photobactin structures. The oxazoline fragment cyclized easier with the *L*-Serine methyl ester than with *L*-Threonine

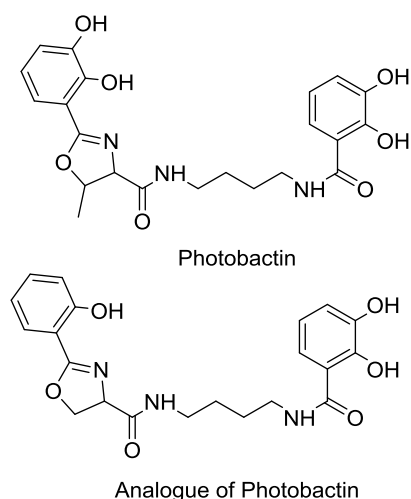


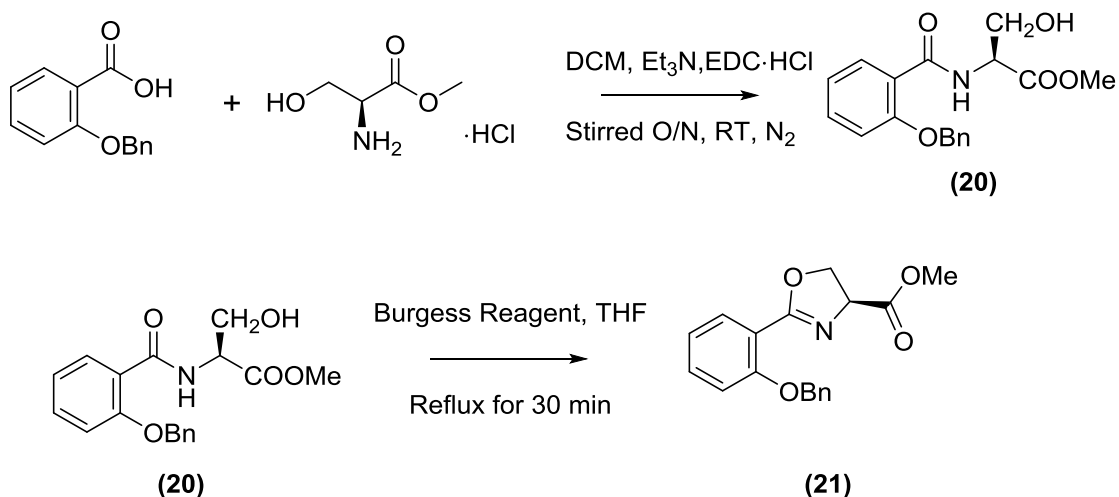
Figure 2.10.1: Structure of Photobactin and the analogue of Photobactin

methyl ester. The Burgess reagent was used to synthesize compound **21**, which is a milder dehydrative reagent than Methyl DAST. Compounds **5** and **6** were not able to synthesize when using the Burgess reagent, this can be due to the extra -OH / -OMe on the phenyl moiety and the -CH₃ group on the *L*-Threonine.

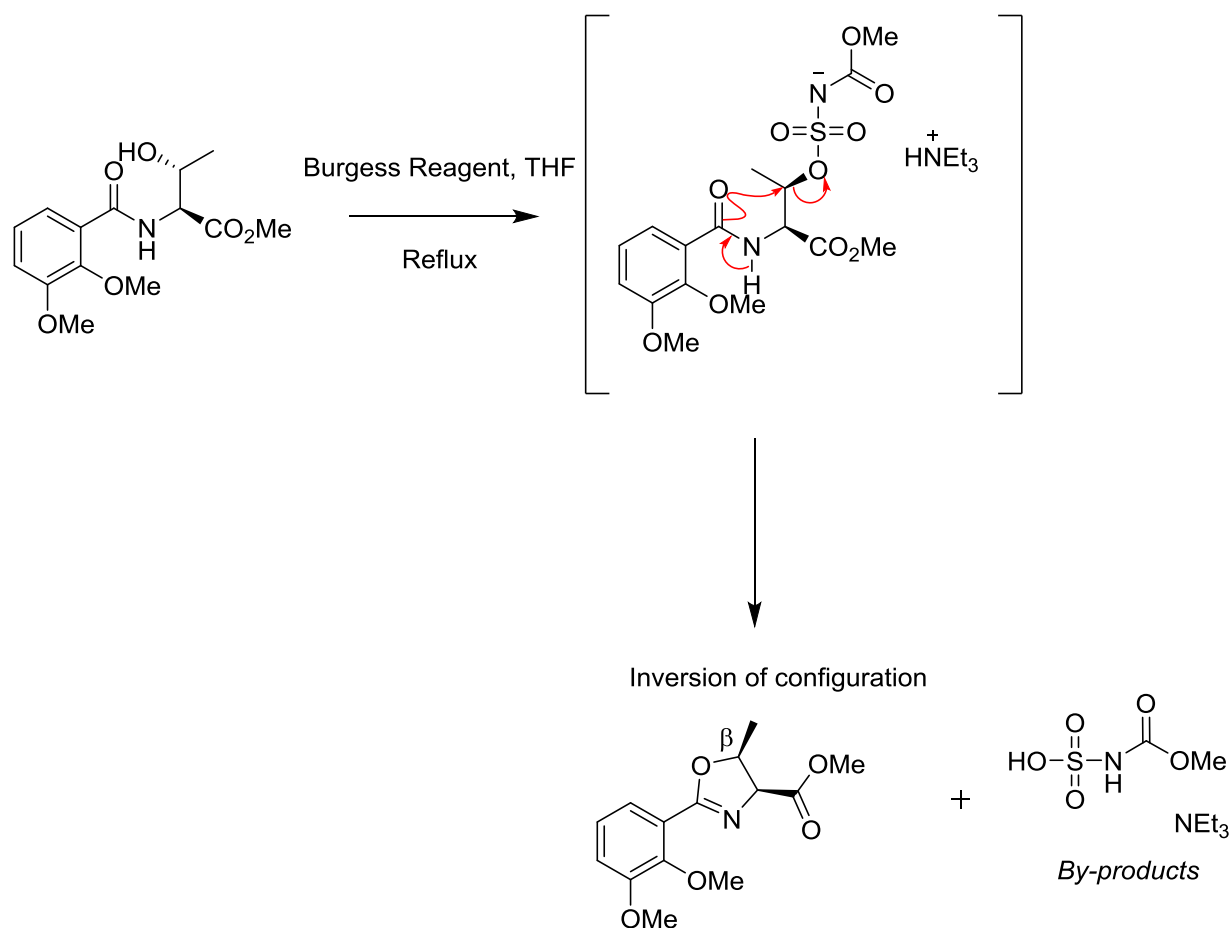
The -CH₃ group on the *L*-Threonine residue can affect cyclization when using the Burgess reagent because invertive cyclization arises at the β-position (**Scheme 26**), which may require a

longer reaction time (> 24 hrs). Also, having two -OMe / -OH on the phenyl makes it much more challenging for cyclization to occur, than having simply one of such groups.

On the other hand, several dehydrating reagents promote the dehydrative cyclization of the amide (*L*-Threonine residue) as mentioned in **Section 2.3**. It is debatable, which dehydrative reagent (e.g. Burgess reagent, Methyl DAST, thionyl chloride) proceeds with an inversion of configuration (*stereochemistry*) at the β -position of the *L*-Threonine residue. Methyl DAST can proceed in an inversion configuration, but it is not definite. If that is the case, *L-allo*-Threonine is required to be used as a substitute in order to prevent inversion.



Scheme 25: Synthesis of compound **21** via Burgess reagent



Scheme 26: Using Burgess reagent to yield an oxazoline

2.10.1 *N*-[2-(benzyloxy)benzoyl]-L-Serine methyl ester (**20**)

Compound **20** was isolated as yellowish-white coloured crystals with a 30% yield after recrystallization with toluene.

The ¹H-NMR spectrum showed (**Figure A1.29**) a singlet with a chemical shift at $\delta = 3.66$ ppm integrating for three protons. This signal was assigned to the methyl group. The multiplets at $\delta = 3.84$ -3.89 ppm and at $\delta = 4.80$ -4.82 ppm were assigned to the -CH₂ and -CH of the amide moiety. The singlet at $\delta = 5.21$ ppm which integrated for two protons was assigned to the -CH₂ of the benzyl functional group. The signals at $\delta = 7.07$ -7.47, and 8.16 ppm were assigned to the aromatic

protons that integrated for nine protons. The doublet at $\delta = 8.74$ ppm was assigned to the amide proton.

2.10.2 (S)-Methyl-2-[2-Benzyloxy)phenyl]-1,3-oxazoline-4-carboxylate (**21**)

(S)-Methyl-2-[2-Benzyloxy)phenyl]-1,3-oxazoline-4-carboxylate (**21**) was synthesized following **Scheme 22**. Compound **21** was a yellow coloured oil with a 60% yield. The $^1\text{H-NMR}$ spectrum (**Figure A1.30**) showed a singlet with a chemical shift (δ) at 3.83 ppm integrating for three protons. The multiplet at $\delta = 4.57$ -4.62 ppm was assigned to the $-\text{CH}_2$ on the oxazoline ring, integrating for two protons. The doublet of doublets at $\delta = 4.99$ ppm was assigned to the $-\text{CH}$ which integrated for one proton on the oxazoline ring. The singlet at $\delta = 5.21$ ppm integrates for two protons and was assigned to the $-\text{CH}_2$ of the benzyl functional group. The nine aromatic protons were shown at $\delta_{\text{H}} = 7.01$, 7.31-7.53, and 7.82 ppm.

2.11 Binding Studies with Fe^{3+}

Binding studies were conducted through UV-Vis and computational chemistry using Spartan'10. The spectroscopic investigation of the binding between Fe^{3+} and the simple material (**15**) was undertaken as a guide, and for training purposes, with the later intention of using similar techniques with Photobactin. Compound **15** displayed a UV-Vis spectrum typical for catechol^{7,13,14} seen in siderophores, with an absorption peak at 318 nm resulting from a π - π^* transition of catechol siderophore (**Figure A2.1**). Upon the addition of FeCl_3 , two absorption peaks were observed, 319 nm and 572 nm, and the solution turned from colourless to bluish-purple (**Figure A2.1**). An absorption peak at 319 nm was assigned to a ligand-to-metal charge transfer (LMCT) band characteristic for Fe^{3+} tetrahedrally coordinated complex. In addition, the broad absorption peak at 572 nm was assigned to the spin forbidden d-d transition.⁶ This suggested that the siderophore was isolated mainly in the iron-free form and formed a complex with iron (Fe^{3+}) upon the addition of iron. Therefore, in LMCT for d^5 complex, there are two absorptions bands one near 250 nm and the other near 600 nm which correlates to **Figure A2.1**. The binding constant was

calculated from carrying out UV-Vis. The binding (*formation*) constant for compound **15** is (K) 421, which is common. The higher the binding constant, the stronger the interaction between the ligands and the metal ion (e.g. Fe^{3+}) which is mentioned in **Section 1.3: Figure 1.3.1**.

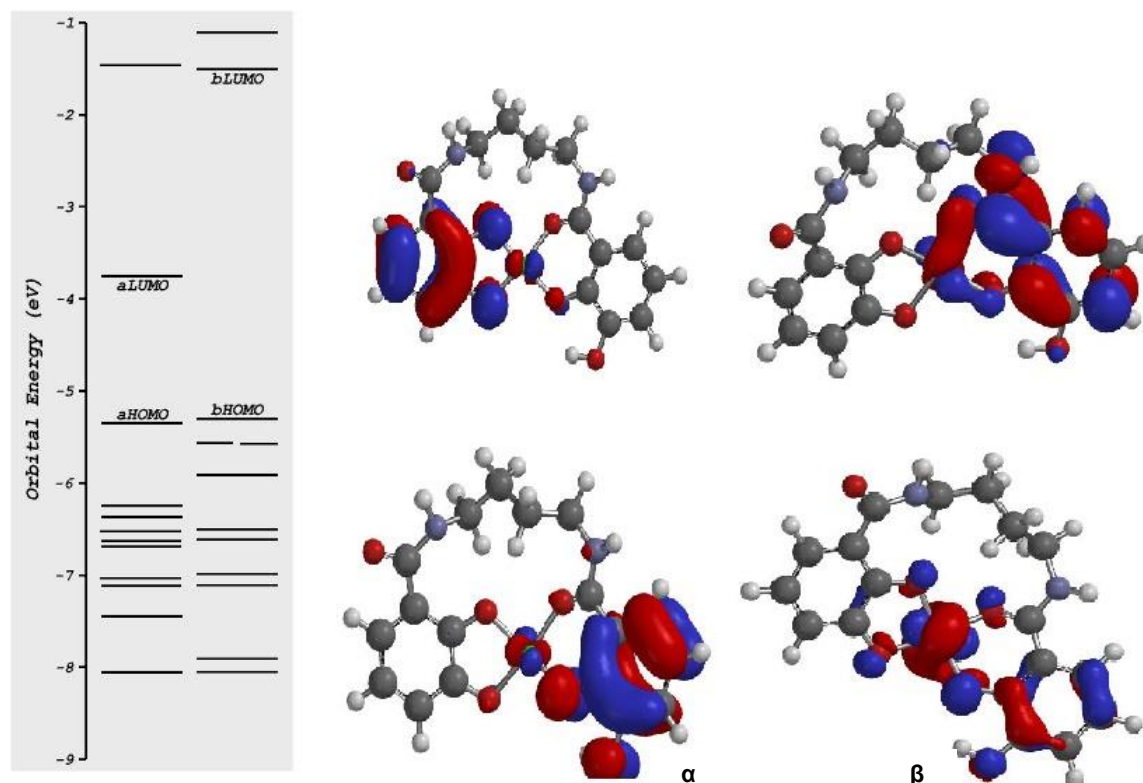


Figure 2.11.1: Orbital energy of compound **15** calculated using DFT (B3LYP/6-31G*)

Frontier orbitals are the most important orbitals in molecules for chemical reactivity. These are called HOMO (*highest occupied molecular orbital*) and LUMO (*lowest unoccupied molecular orbital*).¹⁷ HOMO is the orbital of highest energy that is occupied, it is the easiest to remove electrons from this orbital (electron donor). LUMO is the lowest lying orbital that is empty, so it is easy to add more electrons into this orbital (electron acceptor). In **Figure 2.11.1**, the α -spin HOMO and LUMO are ligand based orbitals and the β -spin HOMO and LUMO are mixed metal-ligand based orbitals. The α HOMO density is largely located on the dihydroxybenzoyl moiety and the

α LUMO density is mainly located on the other dihydroxybenzoyl moiety. The β HOMO and β LUMO densities are mainly located on the metal (Fe) and the dihydroxybenzoyl group (**Figure 2.11.1**).

Moreover, from the UV-Vis for compound **15**, the ϵ_{\max} is 1645.100 L mol⁻¹cm⁻¹ ($\epsilon > 10^3$) which is indicative of the LMCT at λ_{\max} is 319 nm. This specifically means that the absorption band is very intense,³⁵ as displayed in **Figure A2.1**. This LMCT can also be observed in **Figure 2.11.1**, as the electron transfer from α HOMO (*ligand based*) to β LUMO (*mixed metal-ligand based*) in compound **15** with Fe³⁺.

Possible bonding modes have been investigated by molecular modeling where the suggested binding of Photobactin is the loss of the H⁺ from the catechol or amide. The tertiary nitrogen on the oxazoline participates as coordinating ligand based on p*K*_a and resonance mentioned in **Section 1.3**. If placed in an aqueous solution, the oxygen from the water can coordinate to Fe³⁺ as well (**Figure 2.11.2**). The DFT calculations were performed where the B3LYP/6-31G* method is used to predict vibrational frequencies of Fe-Photobactin complexes (Fe³⁺).

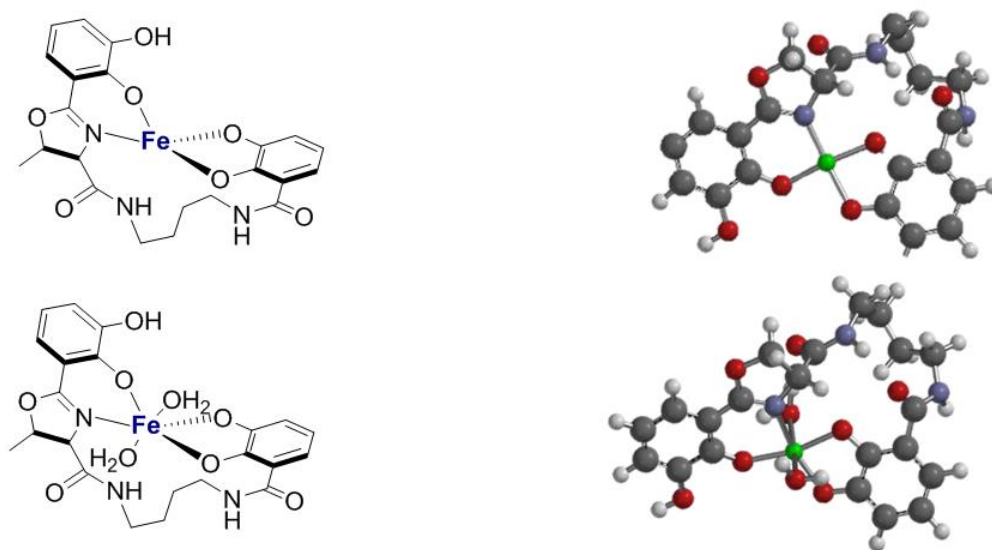


Figure 2.11.2: Possible Fe-Photobactin complexes calculated using DFT (B3LYP/6-31G*)

In **Figure 2.11.2** two molecular models are shown. The top is a distorted square planar while the bottom is the octahedral. The bond lengths and bond angles are slightly distorted. The energies

for the square planar and octahedral complexes are -7367507.02 kJ/mol and -7566545.54 kJ/mol respectively. Based on these calculations, it is hypothesized that Fe-Photobactin complex will be a hexadentate (*6-coordinate ligand*), because the Fe-Photobactin forms a soluble complex, and oxygen from the water will partake in the binding site. Also, the energy for the two molecular models are different, which means octahedral is preferred because it has a larger negative energy than the square planar, that indicates it is more stable. The large negative energy represents how much energy is released when the molecule is formed by bringing together all its nuclei and all its electrons.³⁵

The predicted UV-Vis was also calculated for Photobactin at the B3LYP level of theory (**Figure A2.2**). Fe-Photobactin complex was not calculated due to the maximum number of cycles reached. Comparing the literature to the predicted UV-Vis reveals that they are similar. Two absorbance peaks (λ_{max}) for Photobactin were predicted to be seen at 274 nm and 282 nm. In the literature, it was reported at 257 nm and 316 nm.¹² The absorbance peaks (λ_{max}) were identical to Agrobactin under acidic conditions, which is expected due to the presence of an oxazoline ring.^{13,14} For Vibriobactin, it had a broad band at 320 nm and a sharper more intense band at 258 nm.⁷ The greater absorbance in Vibriobactin is due to the fact it has two oxazoline rings while Agrobactin and Photobactin only have one.

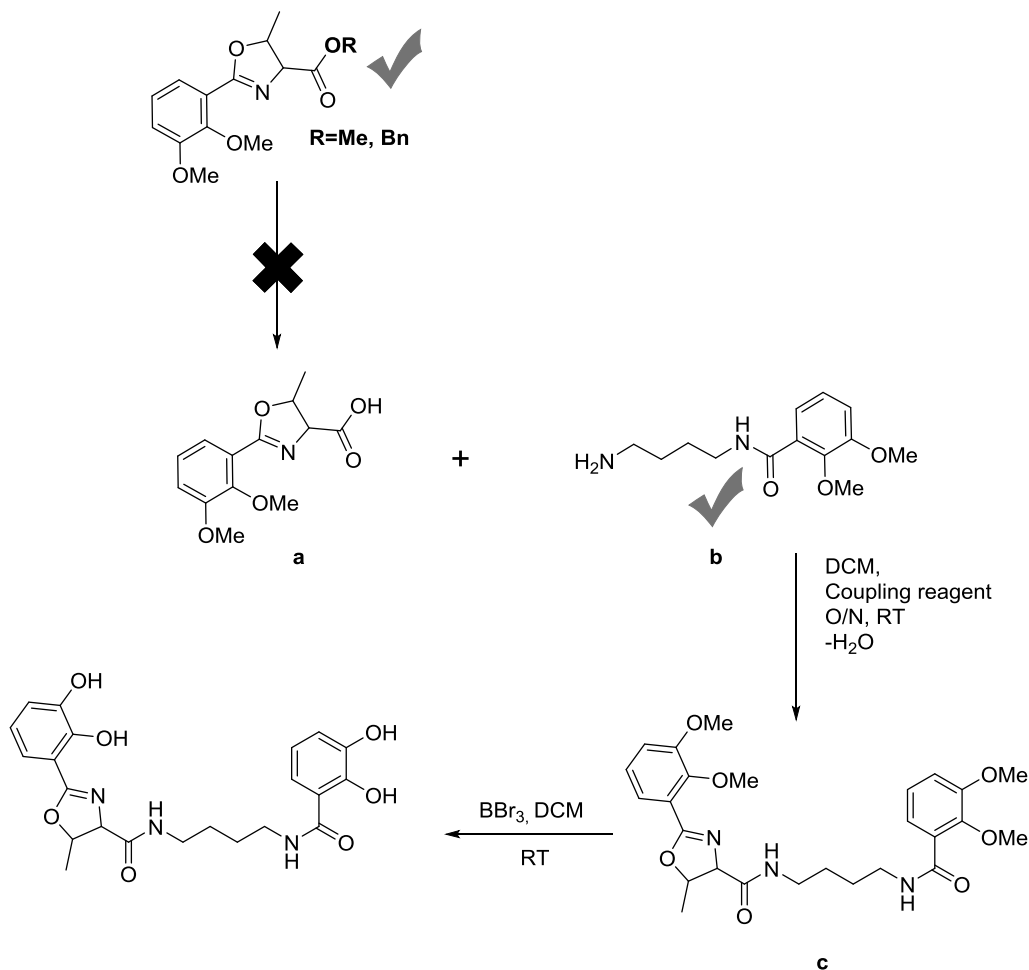
3. Conclusion and Future Work

The goal of this thesis was to synthesize Photobactin and study its binding properties with Fe^{3+} . From the proposed synthesis (**Scheme 6**), which was inspired by Miller *et al.* and Takeuchi *et al.*, one of the steps halted the synthesis of Photobactin. Specifically, the deprotection of the ester from the first building block has been troublesome, and hence the total synthesis of Photobactin has not been accomplished (**Scheme 27**). Once the ester group is cleaved, a coupling reagent can be used to couple the two building blocks together (**Scheme 27 (a) and (b)**), which will result in a protected Photobactin (**Scheme 27 (c)**). The final stage would be deprotection of the methoxy groups with BBr_3 ; this method worked, by studying the deprotection of compound **13** (**Scheme 22**). Following these steps can lead to a successful synthesis of Photobactin.

Moreover, the binding studies of Photobactin were performed by computation calculations (DFT) using Spartan'10 and based on the results, a potential Fe-Photobactin complex can be a distorted square planar or an octahedral conformation where nitrogen from the oxazoline participates as a coordinating ligand. The octahedral conformation, is preferred based on the energy of the molecule (**Figure 2.11.2**).

Future work for a continuation from this thesis project involves increasing the yield of the amides **3** and **4**. Using acyl chloride in this condensation reactions gave higher yields than when using the coupling reagent, EDC·HCl, but exploring different coupling reagents may provide an even higher yield than the acyl chloride. Some recommended amide coupling reagents are DMTMM and HBTU. The other step is deprotecting the ester, which can be accomplished by using different acid base reactions (*saponification*) under different conditions for the methyl ester or choosing a new protecting group besides benzyl or methyl group. Deprotecting the benzyl group can be performed using a different hydrogen source, such as ammonium formate, in the presence of the catalyst palladium on carbon. Another way to cleave benzyl group is conducting the experiment

under higher pressure using a Parr reactor, which will be explored in subsequent studies of these systems.



Scheme 27: The results from proposed synthesis of Photobactin

In conclusion, many experiments and studies have been completed on this siderophore, Photobactin. Even though this compound has not been successfully synthesized there is still potential that it will be synthesized, and hopefully in the near future Fe-Photobactin complex will be used as an application in medical sciences.

“There is no such thing as a failed experiment, only experiments with unexpected outcomes”

-R. Buckminster Fuller

4. Experimental

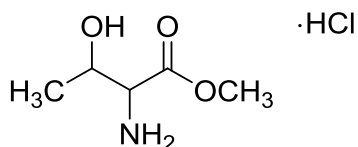
General Section

All reactions were carried out using standard bench top laboratory techniques. Reagents were purchased from Sigma Aldrich Chemical Co. and were used as received. The R_f values quoted were for thin layer chromatography (TLC) on Aldrich TLC plates, silica gel on aluminum. Silica gel 60 (particle size 0.063-0.200 mm) was used as conventional preparative dry column vacuum chromatography. Approximately 75% of the cylindrical sintered glass funnel was filled with silica gel and then tapped to give an even distribution of silica. The glass funnel was placed in a vacuum (Büchner) flask and vacuum was applied. While preparing the column, the compound mixture was pre-adsorbed on silica gel. The mixture was dissolved in a small volume of DCM, and silica was added till it became a slurry mixture. To obtain separation it was required to apply the sample on the column as a thin layer. The filter paper was then placed on top of the compound. The column is developed by gradient elution using hexanes and EtOAc under vacuum. The least polar solvent mixture was added first (100% hexanes) followed by solvent fractions of increasing polarity (0-100 % of EtOAc) in hexanes for elution.

When there was less than 200 mg of crude compound, purification was done using preparative thin layer chromatography (*Prep TLC, Fluka-Silica gel on TLC plates*). Prep TLC was also done when further purification was needed after flash chromatography was performed on the compound and was used for separation of milligram quantities of materials. Once spotted and the plate was developed (hexanes-EtOAc), the materials were separated as long streaks rather than spots. The specific components were scraped off the plate along with the absorbent. Each separate component was then extracted from the stationary phase with a polar solvent (DCM or MeOH)

Proton (^1H -NMR) and Carbon (^{13}C -NMR) Nuclear Magnetic Resonance spectra were recorded on Bruker Avance II-400 spectrometer at 400 MHz and 100 MHz respectively using standard

pulse sequences. Majority of the spectra were recorded in deuterated chloroform (CDCl_3) in 5 mm NMR tubes. The other spectra were recorded in deuterated methanol (CD_3OD) and deuterium oxide (D_2O). Homonuclear and heteronuclear 2D-NMR (COSY, HSQC, and HMBC) experiments were recorded for some compounds, which assisted in assigning chemical shifts. UV-Vis absorption spectra were recorded on Perkin Elmer UV/Vis Spectrometer Lambda 20. Elemental analysis was performed by the Atlantic Microlab, Inc. in Norcross Georgia, and it was analyzed for carbon (C), hydrogen (H), and nitrogen (N) only.

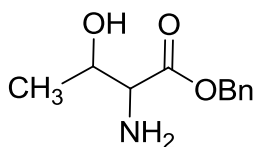


Molecular Weight: 169.61 g/mol

L-Threonine Methyl Ester Hydrochloride (1)

L-Threonine (1.66 g, 13.94 mmol) was placed in a round bottom flask and chlorotrimethylsilane (3.53 mL, 27.80 mmol) was added slowly and stirred with a magnetic stirrer. Methanol (20 mL) was then added and the resulting solution was stirred O/N at RT under N₂. Then the reaction mixture was concentrated on a rotary evaporator to give a yellowish-orange coloured oil as the title product.

$R_f < 0.01$ (hexanes-EtOAc, 1:3); ¹H-NMR (D₂O, 400 MHz) δ 4.43 (qd, ³ J_1 = 6.60 Hz, ³ J_2 = 3.80 Hz, 1H, CH), 4.09 (d, ³ J = 3.80 Hz, 1H, CH), 3.87 (s, 3H, OCH₃), 1.34 (d, ³ J = 6.60 Hz, 3H, CH₃); ¹³C-NMR (D₂O, 100 MHz) δ 65.37 (CH), 58.42 (CH), 53.60 (OCH₃), 18.71 (CH₃).



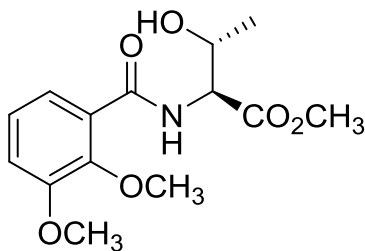
Molecular Weight: 209.24g/mol

L-Threonine Benzyl Ester (2)

In a 125 mL round bottom flask, L-Threonine (1.78 g, 14.9 mmol), and *p*-toluene sulfonic acid monohydrate (3.14 g, 16.5 mmol) were added with 25 mL of benzyl alcohol and 30 mL of benzene (or toluene). This reaction was refluxed for 24 hrs using a Dean Stark apparatus. Approximately 2 mL of water was collected. The yellow mixture was rotovapped to remove volatiles and was then partitioned between EtOAc (20 mL) and H₂O (20 mL). The organic layer was extracted two more times with 20 mL of H₂O. Then, 2.85 g (37.26 mmol) of NaHCO₃ was added to the combined aqueous layer. In addition, the combined aqueous solution was extracted with EtOAc (3 x 20 mL). The organic layers were combined and then dried over MgSO₄, and filtered to give the crude product. The crude product was purified by flash chromatography in a 25 mL sintered glass funnel (elution with increasing amounts of EtOAc in hexanes). Benzyl alcohol eluted first (*fractions* 3-7). The product eluted when the column was flushed with EtOAc ($R_f \leq 0.01$ (hexanes-EtOAc, 1:3)). The pure product following the evaporation of the solvent, was isolated as a yellow-coloured solid (0.62 g, 20%).

¹H-NMR (CDCl₃, 400 MHz) δ 7.39-7.37 (m, 5H, Ar-*H*), 5.20 (s, 2H, CH₂-Ar), 3.94 (m, 1H, CH-OH), 3.33 (d, ³*J* = 4.80 Hz, 1H, CH-NH₂), 2.37 (s, 3H, OH, NH₂), 1.24 (d, ³*J* = 6.40 Hz, 3H, CH₃);
¹³C-NMR (CDCl₃, 100 MHz) δ 140.87 (C=O), 128.59 (ArCH), 127.69 (ArCH), 127.65 (ArCH), 127.00 (ArCH), 68.11 (CH-OH), 65.42 (CH₂), 59.93 (CH-NH₂), 19.79 (CH₃).

The ¹H-NMR was identical to the reported values.¹⁸



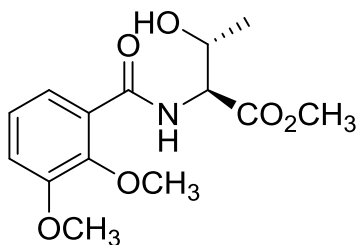
Molecular Weight: 297.31

N-(o, m)-Dimethoxybenzoyl-L-Threonine methyl ester (3)

In a 25 ml round bottom flask, compound **1** (0.540 g, 1.04 mmol), 2,3-dimethoxybenzoic acid (0.580 g, 3.18 mmol), HOBt (0.050 g, 0.370 mmol), and Et₃N (0.44 mL, 3.15 mmol) was added with approximately 10 mL of DCM. The mixture was stirred for 2 min and EDC·HCl (0.68 g, 1.82 mmol) was added to the mixture at 0 °C. The reaction mixture was stirred overnight under N₂ at RT. The reaction mixture was then washed with H₂O (10 mL), 0.5 N HCl (10 mL), 5% Na₂CO₃ solution (10 mL), and then brine (10 mL). The organic layer was then dried over MgSO₄, filtered, and left to evaporate in a small beaker to yield a yellow coloured oil as the product (0.077 g, 25%).

R_f = 0.78 (hexanes-EtOAc,1:3); ¹H-NMR (CDCl₃, 400 MHz) δ 8.89 (d, ³J = 8.50 Hz, 1H, OH), 7.65 (d, ³J = 7.90 Hz, 1H, ArCH), 7.11 (dd, ³J₁ = 7.90 Hz, ³J₂ = 8.10 Hz, 1H, ArCH), 7.04 (d, ³J = 8.10 Hz, 1H, ArCH), 4.78 (dd, ³J₁ = 8.50 Hz, ³J₂ = 2.50 Hz, 1H, CH), 4.30 (qd, ³J₁ = 6.30 Hz, ³J₂ = 2.50 Hz, 1H, CH), 3.95 (s, 3H, CH₃), 3.87 (s, 3H, CH₃), 3.74 (s, 3H, CH₃), 1.24 (d, ³J = 6.30 Hz, 3H, CH₃).

The ¹H-NMR was identical to the reported values.²⁰



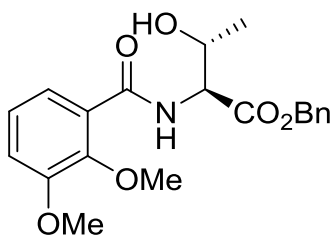
Molecular Weight: 297.31

N-(o, m)-Dimethoxybenzoyl-L-Threonine methyl ester (3)

In a 25 mL round bottom flask 2,3-dimethoxybenzoic acid (0.60 g, 3.24 mmol) was added with DCM (5 mL) and Et₃N (0.70 mL, 4.86 mmol). Thionyl chloride (0.24 mL, 3.24 mmol) was added last at 0 °C and the reaction mixture was stirred for 30 min at the same temperature under N₂. Compound **1** (0.55 g, 3.24 mmol) was then added and the mixture was stirred O/N under N₂. The reaction mixture was washed with saturated NaHCO₃ solution (2 x 5 mL) and then with water (2 x 5 mL). The organic layer was dried over MgSO₄, filtered, and concentrated *in vacuo* which gave a brown coloured oil as the crude product. The residue was purified by flash column chromatography in a 25 mL sintered glass funnel (eluted with increasing amounts of EtOAc in hexanes; *fractions 10-15*) on silica gel afforded the title compound (0.28 g, 29%) as a white solid.

R_f = 0.78 (hexanes-EtOAc,1:3); ¹H-NMR (CDCl₃, 400 MHz) δ 8.88 (d, ³J = 8.40 Hz, 1H, NH), 7.65 (d, ³J = 7.90 Hz, 1H, Ar-H), 7.11 (dd, ³J₁ = 8.10 Hz, ³J₂ = 7.90 Hz, 1H, Ar-H), 7.04 (d, ³J = 8.10 Hz, 1H, Ar-H), 4.79 (dd, ³J₁ = 8.40 Hz, ³J₂ = 2.50 Hz, 1H, CH), 4.38 (qd, ³J₁ = 6.30 Hz, ³J₂ = 2.50 Hz, 1H, CH), 3.95 (s, 3H, O-CH₃), 3.87 (s, 3H, O-CH₃), 3.74 (s, 3H, CH₃), 1.24 (d, ³J = 6.30 Hz, 3H, CH₃); ¹³C-NMR (CDCl₃, 100 MHz) δ 171.70 (C=O), 165.66 (C=O), 152.75 (ArC-OMe), 148.03 (ArC-OMe), 125.88 (ArC-C=O), 124.37 (ArC-H), 122.86 (ArC-H), 115.84 (ArC-H), 68.15 (CH), 61.67 (CH), 57.75 (Ar-OCH₃), 56.14 (Ar-OCH₃), 52.5 (C=O-OCH₃), 20.03 (CH₃).

The ¹H and ¹³C-NMR were identical to the reported values.²⁰

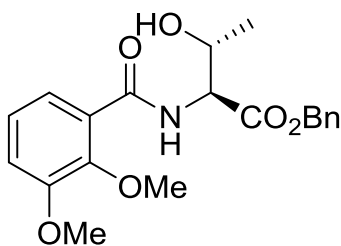


Molecular Weight: 373.40 g/mol

N-(o,m)-Dimethoxybenzoyl-L-Threonine benzyl ester (4)

In a 25 mL round bottom flask, compound **2** (0.218 g, 1.04 mmol), 2,3-dimethoxybenzoic acid (0.206 g, 1.13 mmol), HOBt (0.0163 g, 0.121 mmol), and Et₃N (0.139 mL, 0.99 mmol) were combined together with 20 mL of DCM. The mixture was stirred for two min and then EDC·HCl (0.199 g, 1.04 mmol) was added to the mixture at 0 °C. The mixture was stirred O/N at RT under N₂. When the reaction was deemed to be complete (monitored by TLC) the reaction mixture was then partitioned between DCM (10 mL) and H₂O (10 mL). The organic layer was washed successively with 0.5 N HCl (10 mL), 5% Na₂CO₃ solution (10 mL), and then brine (10 mL). The organic layer was then dried over MgSO₄, filtered, and left to evaporate in a 25 mL beaker. The residue was purified by flash column chromatography in a 25 mL sintered glass funnel (eluted with 0-100% EtOAc in hexanes; *fractions 8-13*) on silica gel, affording the title compound (0.128 g, 33%) as a yellowish-white coloured solid.

$R_f = 0.74$ (hexanes-EtOAc, 1:3) ; ¹H-NMR (CDCl₃, 400 MHz) δ 8.90 (br d, 1H, *NH*), 7.71 (dd, ³*J*₁ = 7.90 Hz, ³*J*₂ = 1.60 Hz, 1H, *Ar-H*), 7.35-7.32 (m, 5H, *Ar-H*), 7.18 (t, *J* = 8.00 Hz, 1H, *Ar-H*), 7.07 (dd, ³*J*₁ = 8.10 Hz, ³*J*₂ = 1.60 Hz, 1H, *Ar-H*), 5.23 (s, 2H, *CH*₂-*Ar*), 4.88 (dd, ³*J*₁ = 8.50 Hz, ³*J*₂ = 2.40 Hz, 1H, *CH*-COO₂Bn), 4.43 (qd, ³*J*₁ = 6.40 Hz, ³*J*₂ = 2.40 Hz, 1H, *CH*-OH), 3.91(s, 6H, *Ar*-OCH₃), 1.27 (d, ³*J* = 6.40 Hz, 3H, *CH*₃); ¹³C-NMR (CDCl₃, 100 MHz) δ 171.01 (C=O), 165.67 (C=O), 152.75 (*Ar*C-OMe), 148.06 (*Ar*C-OMe), 135.33 (*Ar*C-CH₂), 128.29 (*Ar*C-C=O), 128.43 (*Ar*CH), 125.90 (*Ar*CH), 124.89 (*Ar*CH), 122.91 (*Ar*CH), 115.84 (*Ar*CH), 68.27 (CH), 67.29 (CH₂), 61.65 (CH), 57.81 (O-CH₃), 56.15 (O-CH₃), 20.11 (CH₃).

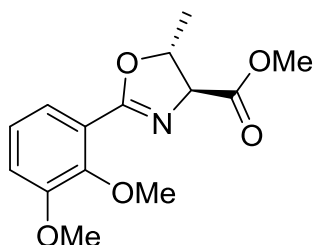


Molecular Weight: 373.40.39 g/mol

N-(o,m)-Dimethoxybenzoyl-L-Threonine benzyl ester (4)

2,3-Dimethoxybenzoic acid (0.0835 g, 0.459 mmol) and Et₃N (0.095 mL, 0.681 mmol) was added to DCM (7 mL) in a 25 mL round bottom flask. The stirring mixture was placed in an ice bath (0 °C) and thionyl chloride (0.033 mL, 0.459 mmol) was added to the mixture stirring for 30 min. After, a solution of compound **2** (0.096 g, 0.459 mmol) in DCM (5 mL) was added to the reaction flask at 0 °C. After being stirred O/N at RT under N₂, the reaction mixture was diluted with 5 mL of DCM and was then extracted with 5% Na₂CO₃ solution (5 mL), and water (5 mL). The organic layer was dried over MgSO₄, filtered, and the evaporation of the solvent gave the title compound as a yellowish-brown coloured solid (0.094 g, 55%).

R_f = 0.76 (hexanes-EtOAc, 1:1); ¹H-NMR (CDCl₃, 400 MHz) δ 8.90 (d, *J* = 8.50 Hz, 1H, *NH*), 7.71 (dd, ³*J*₁ = 7.90 Hz, ³*J*₂ = 1.60 Hz, 1H, *Ar-H*), 7.35-7.32 (m, 5H, *Ar-H*), 7.18 (t, ³*J* = 8.00 Hz, 1H, *Ar-H*), 7.07 (dd, ³*J*₁ = 8.10 Hz, ³*J*₂ = 1.60 Hz, 1H, *Ar-H*), 5.23 (s, 2H, CH₂-Ar), 4.88 (dd, ³*J*₁ = 8.50 Hz, ³*J*₂ = 2.40 Hz, 1H, *CH*), 4.43 (qd, ³*J*₁ = 6.40 Hz, ³*J*₂ = 2.40 Hz, 1H, *CH*), 3.91 (s, 6H, O-CH₃), 1.26 (d, ³*J* = 6.40 Hz, 3H, CH₃). ¹³C-NMR (CDCl₃, 100 MHz) δ 171.01 (C=O), 165.70 (C=O), 152.75 (ArC-OMe), 148.06 (ArC-OMe), 135.36 (ArC-CH₂), 128.62 (ArC-C=O), 128.43 (ArCH), 128.27 (ArCH), 125.90 (ArCH), 124.35 (ArCH), 122.88 (ArCH), 115.84 (ArCH), 68.27 (CH), 67.26 (CH₂), 61.64 (CH), 57.90 (O-CH₃), 56.14 (O-CH₃), 20.11 (CH₃).



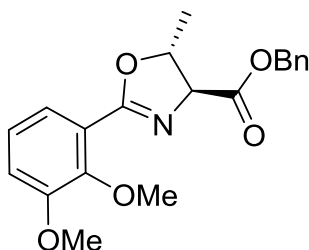
Molecular Weight: 279.29 g/mol

***(4S, 5R)-2-(o, m)-Dimethoxyphenyl)-5-methyl-4-oxazolinecarboxylic acid
methyl ester (5)***

In a 10 mL round bottom flask, compound **3** (0.07 g, 0.235 mmol, 1 eq) along with ~5 mL of DCM was added and cooled to -85 °C (EtOAc/ N₂). Then (dimethylamino)sulfurtrifluoride (Methyl DAST; 0.0344 mL, 0.352 mmol, 1.5 eq) was added to the reaction using a syringe. The reaction mixture was sealed with a septum and was stirred for one hour at -85 °C under N₂. After stirring for one hour, the septum was removed and anhydrous K₂CO₃ (0.05 g, 1.5 eq) was added. This allowed the reaction mixture to reach RT. After stirring for an additional hour, the mixture was washed with saturated NaHCO₃ solution (2 x 10 mL) and lastly with H₂O (10 mL). The organic layer was dried over MgSO₄, filtered, and the evaporation of the solvent gave a yellow coloured oil as the crude product. Purification by flash chromatography using a 15 mL sintered glass funnel (increasing amounts of EtOAc in hexanes as the eluent; *fractions 8-14*) with silica gel afforded the title compound (0.03 g, 46%) as a colourless solid.

R_f = 0.32 (hexanes-EtOAc, 1:1); ¹H-NMR (CDCl₃, 400 MHz) δ 7.36 (d, ³J = 7.50, 1H, Ar-*H*), 7.07-7.03 (dd, *J*₁ = 7.80 Hz, *J*₂ = 7.50 Hz, 2H, Ar-*H*), 5.06-5.03 (qd, ³*J*₁ = 6.20 Hz, ³*J*₂ = 2.20 Hz, 1H, CH), 4.98 (d, ³*J* = 2.20 Hz, 1H, CH), 3.87 (s, 6H, OCH₃), 3.77 (d, ³*J* = 2.30 Hz, 3H, COOCH₃), 1.38 (dd, ³*J*₁ = 6.20 Hz, ³*J*₂ = 2.30 Hz, 3H, CH₃); ¹³C-NMR (CDCl₃, 100 MHz) δ 170.44 (C=O), 165.39 (C=N), 153.43 (ArC-OMe), 149.03 (ArC-OMe), 123.88 (ArC-C=N), 122.67 (ArCH), 122.47 (ArCH) 115.57 (ArCH), 76.76 (CH), 71.72 (CH), 61.50 (OCH₃), 56.17 (OCH₃), 52.04 (COOCH₃), 16.13 (CH₃).

The ¹H and ¹³C-NMR were identical to the reported values.²⁰



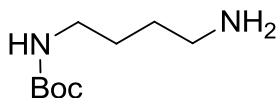
Molecular Weight: 355.38 g/mol

(4S, 5R)-2-(o, m)-Dimethoxyphenyl-5-methyl-4-oxazolinecarboxylic acid

benzyl ester (6)

In a 10 mL round bottom flask, compound **4** (0.01 g, 1 eq) was dissolved in 5 mL of DCM. The solution was stirred for 5 min at -84 °C (EtOAc and N₂), then approximately 3 µL (1.1 eq) of methyl DAST was added to the solution and the reaction was sealed with a septum and stirred for one hour at -84 °C under N₂. After one hour of stirring, the septum was removed and anhydrous K₂CO₃ (0.06 g, 1.5 eq) was added and the reaction mixture was allowed to reach RT. After stirring for another hour, the reaction mixture was partitioned between DCM (5 mL) and H₂O (5 mL). The organic layer was washed successively with saturated NaHCO₃ solution (2 X 10 mL) and lastly with water (10 mL). The organic layer was dried over MgSO₄, filtered, and then left to evaporate. Purification by flash chromatography using a 15 mL sintered glass funnel (eluted with increasing amounts of EtOAc in hexanes; *fractions 7-11*) with silica gel afforded the title compound (0.01 g, > 99%) as an oil.

R_f = 0.60 (hexanes-EtOAc, 1:3); ¹H-NMR (CDCl₃, 400 MHz) δ 7.37-7.32 (m, 6H, Ar-*H*) 7.09-7.02 (m, 2H, Ar-*H*), 5.22 (s, 2H, CH₂-Ar), 5.04-4.99 (m, 2H, CH), 3.87 (s, 3H, OCH₃), 3.86 (s, 3H, OCH₃), 1.33 (d, ³J = 6.00 Hz, 3H, CH₃); ¹³C-NMR (CDCl₃, 100 MHz) δ 169.79 (C=O), 165.41 (C=N), 153.42 (ArC-OMe), 148.92 (ArC-OMe), 135.33 (ArC-CH₂), 128.73 (ArC-C=N), 128.59 (ArCH), 128.50 (ArCH), 123.87 (ArCH), 122.68 (ArCH), 122.44 (ArCH), 115.58 (ArCH), 77.55 (CH-CH₃), 71.67 (CH-C=O), 66.94 (CH₂), 61.50 (O-CH₃), 56.18 (O-CH₃), 16.10 (CH₃).



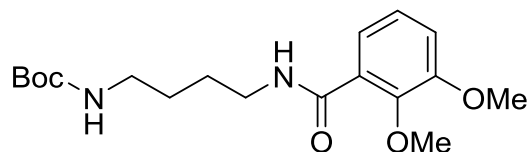
Molecular Weight: 188.27 g/mol

Boc-1, 4-diaminobutane (8)

In a 25 mL round bottom flask 1,4-diaminobutane (2 mL, 19.89 mmol) was dissolved in CHCl_3 (~10 mL). Then a solution of Boc_2O (di-tert-butyl dicarbonate; 1.16 mL, 5.05 mmol) in 5 mL of CHCl_3 was added dropwise over a period of 30 min at 0 °C. The reaction mixture was then stirred at RT for 24 hrs. The reaction mixture was partitioned between CHCl_3 and H_2O (15 mL). The organic layer was washed with brine (15 mL) and dried over MgSO_4 , filtered, and concentrated in a 25 mL beaker. This resulted in a yellow coloured gooey liquid as the crude product (2.00 g, 53%).

$^1\text{H-NMR}$ (CDCl_3 , 400 MHz) δ 4.79 (br s, 1H, NH), 3.05 (d, J = 6.10 Hz, 2H, CH_2), 2.64 (t, J = 6.50 Hz, 2H, CH_2), 1.46-1.37 (m, 15H, CH_3 , CH_2 , NH_2).

The $^1\text{H-NMR}$ was identical to the reported values.²⁵

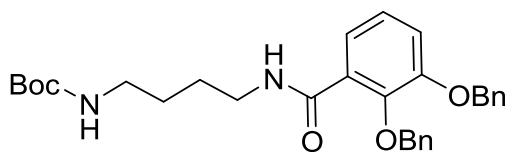


Molecular Weight: 352.43 g/mol

N-Boc (1,4-aminobutyl)-2,3-(dimethoxyphenyl) benzamide (9)

Compound **8** (0.107 mL, 56 mmol) was placed in a round bottom flask along with 15 mL of DCM. 2,3-Dimethoxybenzoic acid (0.101 g, 0.56 mmol), HOBt (0.140 g 1.036 mmol), and Et₃N (0.0685 mL, 0.49 mmol) were added after and stirred for couple of minutes at RT. EDC·HCl (0.161 g, 0.840 mmol) was added last to the stirring mixture at 0 °C. The mixture was stirred O/N at RT under N₂ then partitioned between DCM (10 mL) and H₂O (10 mL). The organic layer was washed with saturated NaHCO₃ solution (10 mL), and brine (10 mL). The organic layer was dried over MgSO₄, filtered, and left to evaporate in a 25 mL beaker. The crude product was purified using flash chromatography on silica gel using a mixture of increasing amounts of EtOAc in hexanes (*fractions 9-11*). This gave a yellow coloured oil as the desired product (0.049 g, 25%).

R_f = 0.77 (hexanes-EtOAc, 1:3); ¹H-NMR (CDCl₃, 400 MHz) δ 7.99 (br s, 1H, NH), 7.67 (dd, ³ J_1 = 7.96 Hz, ³ J_2 = 1.62 Hz, 1H, Ar-H), 7.14 (dd, ³ J_1 = 9.60 Hz, ³ J_2 = 6.50 1H, Ar-H), 7.03 (dd, ³ J_1 = 8.14 Hz, ³ J_2 = 1.60 Hz, 1H, Ar-H), 4.61 (br s, 1H, NH), 3.89 (s, 6H, O-CH₃), 3.47 (dd, ³ J_1 = 12.68 Hz, ³ J_2 = 6.75 Hz, 2H, CH₂), 3.18-3.15 (m, 2H, CH₂), 1.62 (m, 4H, CH₂), 1.42 (s, 9H, CH₃); ¹³C-NMR (CDCl₃, 100 MHz) δ 165.21 (C=O), 162.55 (C=O), 152.55 (ArC-OCH₃), 147.39 (ArC-OCH₃), 126.84 (ArC-C=O), 124.44 (ArCH), 122.79 (ArCH), 115.26 (ArCH), 61.28 (O-CH₃), 56.19 (O-CH₃), 39.27 (CH₂), 33.71 (CH₂), 29.68 (CH₃), 27.62 (CH₂), 27.00 (CH₂). Anal. Calcd. For C₁₈H₂₈N₂O₅ (%): C 61.34, H 8.01, N 7.95; Found: C 61.62, H 8.07, N 6.54.

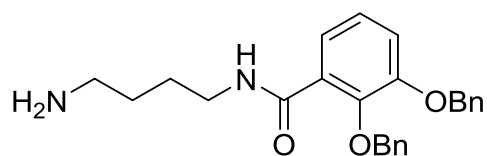


Molecular Weight: 504.63 g/mol

N-Boc(1,4-aminobutyl)-[2,3-bis(benzyloxy)phenyl]benzamide (10)

In a 25 mL round bottom flask, compound **8** (0.107 mL, 0.560 mmol), 2,3-bis(benzyloxy) benzoic acid (0.18 g, 0.538 mmol), HOBt (0.14 g, 1.04 mmol), and 15 mL of DCM was added and stirred for two min at RT. Then of EDC·HCl (0.16 g, 0.835 mmol) was added at 0 °C. The reaction mixture was stirred O/N at RT under N₂. When the reaction was complete (monitored by TLC), the solution was washed with saturated NaHCO₃ solution (10 mL), H₂O (10 mL), and brine (10 mL). The organic layer was dried over MgSO₄, filtered, and concentrated *in vacuo*. Purification by flash chromatography (eluted with 0-100% of EtOAc in hexanes) on silica gel provided with the title compound (*fractions 8-9*, 0.11 g, 40%) as a yellow coloured solid.

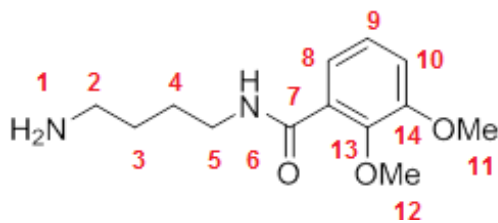
R_f = 0.56 (hexanes-EtOAc, 1:3); ¹H-NMR (CDCl₃, 400 MHz) δ 7.95 (br s, 1H, NH), 7.75-7.73 (m, 1H, Ar-H), 7.49-7.36 (m, 10H, Ar-H), 7.16 (dd, *J*₁ = 6.80 Hz, *J*₂ = 2.70 Hz, 2H, Ar-H), 5.16 (s, 2H, CH₂-Ar), 5.09 (s, 2H, CH₂-Ar), 4.44 (br s, 1H, NH), 3.27 (q, *J* = 6.80 Hz, 2H, CH₂), 3.03 (d, *J* = 5.60 Hz, 2H, CH₂), 1.44 (s, 9H, CH₃), 1.35 (m, 4H). Anal. Calcd. For C₃₀H₃₆N₂O₅ (%): C 71.40, H 7.19, N 5.55; Found: C 71.52, H 7.32, N 4.11.



Molecular Weight: 404.51 g/mol

1,4-Aminobutyl-[2,3-bis(benzyloxy)phenyl] benzamide (11)

In a 10 mL round bottom flask, compound **10** (2.5 mg, 4.96×10^{-3} mmol) was dissolved in DCM (0.25 mL, 1 eq). The reaction mixture was placed in an ice bath and TFA (0.25 mL, 1 eq) was added dropwise. The reaction occurred immediately once TFA was added. The mixture was monitored by TLC. Once complete 6 N NaOH (0.55 mL, 2.2 eq) was added to the mixture and then extraction was performed adding an extra 5 mL of DCM. The organic layer was washed with water (5 mL) and then brine (5 mL). The organic layer was dried over MgSO_4 , filtered, and left to evaporate in a 25 mL beaker. This afforded the white solid as the desired product (1.2 mg, 60%).

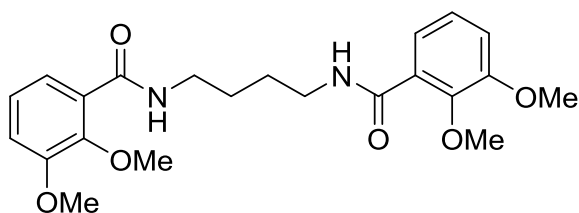


Molecular Weight: 252.31 g/mol

***N*-(2,3-dimethoxybenzoyl)-1,4-diaminobutane (12)**

1,4-Diaminobutane (0.23 mL, 2.28 mmol) and 2,3-dimethoxybenzoic acid (0.166 g, 0.911 mmol) were placed in a 25 mL round bottom flask with DCM (~15 mL), and stirred for 10 min. DMTMM (0.630 g, 2.28 mmol) was then added to the mixture and it was stirred for approximately 19 hrs at RT under N₂. The crude product was washed with saturated NaHCO₃ solution (10 mL), water (10 mL), 0.5 N HCl (10 mL), water (10 mL), and then brine (10 mL). The organic layer was dried over MgSO₄, filtered, and concentrated *in vacuo* to afford the product as a white solid. The crude product was purified using flash chromatography on silica gel eluting with EtOAc (*fractions 2-7*). The product isolated by flash chromatography was further purified by preparative TLC on a silica gel. Two bands (#1 and #2) were shown and were scraped off and dissolved with small amounts of methanol, filtered and left to evaporate. Both bands were characterized by ¹H-NMR. Band #2 had the desired product (0.02 g, 9%) as a white solid.

¹H-NMR (CDCl₃, 400 MHz) δ 8.01 (br s, 1H, NH), 7.67 (d, *J* = 7.90 Hz, 1H, Ar-*H*), 7.14 (dd, *J*₁ = 8.10 Hz, *J*₂ = 7.90 Hz, 1H, Ar-*H*), 7.03 (d, *J* = 8.10 Hz, 1H, Ar-*H*), 5.52 (br s, 1H), 3.88 (d, *J* = 4.90 Hz, 6H, O-CH₃), 3.52-3.49 (m, 3H, CH₂), 1.73-1.66 (m, 5H, CH₂).



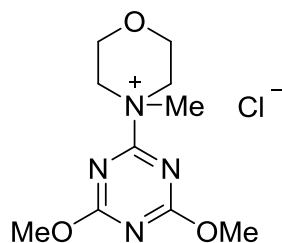
Molecular Weight: 416.47 g/mol

***N,N'*-Bis(2,3 –bis(methoxy)benzoyl)-1,4 -diaminobutane (13)**

In a 25 mL round bottom flask, 2,3-dimethoxybenzoic acid (0.084 g, 0.46 mmol) and Et₃N (0.096 mL, 0.69 mmol) were added along with 3 mL of DCM. The reaction flask was placed in an ice bath and then thionyl chloride (0.033 mL, 0.46 mmol) was added dropwise. The mixture was stirred for 30 min at RT under N₂. 1,4-Diaminobutane (0.092 mL, 0.92 mmol) was then added to the reaction mixture and continues stirring O/N at RT under N₂. Approximately 7 mL of DCM was added to the mixture and was washed with saturated NaHCO₃ solution (10 mL) and then with H₂O (10 mL). The organic layer was dried over MgSO₄, filtered, and the evaporation of the solvent afforded white crystals as the pure product (50 mg, 27%).

R_f =< 0.01 (hexanes-EtOAc, 1:1) ¹H-NMR (CDCl₃, 400 MHz) δ 8.00 (s, 2H, NH), 7.65 (dd, *J*₁ = 7.90 Hz, *J*₂ = 1.00 Hz, 2H, Ar-*H*), 7.12 (t, *J* = 8.00 Hz, 2H, Ar-*H*), 7.01 (dd, *J*₁ = 8.00 Hz, *J*₂ = 1.00 Hz, 2H, Ar-*H*), 3.87 (s, 12H, O-CH₃), 3.51-3.49 (m, 4H, CH₂-NH) 1.72-1.71 (m, 4H, C-CH₂-C).

The ¹H-NMR was identical to the reported values.³⁰



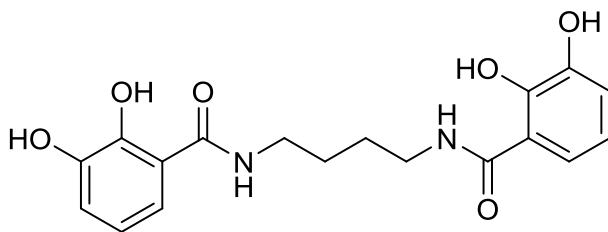
Molecular Weight: 276.12 g/mol

**4-(4,6-dimethoxy-1,3,5-triazin-2-yl)-4-methylmorpholinium chloride
(DMTMM) (14)**

In a 125 mL round bottom flask 2-chloro-4,6-dimethoxy-1,3,5-triazine (CDMT, 3.86 g, 22 mmol) was added into THF (60 mL). *N*-Methylmorpholine (NMM, 2.20 mL, 20 mmol) was slowly added into the stirring mixture and stirred for 30 min; white precipitate was found. The organic material was then filtered by vacuum filtration to yield a white solid (5.42 g, 98%)

$^1\text{H-NMR}$ (CD_3OD , 400 MHz) δ 4.52-4.55 (m, 2H, CH_2), 4.18 (s, 5H, O-CH_3), 4.08-4.06 (m, 2H, CH_2), 3.89-3.83 (m, 4H, CH_2), 3.51 (s, 3H, N-CH_3).

The $^1\text{H-NMR}$ was identical to the reported values.²⁹



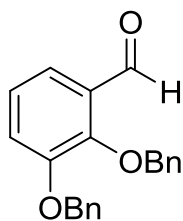
Molecular Weight: 360.37 g/mol

***N,N'*-Bis (2,3-dihydroxybenzoyl)-1-4-diaminobutane (15)**

In a 10 mL round bottom flask compound **13** (0.03 g, 0.072 mmol) was added along with 2 mL of dry DCM. The reaction was sealed with a septum under N₂. Then the reaction was placed in a -84 °C bath and BBr₃ was added (0.100 mL, 1.053 mmol). The reaction immediately turned yellow from a colourless liquid upon the addition of BBr₃. The reaction was stirred for 2 hrs at -84 °C and then at RT for 18 hrs. The reaction was then cooled to -84 °C and anhydrous MeOH (0.7 mL), saturated NaHCO₃ solution (0.7 mL), and then H₂O (4 mL) was added. The cooling bath was removed and allowed the reaction to reach room temperature. The septum was removed and extraction took place with EtOAc (3 x 10 mL). The evaporation of the solvent in the aqueous layer afforded a whitish-grey coloured solid as the product (0.02 g, 77%).

λ_{max} = 318 nm; ¹H-NMR (CD₃OD, 400 MHz) δ 8.87 (br s, 2H, NH), 7.15-7.11 (m, 2H, Ar-H), 6.75-6.72 (m, 2H, Ar-H), 6.62 (dd, ³J₁ = 15.30 Hz, ⁴J₂ = 7.60 Hz, 2H, Ar-H), 3.48-3.46 (m, 4H, NH-CH₂), 1.73-1.71 (m, 4H, C-CH₂-C).

The ¹H-NMR was identical to the reported values.³⁰



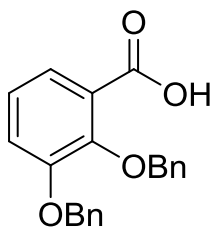
Molecular weight: 318.37 g/mol

2,3-Dibenzoyloxybenzaldehyde (16)

In a 25 mL 3-neck round bottom flask, 2,3-dihydroxybenzaldehyde (0.90 g, 6.52 mmol) was added along with benzyl chloride (1.80 mL, 15.00 mmol) in EtOH (20 mL). Lastly, K_2CO_3 (1.13 g, 8.15 mmol) was added and the reaction mixture was refluxed for 20 hrs in air. The reaction mixture was then pumped down and partitioned between EtOAc (25 mL) and H_2O (25 mL). The organic layer was dried over $MgSO_4$, filtered, and the evaporation of the solvent gave a brownish-beige coloured solid as the title compound (0.65 g, 31%).

1H -NMR ($CDCl_3$, 400 MHz) δ 10.20 (s, 1H, $C=OH$), 7.42-7.03 (m, 13H, Ar- H), 5.13 (s, 4H, CH_2).

The 1H -NMR was identical to the reported values.³⁴



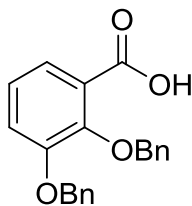
Molecular Weight: 334.37 g/mol

2,3-bis (benzyloxy) benzoic acid (17)

In a 25 mL round bottom flask, 2,3-dibenzyloxybenzaldehyde (0.57 g, 1.79 mmol) was dissolved in acetone (5 mL) and diluted with H₂O (5 mL). While stirring, sulfamic acid (0.244 g, 2.51 mmol) and sodium chlorite (0.170 g, 1.87 mmol) were added in a portion of 15 min to the opaque reaction mixture. The resulting solution was stirred for one hour at RT in air. Acetone was evaporated which yielded the product as a precipitate in the remaining aqueous mixture. The mixture was filtered and the crude was collected from the filter paper as a light brown coloured solid (0.50 g, 84%) as the product.

R_f = 0.74 (hexanes-EtOAc, 1:3); ¹H-NMR (CDCl₃, 400 MHz) δ 10.26 (s, 1H, OH), 7.76-7.19 (m, 13H, Ar-H), 5.27 (s, 2H, CH₂), 5.19 (s, 2H, CH₂).

The ¹H-NMR was identical to the reported values.³⁴

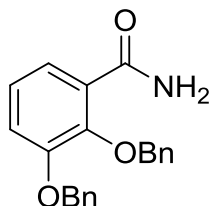


Molecular Weight: 334.37 g/mol

2,3-bis (benzyloxy) benzoic acid (17)

2,3-Bis(benzyloxy)benzoate (2.00 g, 4.71 mmol) was added to 12% (w/v) K_2CO_3 (~16 mL) in MeOH and heated under reflux in air for 20 hrs. The reaction stopped and water (3 mL) was added. Then cold concentrated HCl was added dropwise to the mixture until it reached pH 2. Peachy coloured solid precipitated out of the mixture, reaction flask was placed in the freezer for a couple of hrs. The solid compound was then filtered and recrystallized with 95% ethanol to afford the product as brownish-peach coloured crystals (1.07 g, 68%).

$R_f = 0.74$ (hexanes-EtOAc, 1:3); 1H -NMR ($CDCl_3$, 400 MHz) δ 11.33 (s, 1H, OH), 7.76 (dd, $J_1 = 7.90$ Hz, $J_2 = 1.70$ Hz, 1H, Ar-H), 7.53-7.21 (m, 12H, Ar-H), 5.28 (s, 2H, CH_2), 5.21 (s, 2H, CH_2).



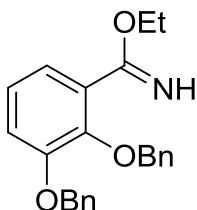
Molecular Weight: 333.39 g/mol

2,3-bis(benzyloxy)benzamide (18)

In a 50 mL round bottom flask, 2,3-dibenzyloxybenzoic acid (0.30 g, 0.89 mmol), DCM (20 mL) and Et₃N (0.188 mL, 1.35 mmol) were added. At 0 °C, thionyl chloride (0.065 mL, 1.35 mmol) was added to the stirring mixture which was continued stirring for 30 min under the same condition. Lastly, concentrated NH₄OH (2.2 mL) was added slowly at 0 °C, and continued stirring for 24 hrs at RT under N₂. The reaction mixture was then partitioned between DCM (15 mL) and H₂O (15 mL). The organic layer was washed with 5% Na₂CO₃ (15 mL) and then water (15 mL). The organic layer was then dried over MgSO₄, filtered, and concentrated to yield the crude product as a brown coloured solid. Recrystallization with 50% aqueous EtOH gave a white solid as the pure product (0.130 g, 44%).

¹H-NMR (CDCl₃, 400 MHz) δ 7.81 (br s, 1H, NH), 7.75-7.72 (m, 1H, Ar-*H*), 7.48-7.32 (m, 10H, Ar-*H*), 7.17-7.16 (m, 2H, Ar-*H*), 5.16 (s, 2H, CH₂), 5.09 (s, 2H, CH₂).

The ¹H-NMR was identical to the reported values.³³



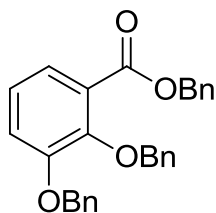
Molecular Weight: 361.44 g/mol

Ethyl-2,3-bis(benzyloxy)benzimidate (19)

In a 5 mL round bottom flask, 2,3-bis(benzyloxy)benzamide (0.01 g, 0.0299 mmol) and 1 mL of DCM were added. Then triethyloxonium hexafluorophosphate (0.009 g, 0.0363 mmol) and another 1 mL of DCM were added. The reaction mixture was stirred O/N at RT under N₂. Once the reaction was completed (monitored by TLC), cold 1M Na₂CO₃ (10 mL) was poured into a separatory funnel along with the reaction mixture. This was then extracted. The aqueous layer was re-extracted with DCM (2 x 10 mL) and the organic layer was dried over MgSO₄, filtered, and concentrated *in vacuo*. Purification by flash chromatography using a 15 mL sintered glass funnel (eluted with increasing amounts of EtOAc in hexanes; *fractions 2-3*) with silica gel afforded the title compound (0.02 g, > 99%) as a clear oil.

R_f = 0.90 (hexanes-EtOAc, 1:1); ¹H-NMR (CDCl₃, 400 MHz) δ 7.45-7.26 (m, 11H, Ar-*H*), 7.15-7.06 (m, 2H, Ar-*H*), 5.13 (d, *J* = 9.10Hz, 4H, CH₂), 4.32 (q, *J* = 7.10 Hz, 2H, CH₂), 1.31 (t, *J* = 7.10 Hz, 3H, CH₃).

The ¹H-NMR was identical to the reported values.³³

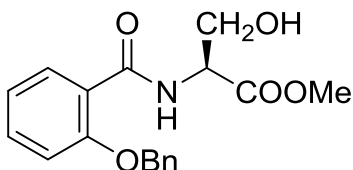


Molecular Weight: 424.50 g/mol

Benzyl - 2,3-bis (benzyloxy) benzoate

2,3-Dihydroxybenzoic acid (1.00 g, 6.49 mmol) was dissolved in acetone (50 mL). Anhydrous K_2CO_3 (4.03 g, 29.16 mmol) was added to the mixture and left to stir for 5 min at RT. Benzyl bromide (3.50 mL, 29.16 mmol) was added to the stirring mixture and then it was heated under reflux for 20 hrs in air. The solvent was removed under reduced pressure affording the product as peach coloured solid (2.13 g, 77%).

1H -NMR ($CDCl_3$, 400 MHz) δ 7.48-7.30 (m, 16H, Ar-*H*), 7.17 (d, J = 8.10 Hz, 1H, Ar-*H*), 7.12 (t, J = 7.90 Hz, 1H, Ar-*H*), 5.36 (s, 2H, CH_2), 5.16 (s, 2H, CH_2), 5.12 (s, 2H, CH_2).

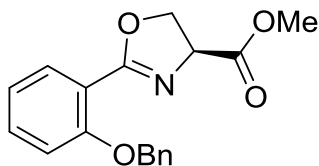


Molecular Weight: 329.35 g/mol

N-[2-(benzyloxy)benzoyl]-L-Serine methyl ester (20)

In a 50 mL round bottom flask, 2-(benzyloxy)benzoic acid (1.00 g, 4.38 mmol) and L-serine methyl ester hydrochloride (0.62 g, 3.96 mmol) was dissolved in 25 mL of DCM. Et₃N (0.59 mL, 4.23 mmol) and EDC·HCl (0.84 g, 4.38 mmol) was added to the reaction mixture, sealed with a septum and stirred O/N under N₂. The reaction mixture was diluted with DCM (10 mL) and washed with H₂O (35 mL), 5% NaHCO₃ solution (35 mL), 5% citric acid solution (35 mL), H₂O (35 mL), and brine (35 mL). The organic layer was dried over MgSO₄, filtered, and concentrated in *vacuo* which gave a yellow coloured oil as the crude product. The crude product was then recrystallized with toluene which afforded the product (0.39 g, 30%) as yellowish-white coloured crystals.

¹H-NMR (CDCl₃, 400 MHz) δ 8.74 (d, ³J = 6.90 Hz, 1H, NH), 8.16 (dd, *J*₁ = 7.80, *J*₂ = 1.90 Hz, 1H, Ar-*H*), 7.47-7.36 (m, 6H, Ar-*H*), 7.07-7.03 (m, 2H, Ar-*H*), 5.21 (d, *J* = 3.90 Hz, 2H, CH₂), 4.82-4.80 (m, 1H, CH), 3.89-3.84 (m, 2H, CH₂), 3.66 (s, 3H, CH₃).



Molecular Weight: 311.34 g/mol

(S)-Methyl 2-[2-(Benzyloxy)phenyl]-1,3-oxazoline-4-carboxylate (21)

In a 10 mL round bottom flask, *N*-[2-(benzyloxy)benzoyl]-L-serine methyl ester (**20**) (0.10 g, 0.30 mmol) was dissolved in THF (~5 mL) and Burgess reagent (0.079 g, 0.33 mmol) was added. The reaction mixture was refluxed for 30 min under N₂. The reaction was then diluted with EtOAc (10 mL) and washed with H₂O (15 mL) and then brine (15 mL). The organic layer was dried over Mg₂SO₄, filtered, and allowed to evaporate in a 50 mL beaker to yield a yellow coloured oil as the desired product (**22**) (0.056 g, 60%).

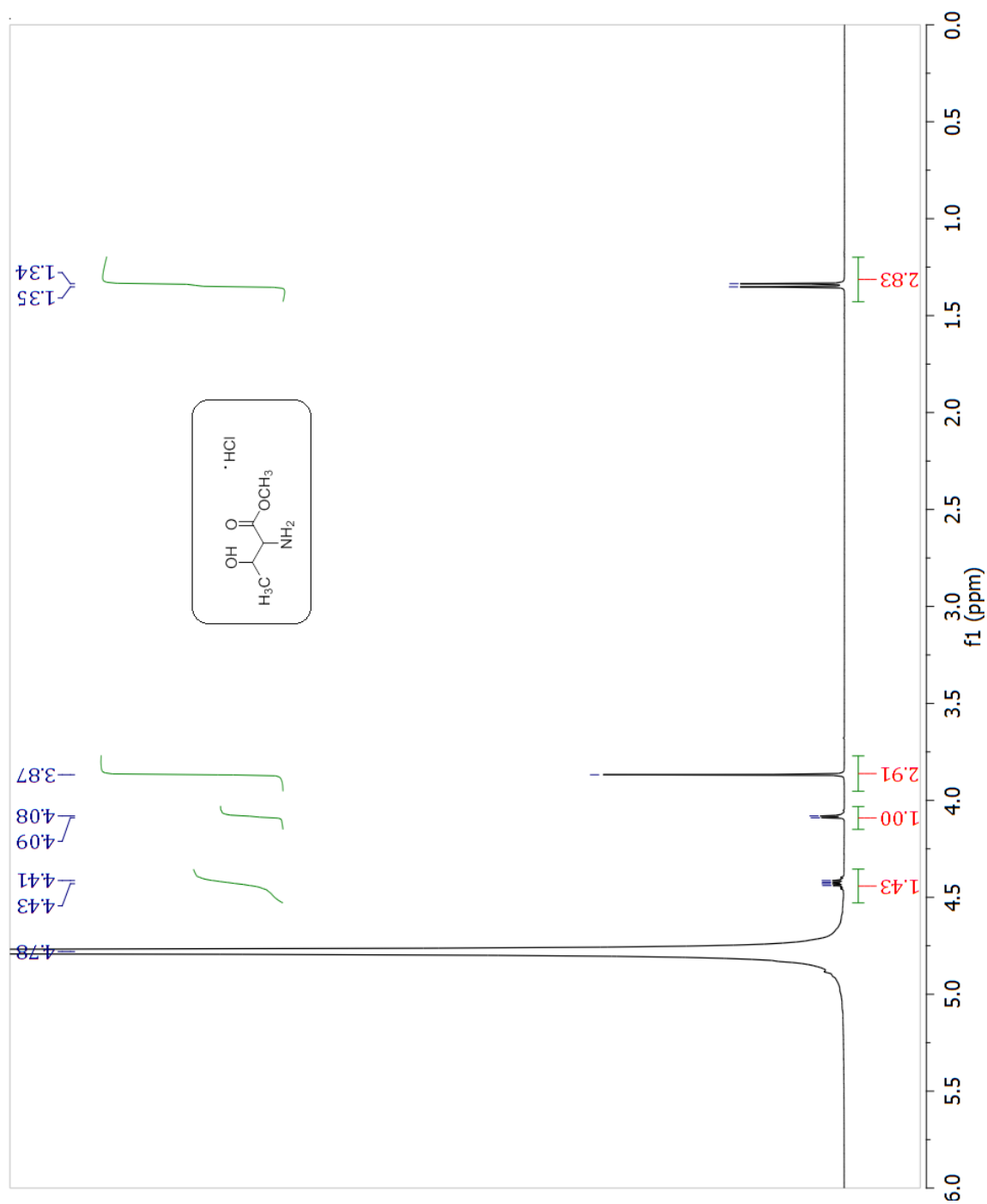
No purifications were performed for this product.

¹H-NMR (CDCl₃, 400 MHz) δ 7.82 (dd, *J*₁ = 7.50 Hz, *J*₂ = 1.80 Hz, 1H, Ar-*H*), 7.53-7.31 (m, 6H, Ar-*H*), 7.01 (dd, *J*₁ = 8.30 Hz, *J*₂ = 0.80 Hz, 2H, Ar-*H*), 5.21 (s, 2H, CH₂), 4.99 (dd, ³*J*₁ = 10.60 Hz, ³*J*₂ = 8.10 Hz, 1H, CH), 4.62-4.57 (m, 2H, CH₂), 3.83 (s, 3H, CH₃).

5. Appendix

Figure A1.1:	¹ H-NMR of L-Threonine Methyl Ester Hydrochloride (1) in D ₂ O	79
Figure A1.2:	¹³ C-NMR of L-Threonine Methyl Ester Hydrochloride (1) in D ₂ O	80
Figure A1.3:	¹ H-NMR of L-Threonine Benzyl Ester (2) in CDCl ₃	81
Figure A1.4:	¹³ C-NMR of L-Threonine Benzyl Ester (2) in CDCl ₃	82
Figure A1.5:	¹ H-NMR of <i>N</i> -(<i>o,m</i>)-Dimethyloxybenzoyl-L-Threonine methyl ester (3) in CDCl ₃	83
Figure A1.6:	¹³ C-NMR of <i>N</i> -(<i>o,m</i>)-Dimethyloxybenzoyl-L-Threonine methyl ester (3) in CDCl ₃	84
Figure A1.7:	¹ H-NMR of <i>N</i> -(<i>o,m</i>)-Dimethoxybenzoyl-L-Threonine benzyl ester (4) in CDCl ₃	85
Figure A1.8:	¹³ C-NMR of <i>N</i> -(<i>o,m</i>)-Dimethoxybenzoyl-L-Threonine benzyl ester (4) in CDCl ₃	86
Figure A1.9:	¹ H-NMR ((<i>4S,5R</i>)-2-(<i>o,m</i>)-Dimethoxyphenyl)-5-methyl-4- oxazolinecarboxylic acid methyl ester (5) in CDCl ₃	87
Figure A1.10:	¹³ C-NMR ((<i>4S,5R</i>)-2-(<i>o,m</i>)-Dimethoxyphenyl)-5-methyl-4- oxazolinecarboxylic acid methyl ester (5) in CDCl ₃	88
Figure A1.11:	¹ H-NMR of (<i>4S,5R</i>)-2-(<i>o,m</i>)-Dimethoxyphenyl)-5-methyl-4- oxazolinecarboxylic acid benzyl ester (6) in CDCl ₃	89
Figure A1.12:	¹³ C-NMR of (<i>4S,5R</i>)-2-(<i>o,m</i>)-Dimethoxyphenyl)-5-methyl-4- oxazolinecarboxylic acid benzyl ester (6) in CDCl ₃	90
Figure A1.13:	¹ H-NMR of Boc-1, 4-diaminobutane (8) in CDCl ₃	91
Figure A1.14:	¹ H-NMR of <i>N</i> -Boc (1,4-aminobutyl)-2,3-(dimethoxyphenyl) benzamide (9) in CDCl ₃	92

Figure A1.15:	^{13}C -NMR of <i>N</i> -Boc (1,4-aminobutyl)-2,3-(dimethoxyphenyl) benzamide (9) in CDCl_3	93
Figure A1.16:	^1H -NMR of <i>N</i> -Boc(1,4-aminobutyl)-[2,3-bis(benzyloxy)phenyl]benzamide (10) in CDCl_3	94
Figure A1.17:	^1H -NMR of <i>N</i> -(2,3-dimethoxybenzoyl)-1,4-diaminobutane (12) in CDCl_3	95
Figure A1.18:	2D (^1H , ^1H)-COSY-NMR of <i>N</i> -(2,3-dimethoxybenzoyl)-1,4-diaminobutane (12) in CDCl_3	96
Figure A1.19:	2D (^1H , ^{13}C)-HSQC-NMR of <i>N</i> -(2,3-dimethoxybenzoyl)-1,4-diaminobutane (12) in CDCl_3	97
Figure A1.20:	2D (^1H , ^{13}C)-HMBC-NMR of <i>N</i> -(2,3-dimethoxybenzoyl)-1,4-diaminobutane (12) in CDCl_3	98
Figure A1.21:	^1H -NMR of <i>N,N</i> -Bis(2,3 –bis(methoxy)benzoyl)-1,4 –diaminobutane (13) in CDCl_3	99
Figure A1.22:	^1H -NMR of DMTMM (14) in CD_3OD	100
Figure A1.23:	^1H -NMR of <i>N</i> -Bis-(2,3-Dimethoxybenzoyl)-1,4-diaminobutane (15) in CD_3OD	101
Figure A1.24:	^1H -NMR of 2, 3-Dibenzyloxybenzaldehyde (16) in CDCl_3	102
Figure A1.25:	^1H -NMR of 2, 3-Bis (benzyloxy) benzoic acid (17) in CDCl_3	103
Figure A1.26:	^1H -NMR of 2, 3-Bis (benzyloxy) benzamide (18) in CDCl_3	104
Figure A1.27:	^1H -NMR of Ethyl-2, 3-Bis (benzyloxy) Benzimidate (19) in CDCl_3	105
Figure A1.28:	^1H -NMR of Benzyl-2, 3-Bis (Benzyloxy) Benzoate in CDCl_3	106
Figure A1.29:	^1H -NMR of <i>N</i> -[2-(benzyloxy) benzoyl]-L-Serine methyl ester (20) in CDCl_3	107
Figure A1.30:	^1H -NMR of (S)-Methyl 2-[2-Benzyloxy) phenyl]-1,3-oxazoline-4-carboxylate (21) in CDCl_3	108



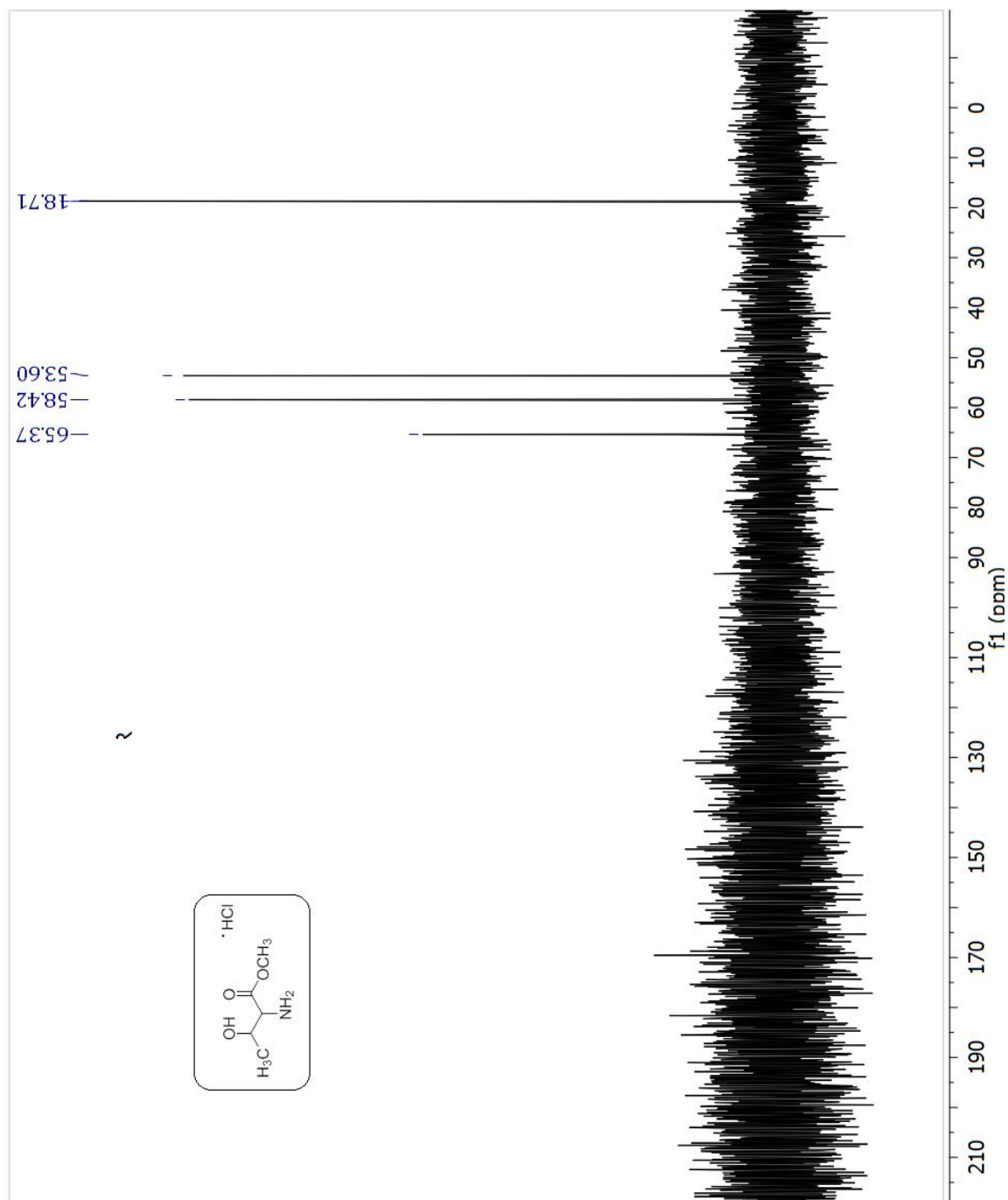


Figure A1.2: ^{13}C -NMR of L-Threonine Methyl Ester Hydrochloride (1) in D_2O

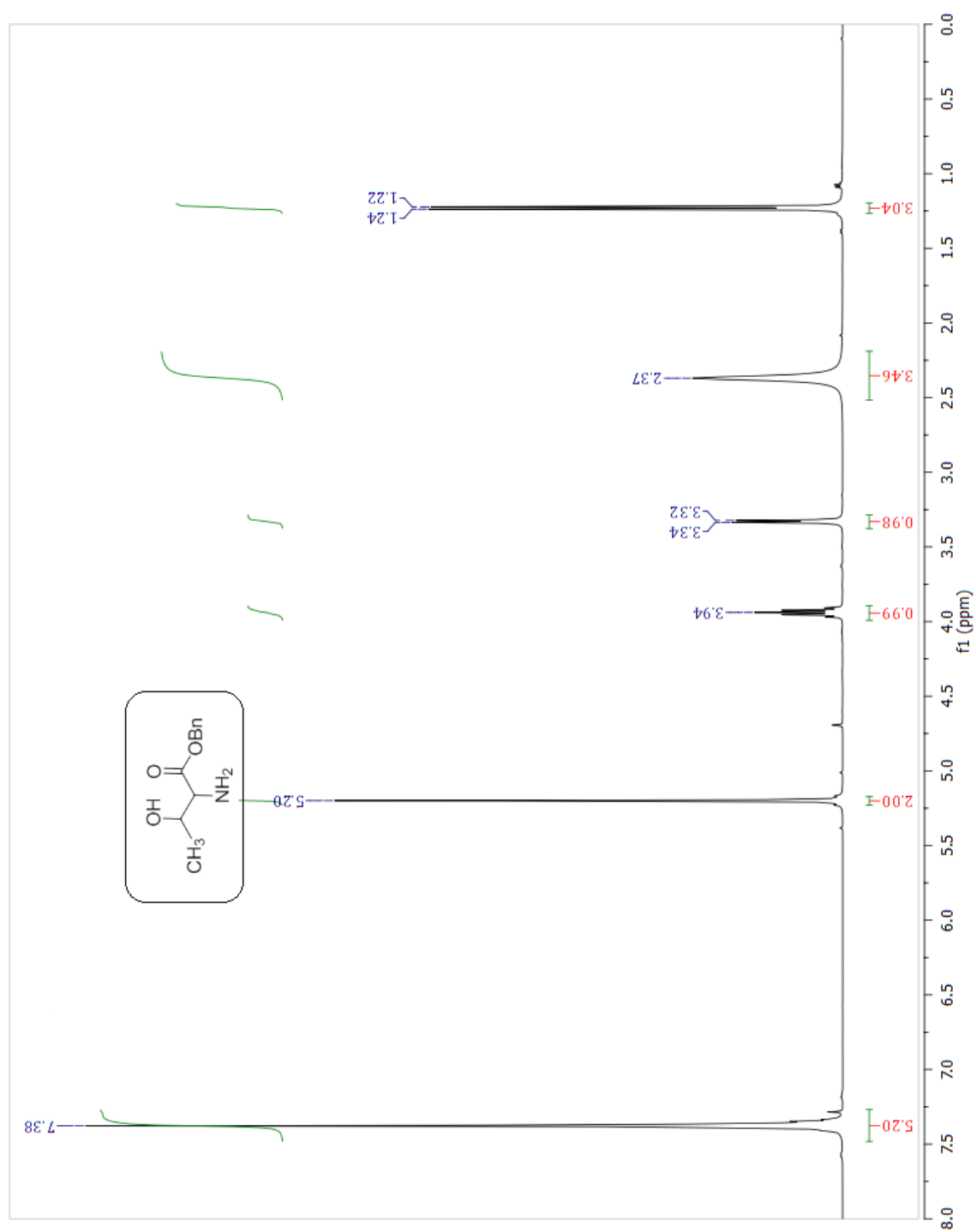


Figure A1.3: ^1H -NMR of L-Threonine Benzyl Ester (2) in CDCl_3

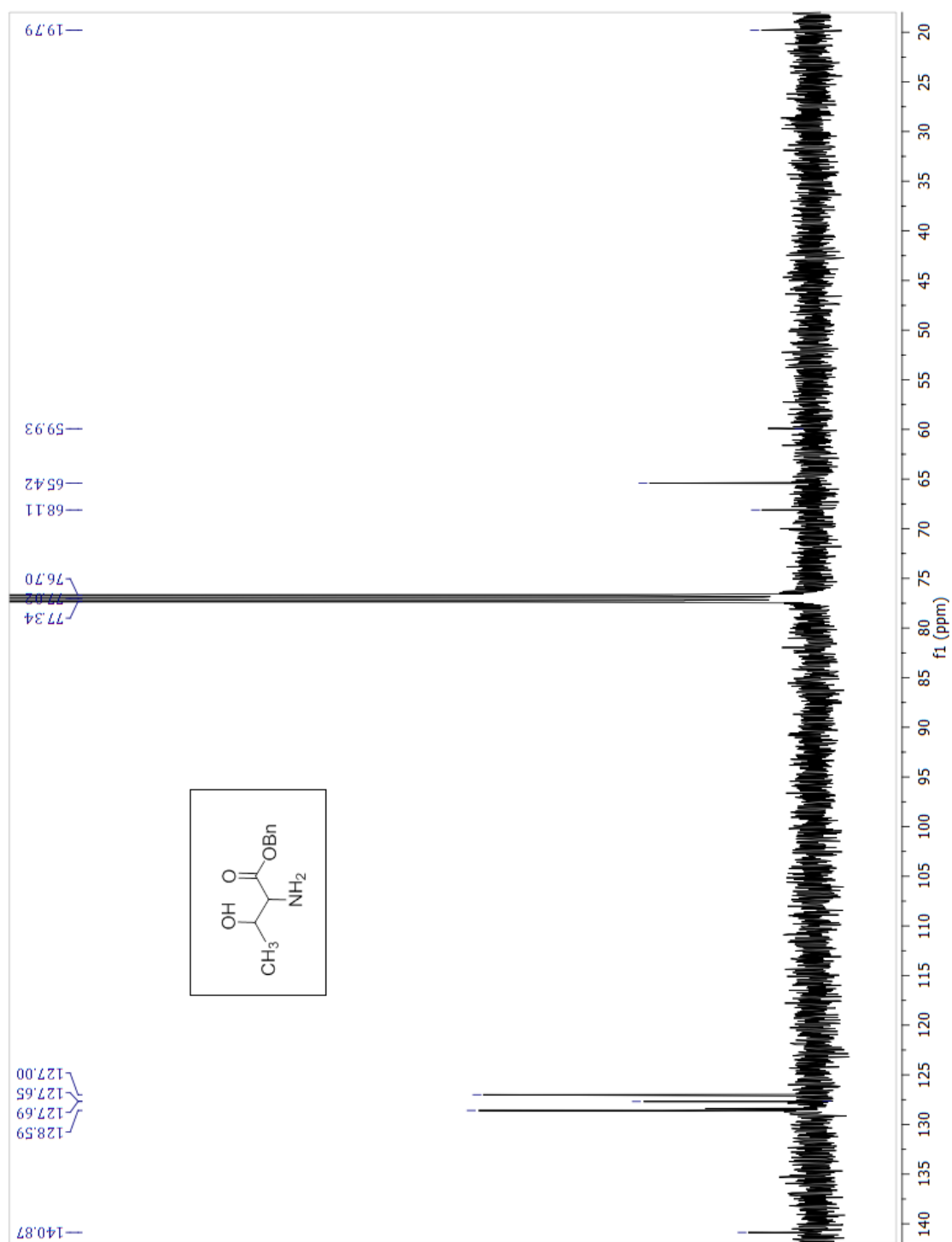


Figure A1.4: ¹³C-NMR of L-Threonine Benzyl Ester (2) in CDCl₃

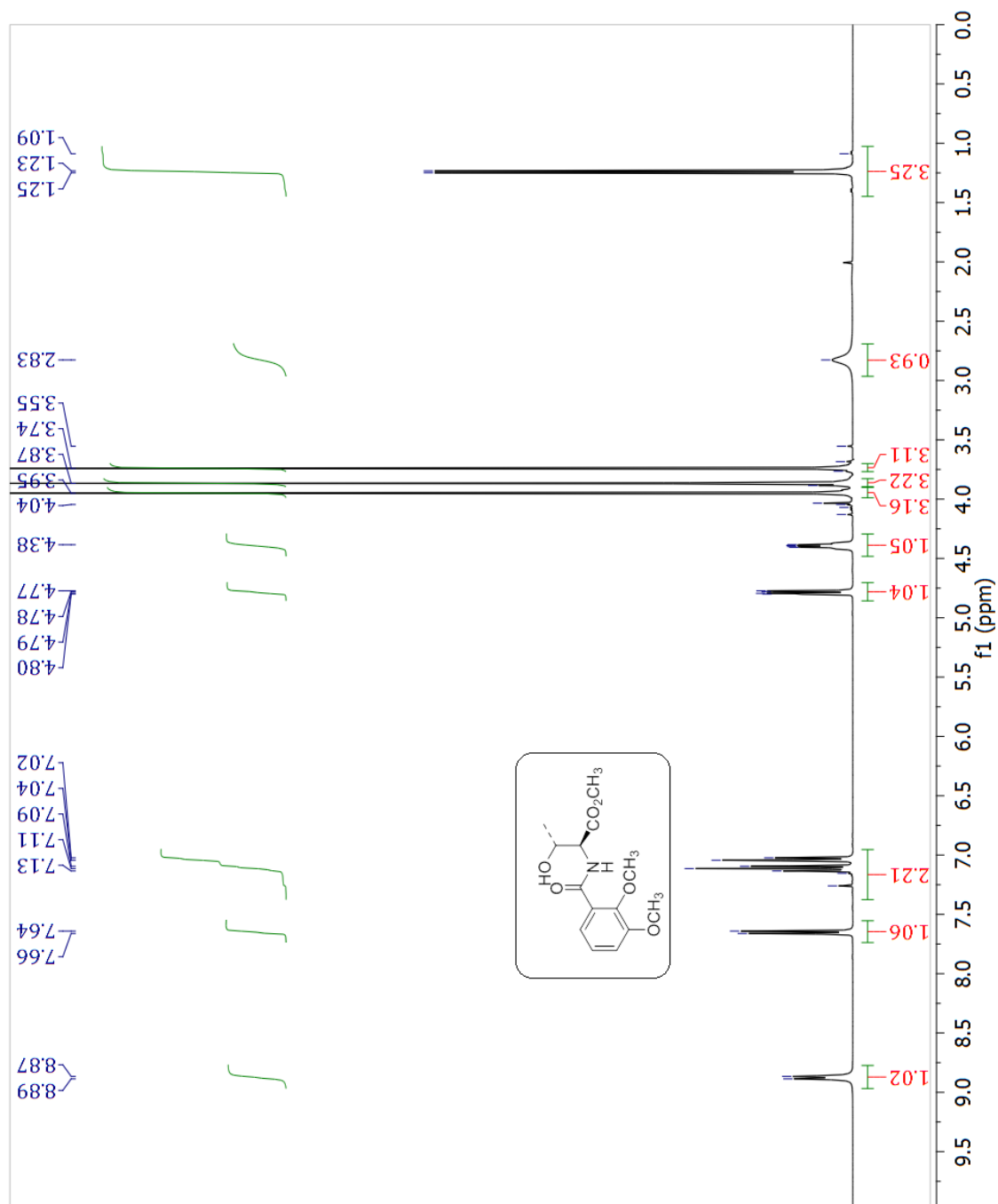


Figure A1.5: ¹H-NMR of *N*-(*o,m*)-Dimethyloxybenzyl-L-Threonine methyl ester (**3**) in CDCl₃

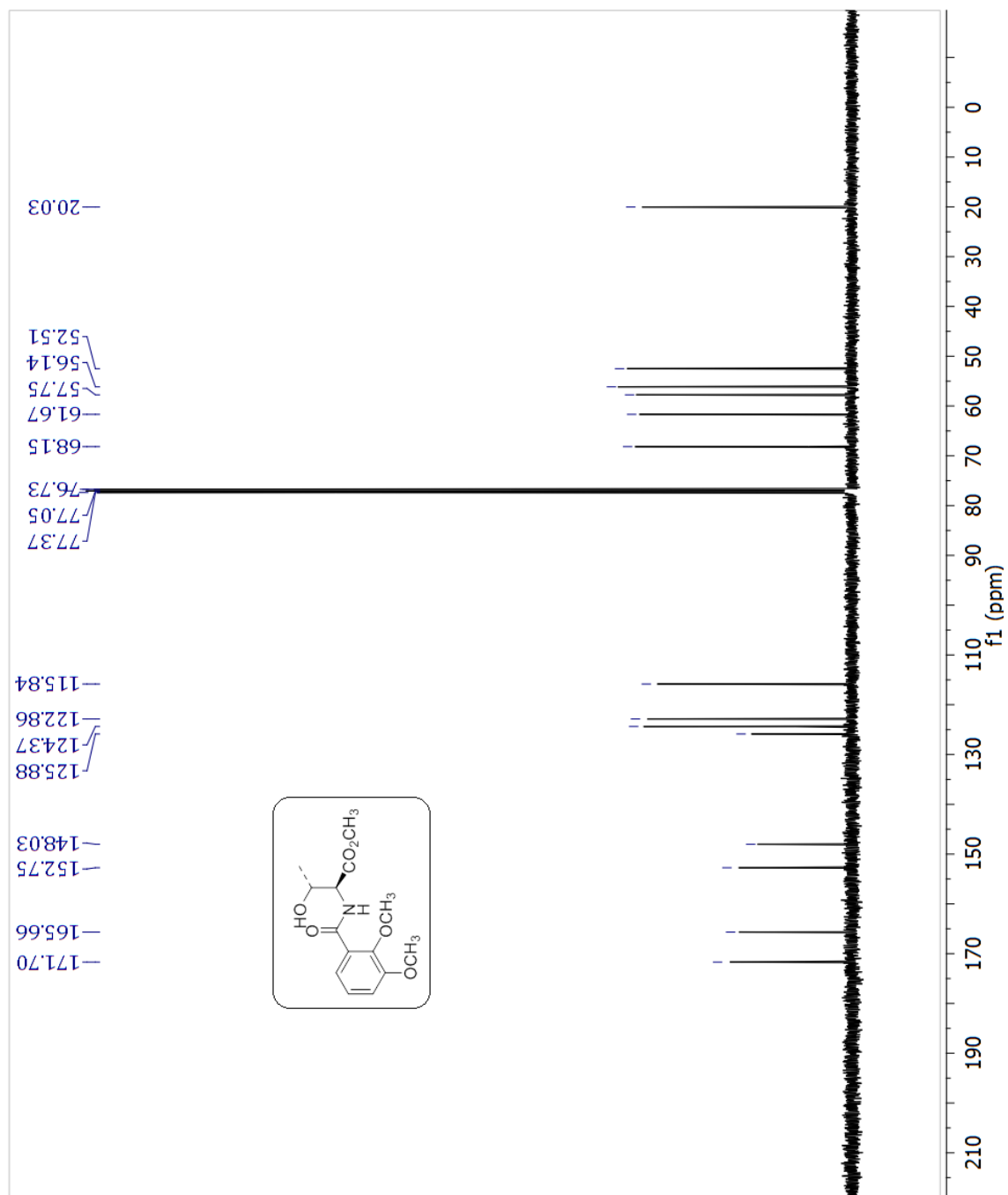


Figure A1.6: ¹³C-NMR of *N*-(*o,m*)-Dimethyloxybenzoyl-L-Threonine methyl ester (**3**) in CDCl₃

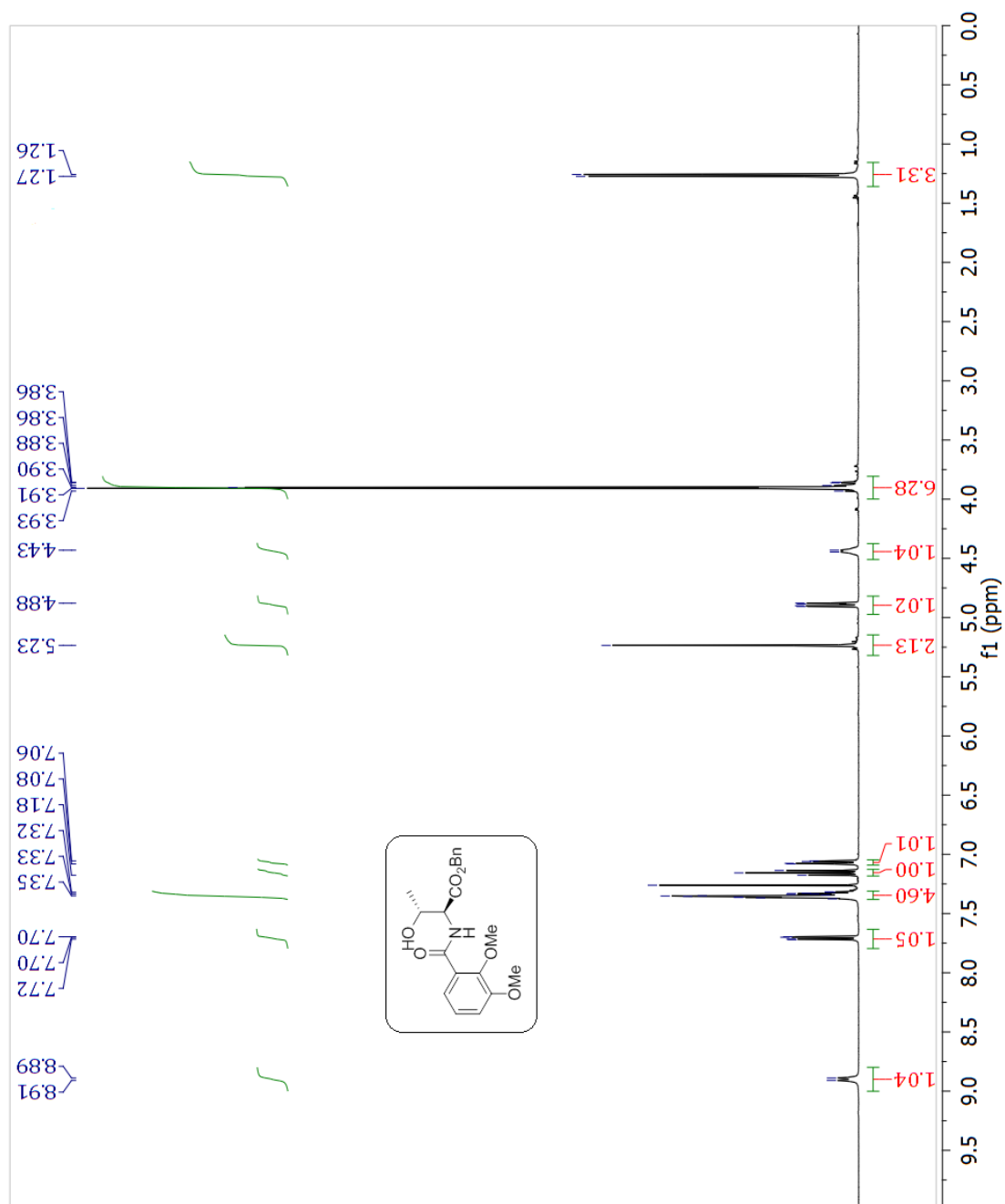


Figure A1.7: ¹H-NMR of *N*-(*o,m*)-Dimethoxybenzoyl-L-Threonine benzyl ester (**4**) in CDCl₃

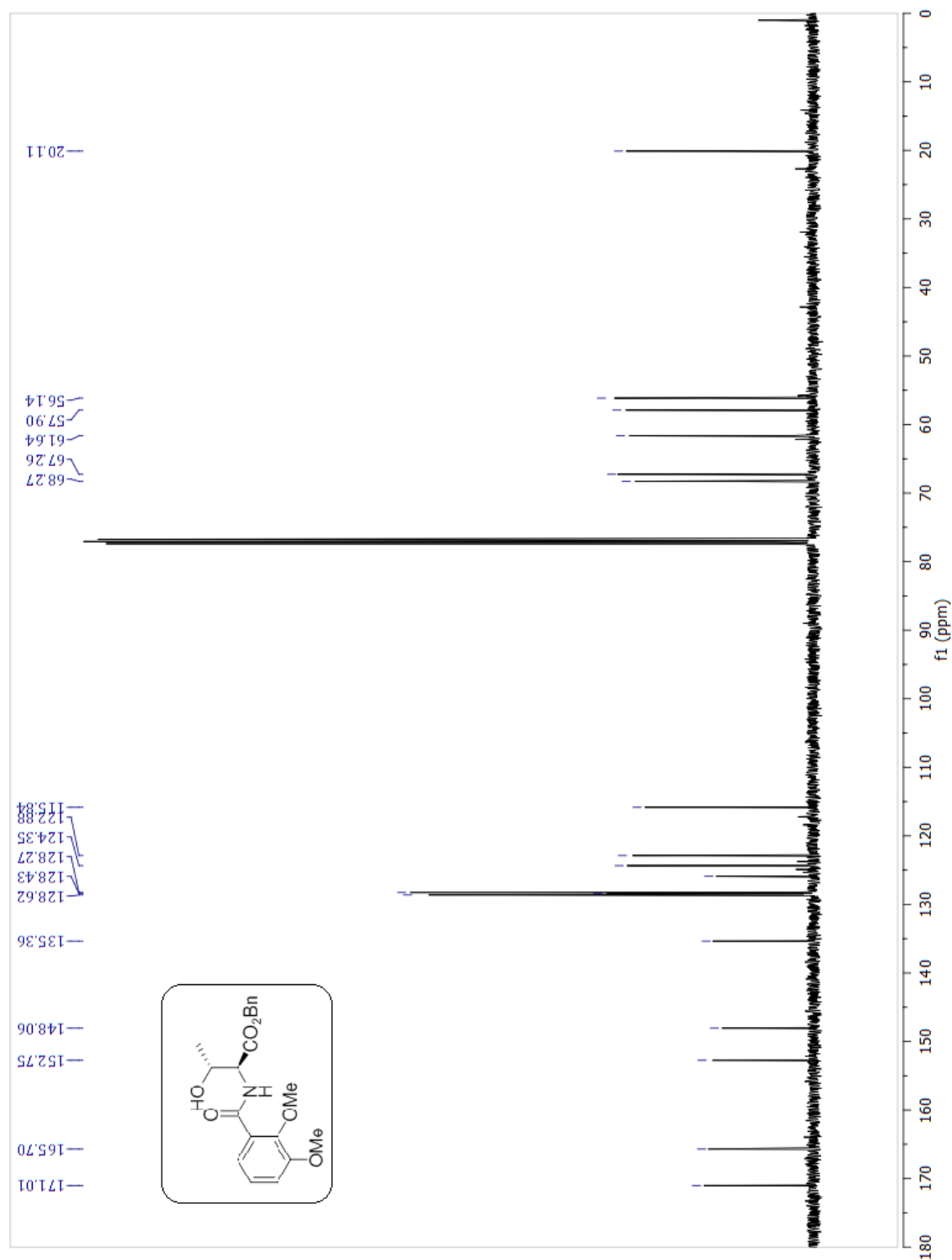


Figure A1.8: ¹³C-NMR of *N*-(*o,m*)-Dimethoxybenzoyl-L-Threonine benzyl ester (**4**) in CDCl₃

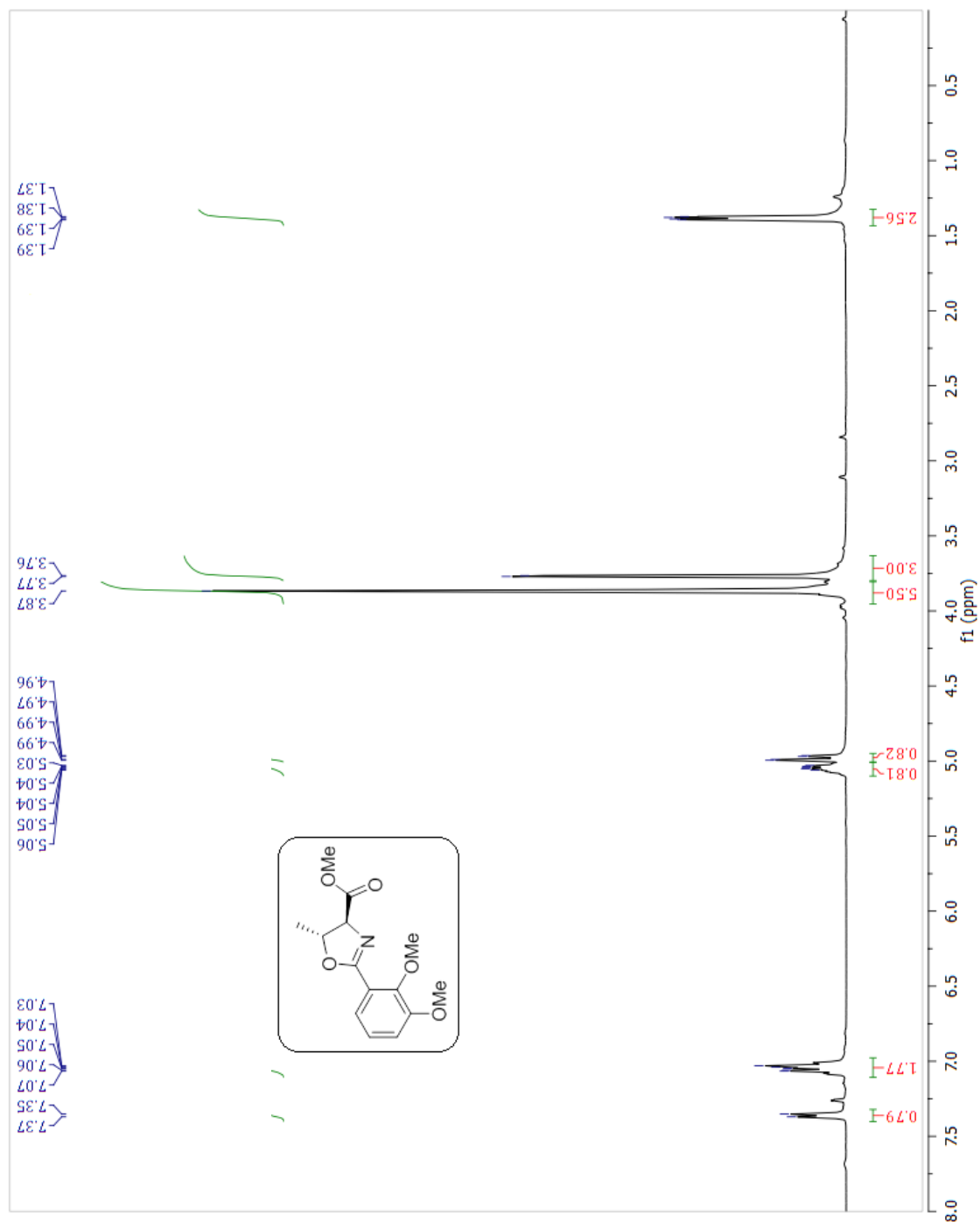


Figure A1.9: ¹H-NMR ((4*S*, 5*R*)-2-(*o,m*)-Dimethoxyphenyl)-5-methyl-4-oxazolinecarboxylic acid methyl ester (**5**) in CDCl₃

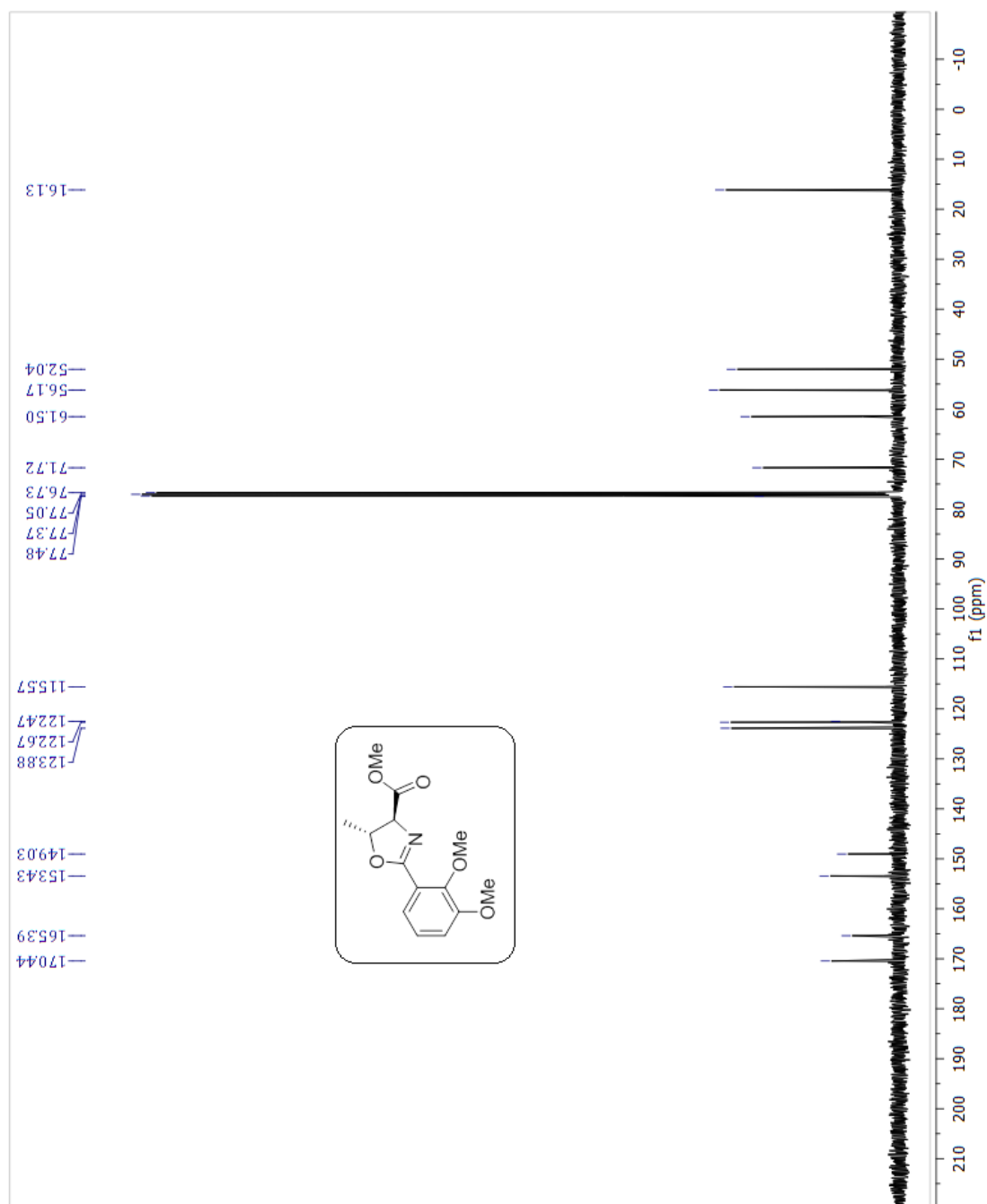


Figure A1.10: ¹³C-NMR ((4*S*,5*R*)-2-(*o,m*)-Dimethoxyphenyl)-5-methyl-4-oxazolinecarboxylic acid methyl ester (**5**) in CDCl₃

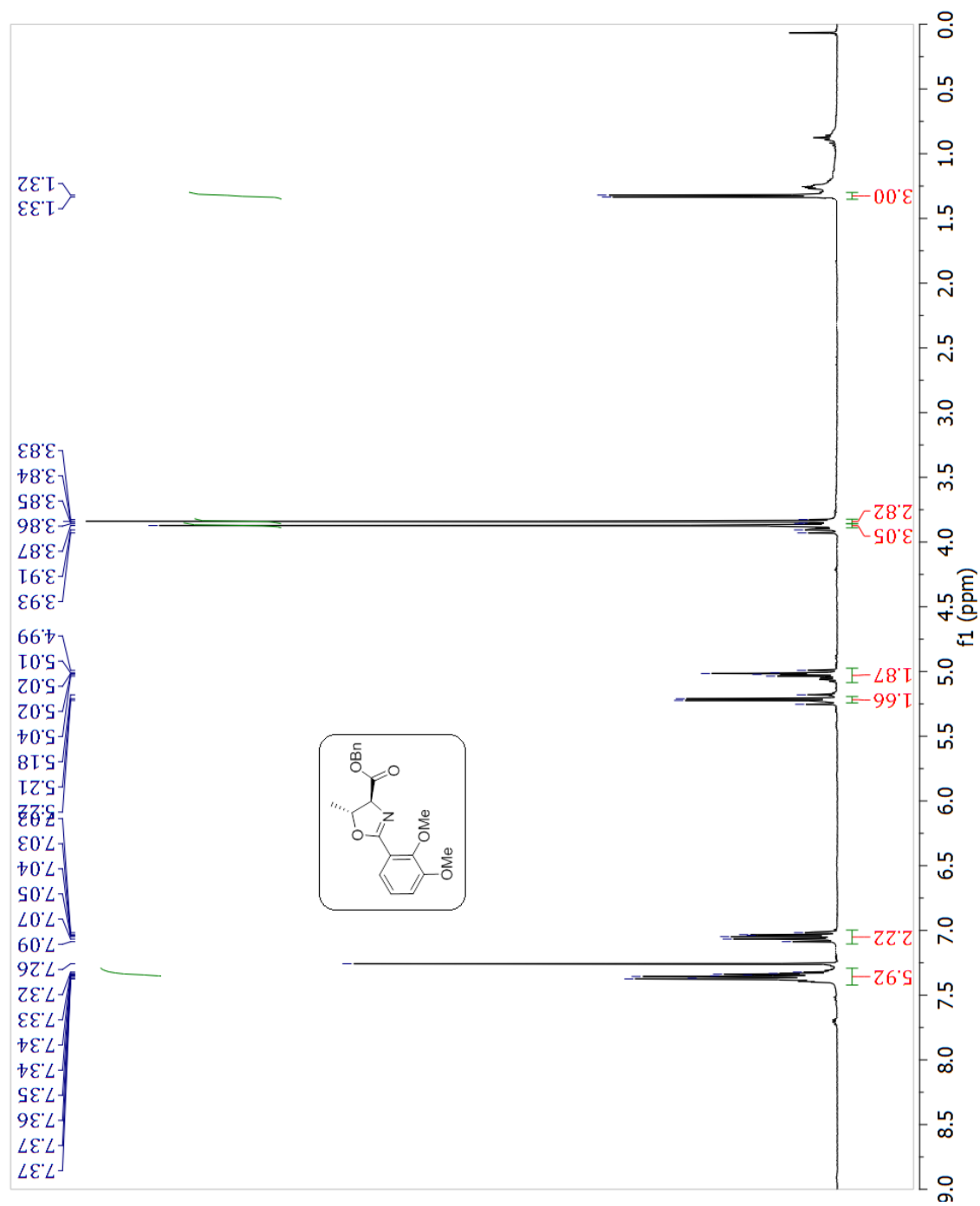


Figure A1.11: ¹H-NMR of (4S,5R)-2-(o,m)-Dimethoxyphenyl)-5-methyl-4-oxazolinecarboxylic acid benzyl ester (**6**) in CDCl₃

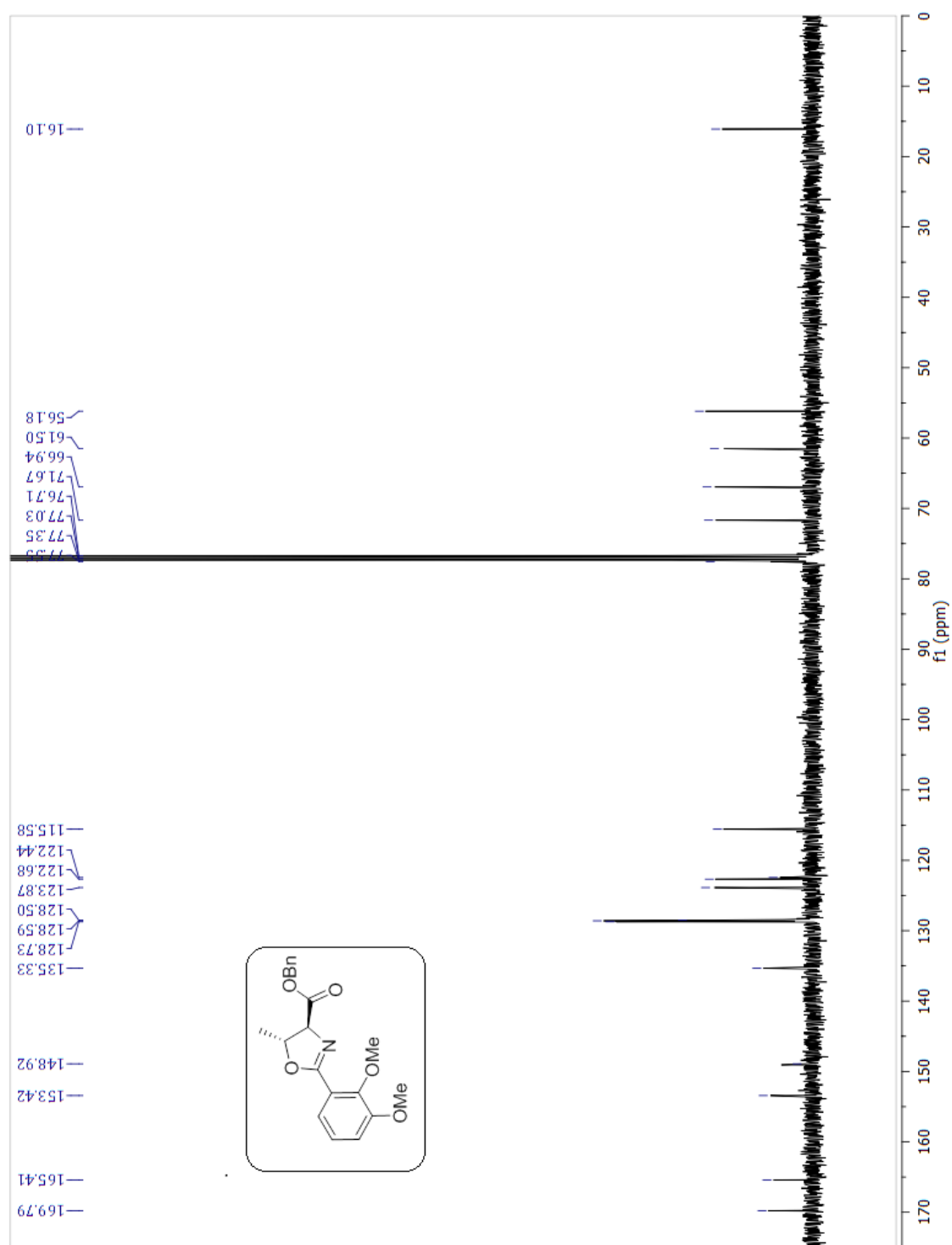


Figure A1.12: ^{13}C -NMR of (4*S*,5*R*)-2-(*o,m*)-Dimethoxyphenyl)-5-methyl-4-oxazolinecarboxylic acid benzyl ester (**6**) in CDCl_3

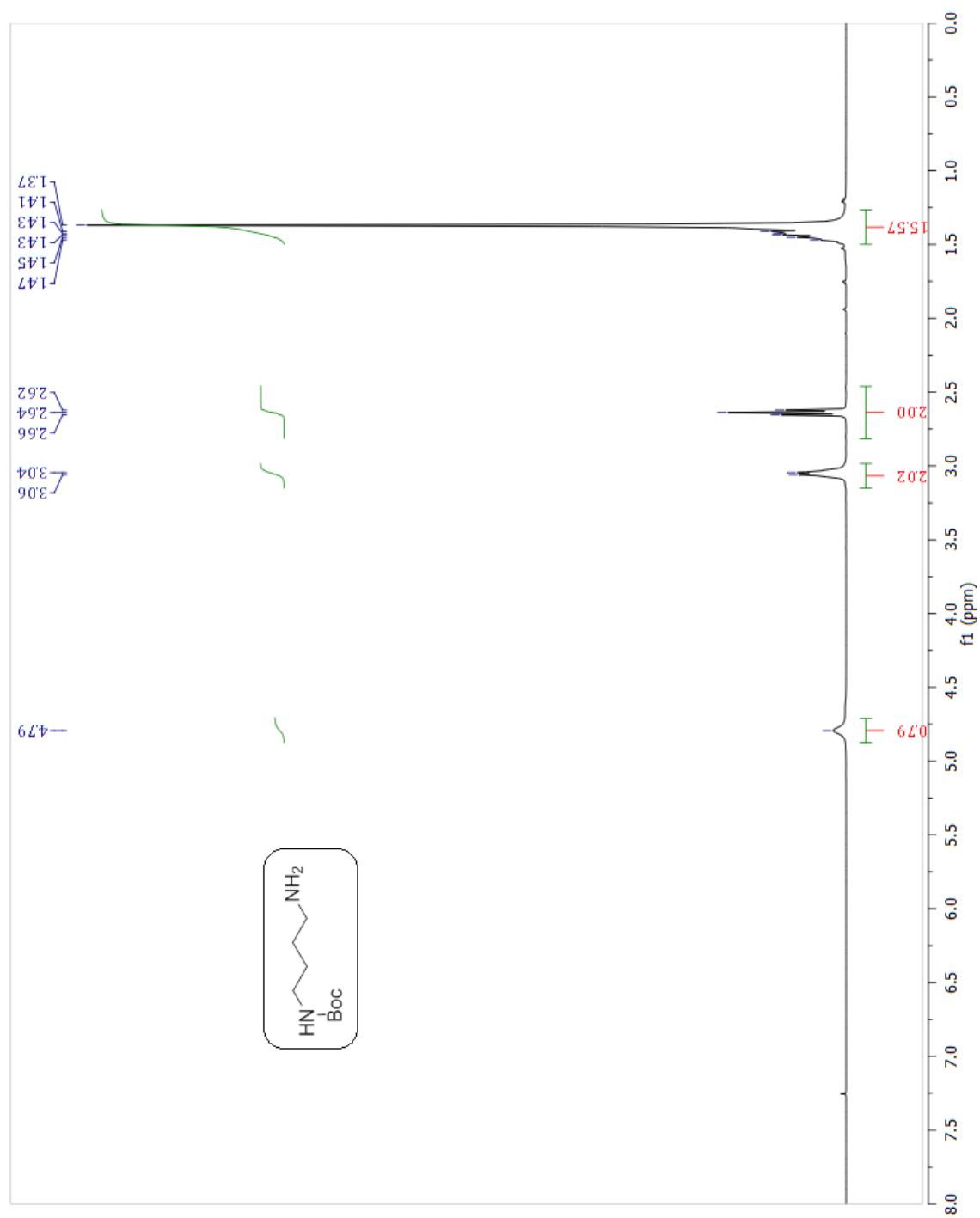


Figure A1.13: ¹H-NMR of Boc-1, 4-diaminobutane (8) in CDCl₃

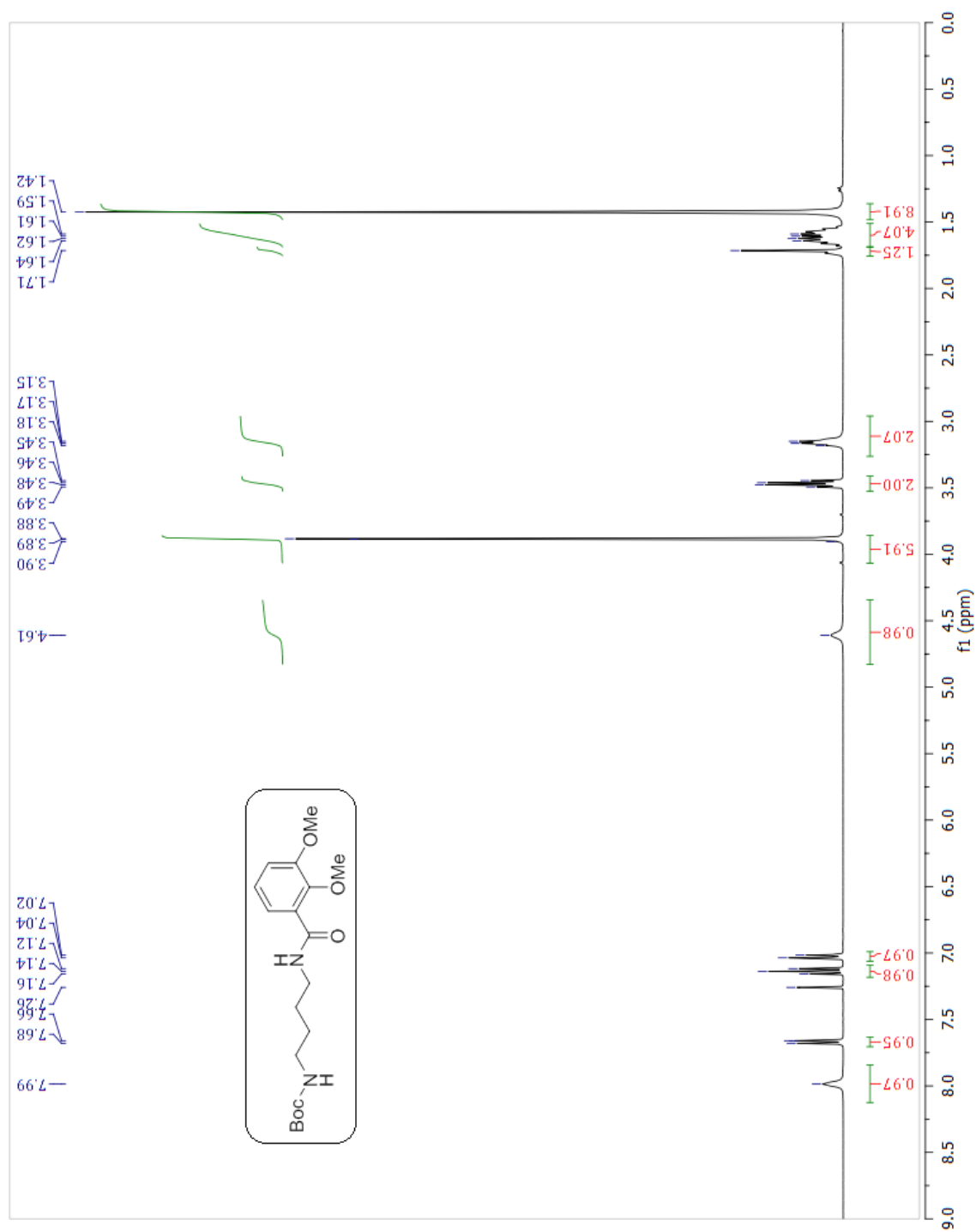


Figure A1.14: ¹H-NMR of *N*-Boc (1,4-aminobutyl)-2,3,3-(dimethoxyphenyl) benzamide (**9**) in CDCl₃

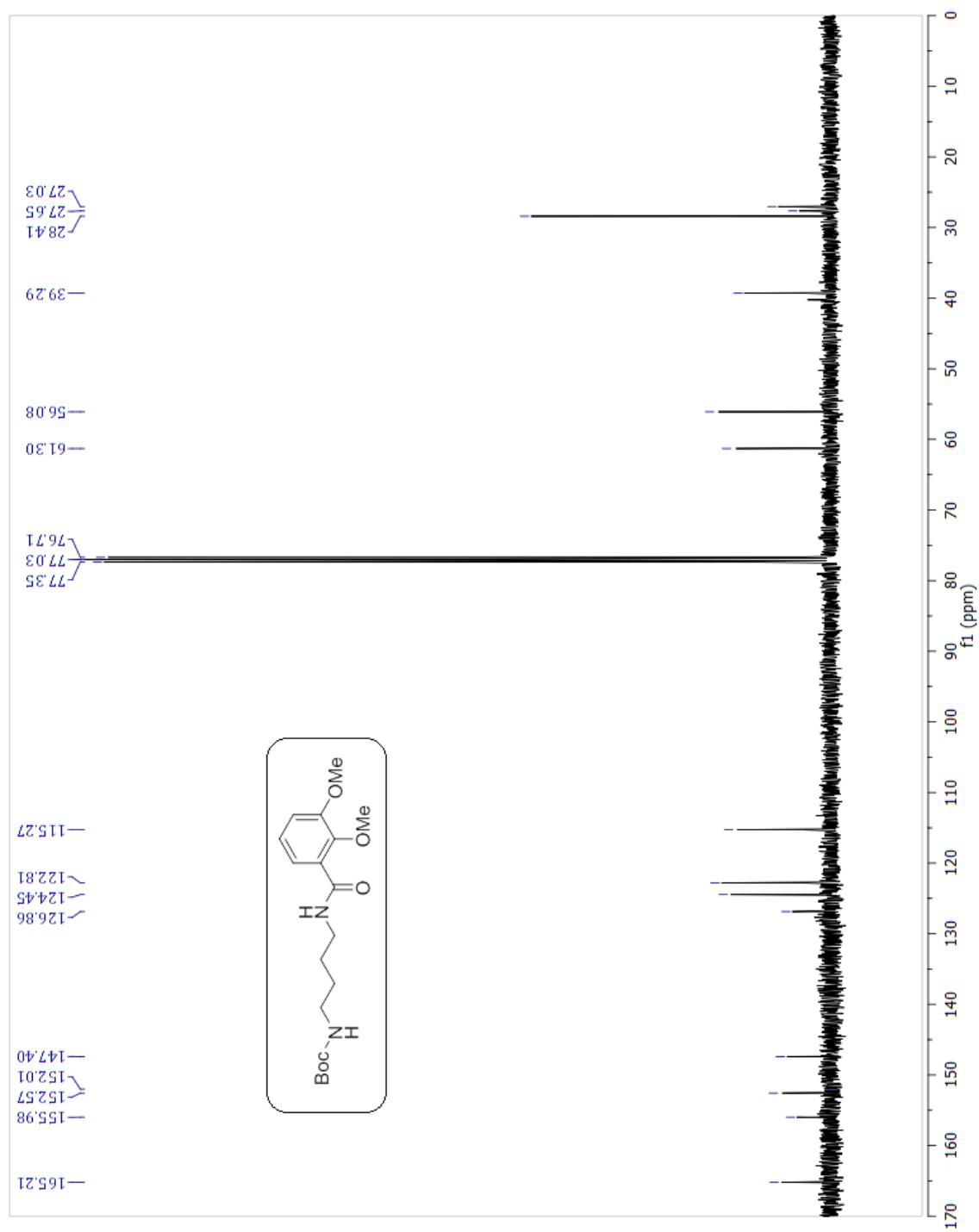


Figure A1.15: ^{13}C -NMR of N-Boc (1,4-aminobutyl)-2,3-(dimethoxyphenyl) benzamide (**9**) in CDCl_3

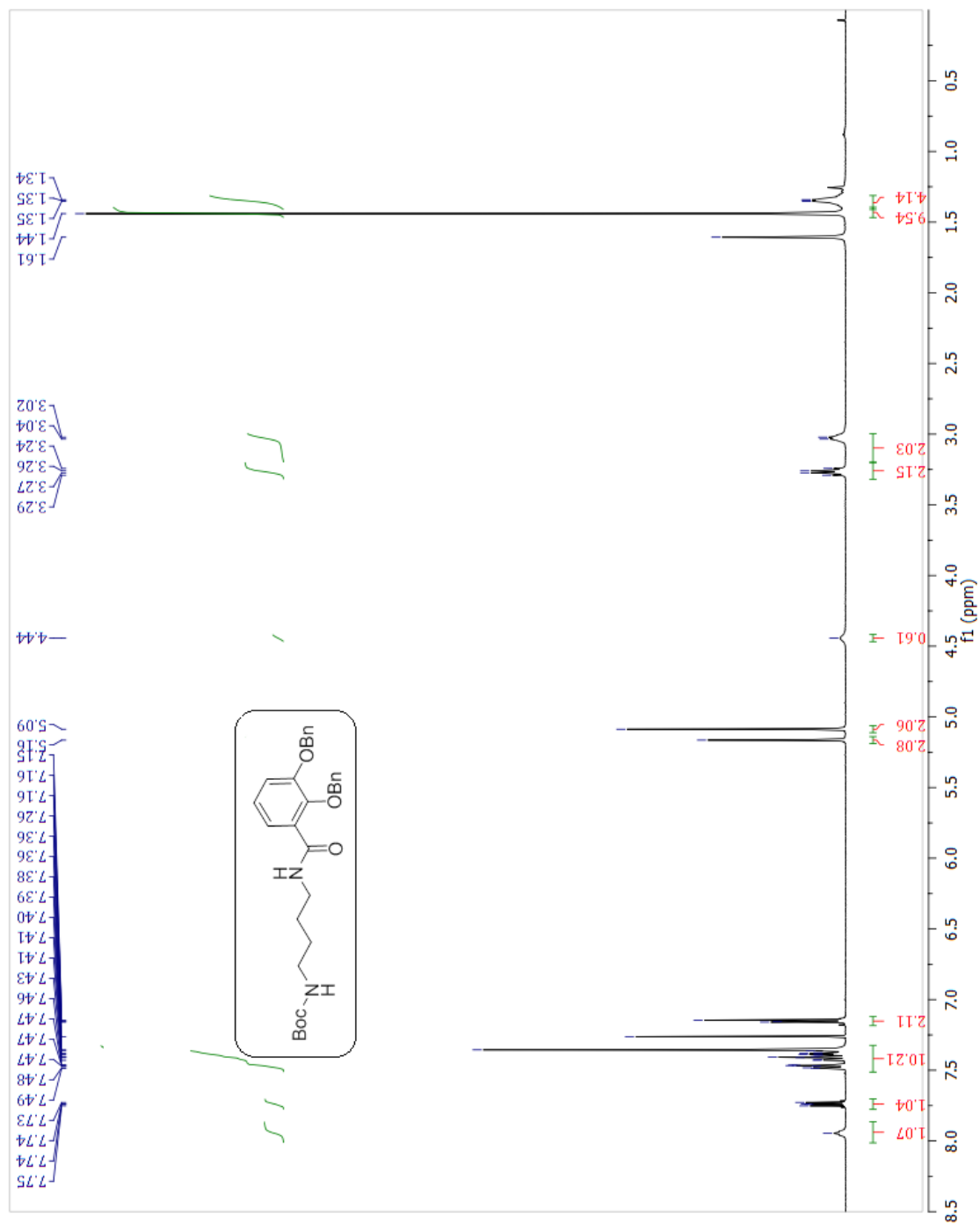


Figure A1.16: ¹H-NMR of *N*-Boc(1,4-aminobutyl)-[2,3-bis(benzyloxy)phenyl]benzamide (**10**) in CDCl₃

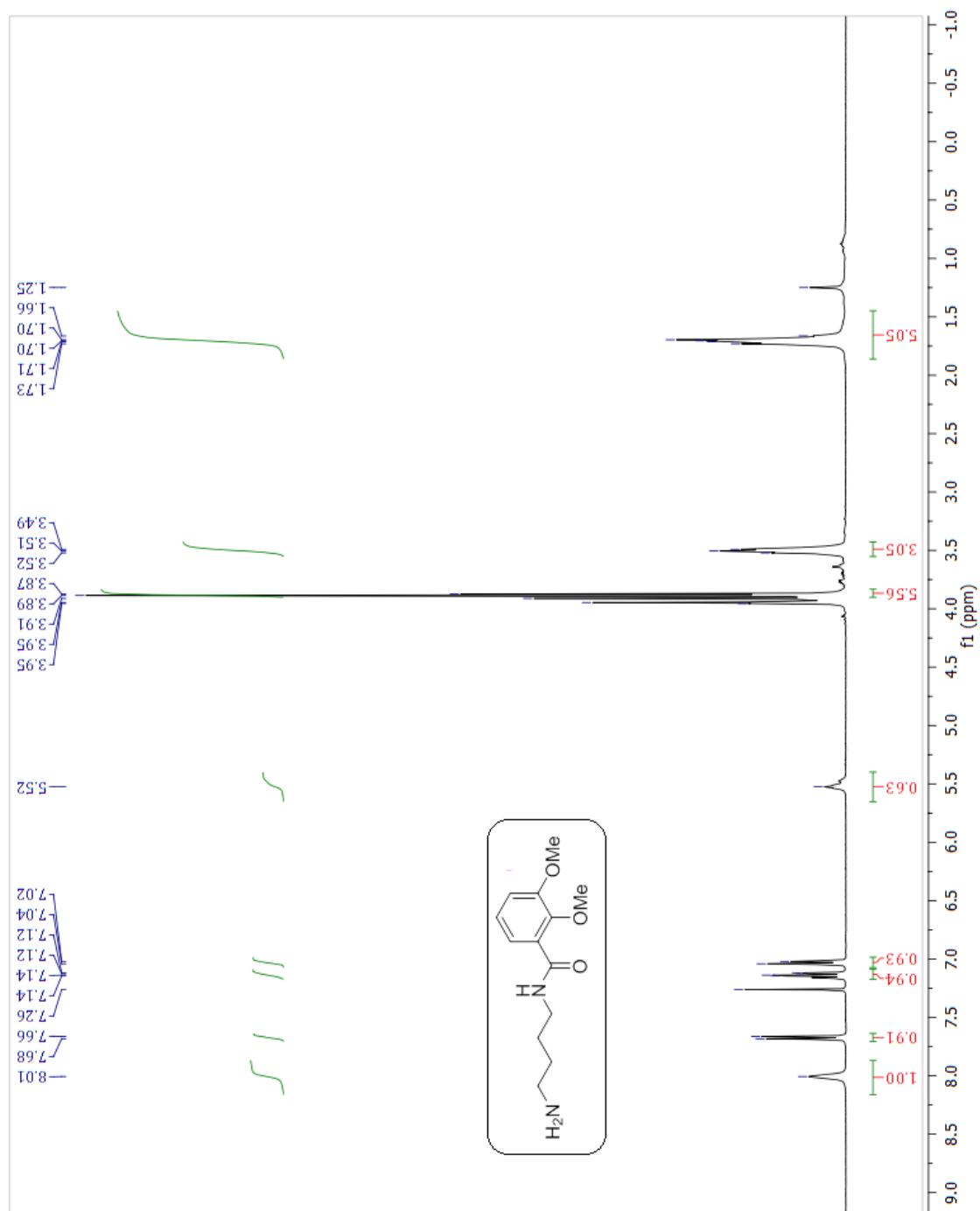


Figure A1.17: ¹H-NMR of *N*-(2,3-dimethoxybenzoyl)-1,4-diaminobutane (**12**) in CDCl₃

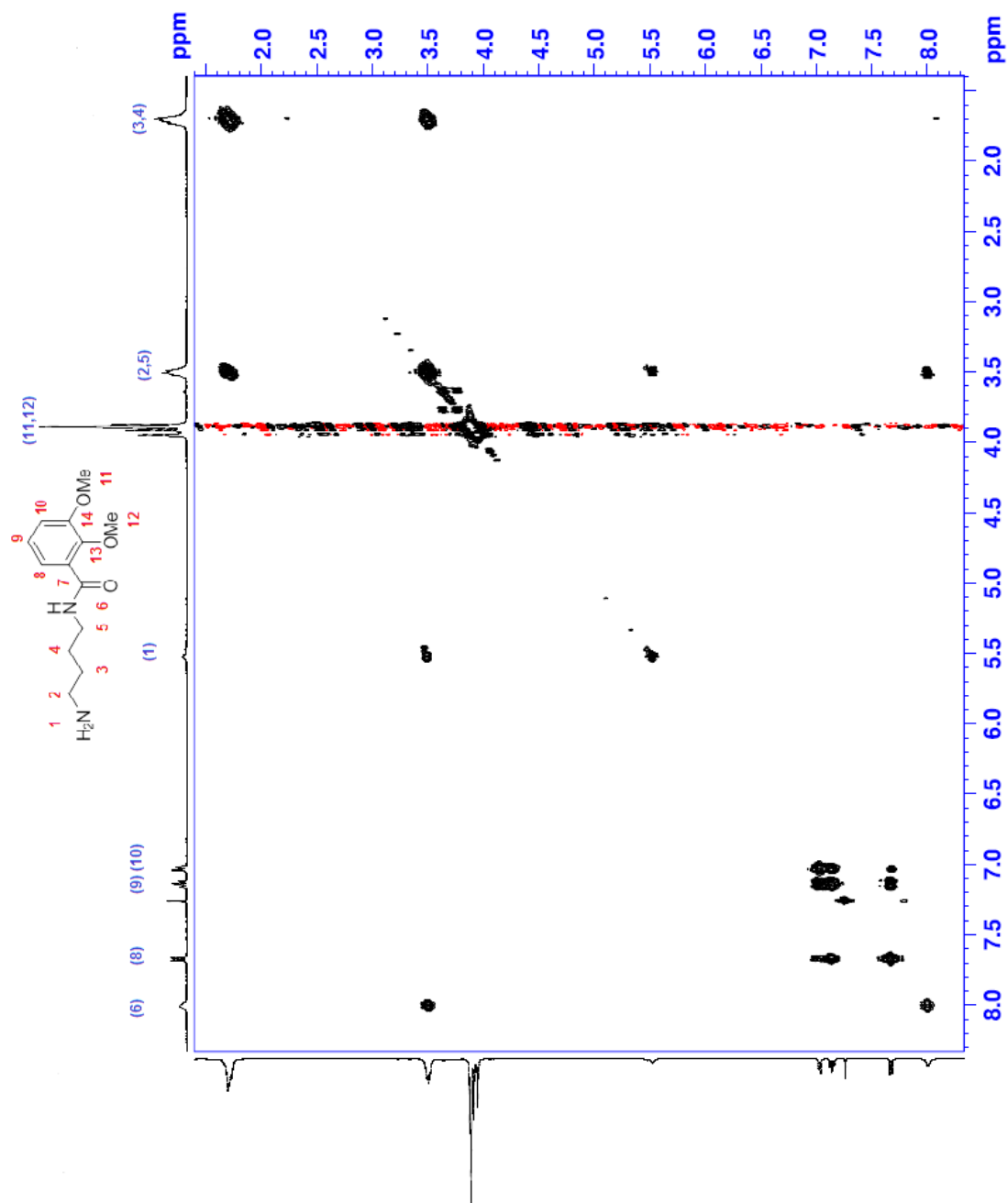


Figure A1.18: 2D (^1H , ^1H)-COSY-NMR of *N*-(2,3-dimethoxybenzoyl)-1,4-diaminobutane (12) in CDCl_3

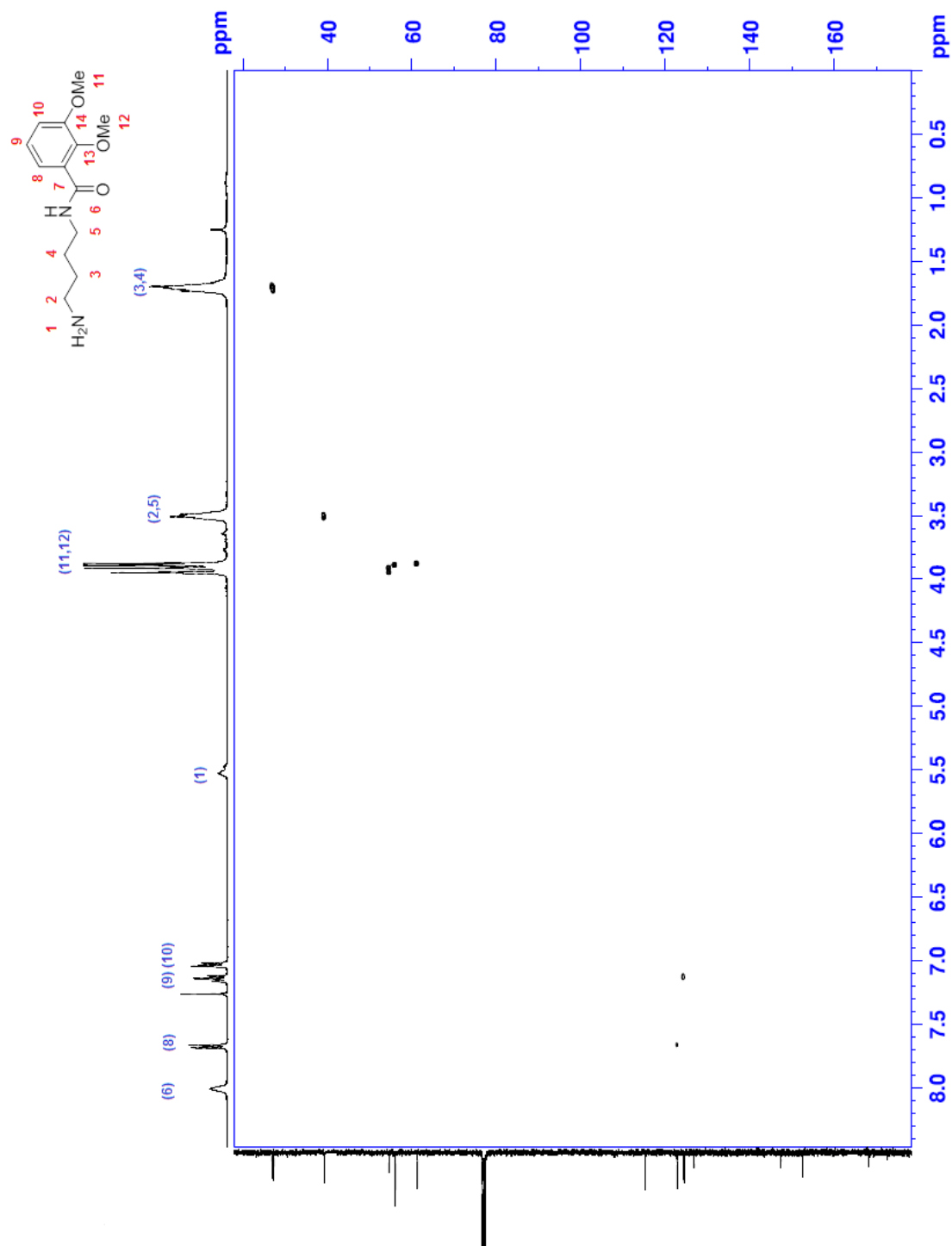


Figure A1.19: 2D (¹H, ¹³C)-HSQC-NMR of *N*-(2,3-dimethoxybenzoyl)-1,4-diaminobutane (**12**) in CDCl₃

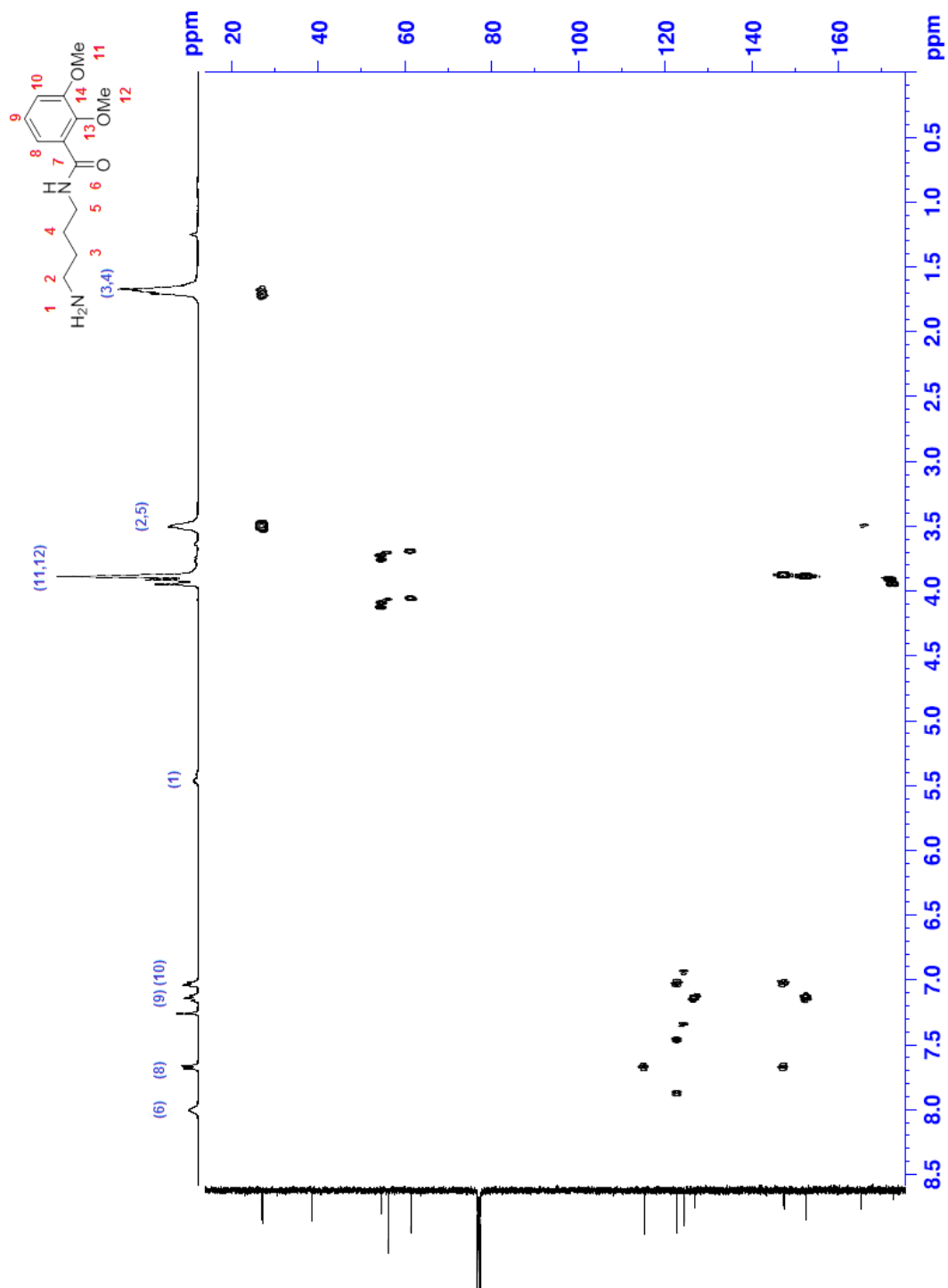


Figure A1.20: 2D (¹H, ¹³C)-HMBC-NMR of *N*-(2,3-dimethoxybenzoyl)-1,4-diaminobutane (**12**) in CDCl₃

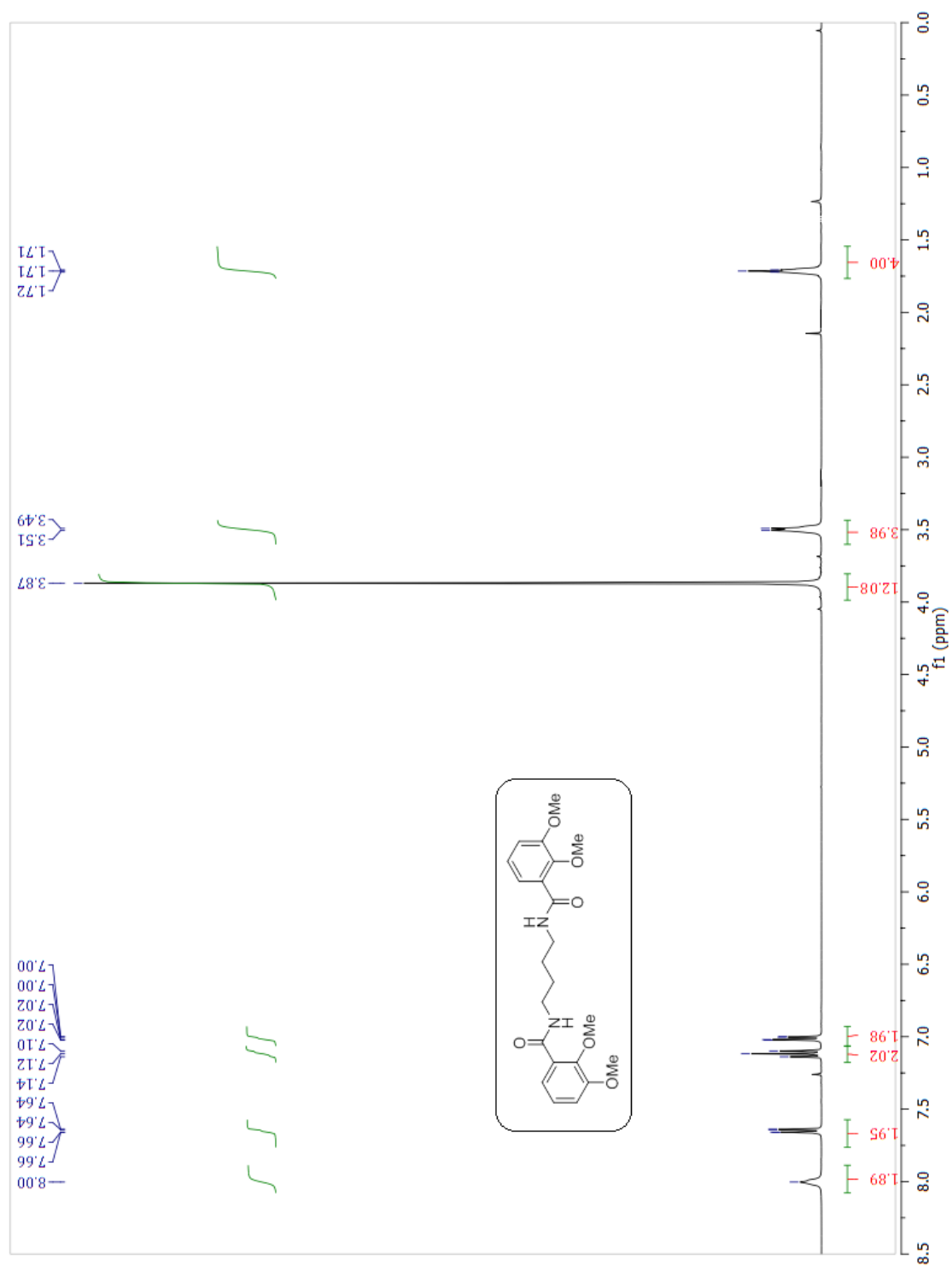


Figure A1.21: ¹H-NMR of *N,N*-Bis(2,3-bis(methoxy)benzoyl)-1,4-diaminobutane (**13**) in CDCl₃

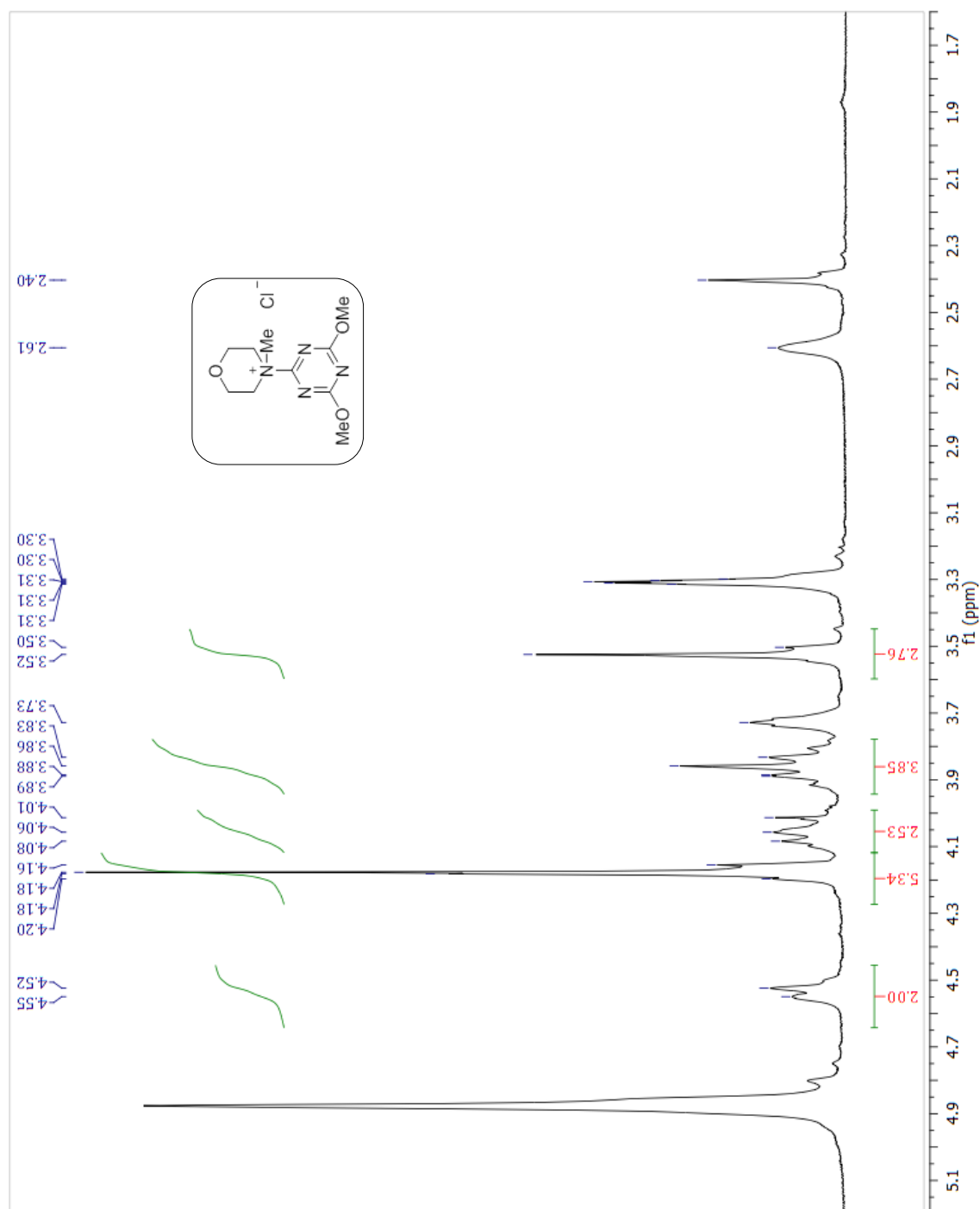


Figure A1.22: ¹H-NMR of DMTMM (**14**) in CD₃OD

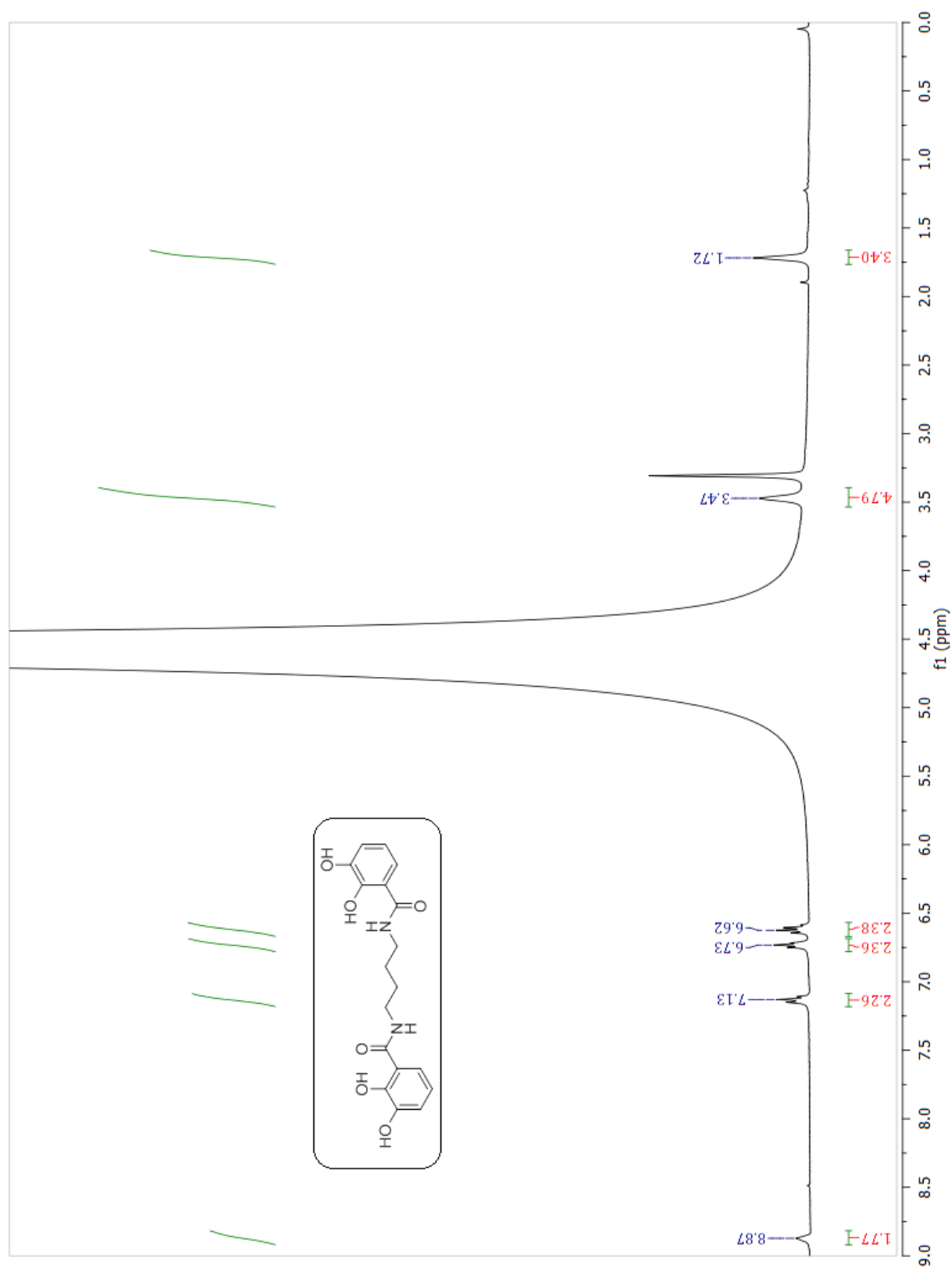


Figure A1.23: ^1H -NMR of *N*-Bis-(2,3-Dimethoxybenzoyl)-1,4-diaminobutane (**15**) in CD_3OD

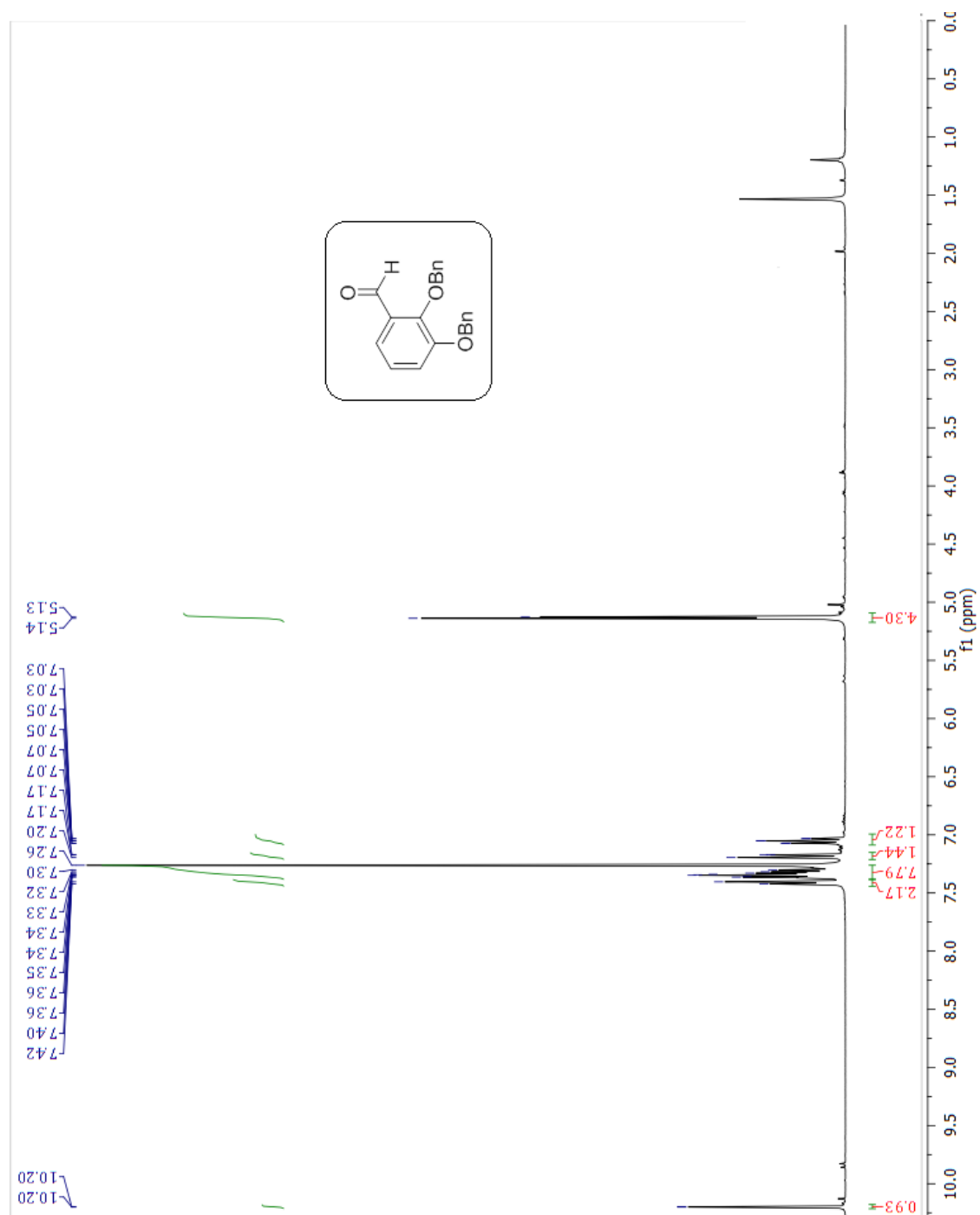


Figure A1.24: ¹H-NMR of 2, 3-Dibenzoyloxybenzaldehyde (**16**) in CDCl₃

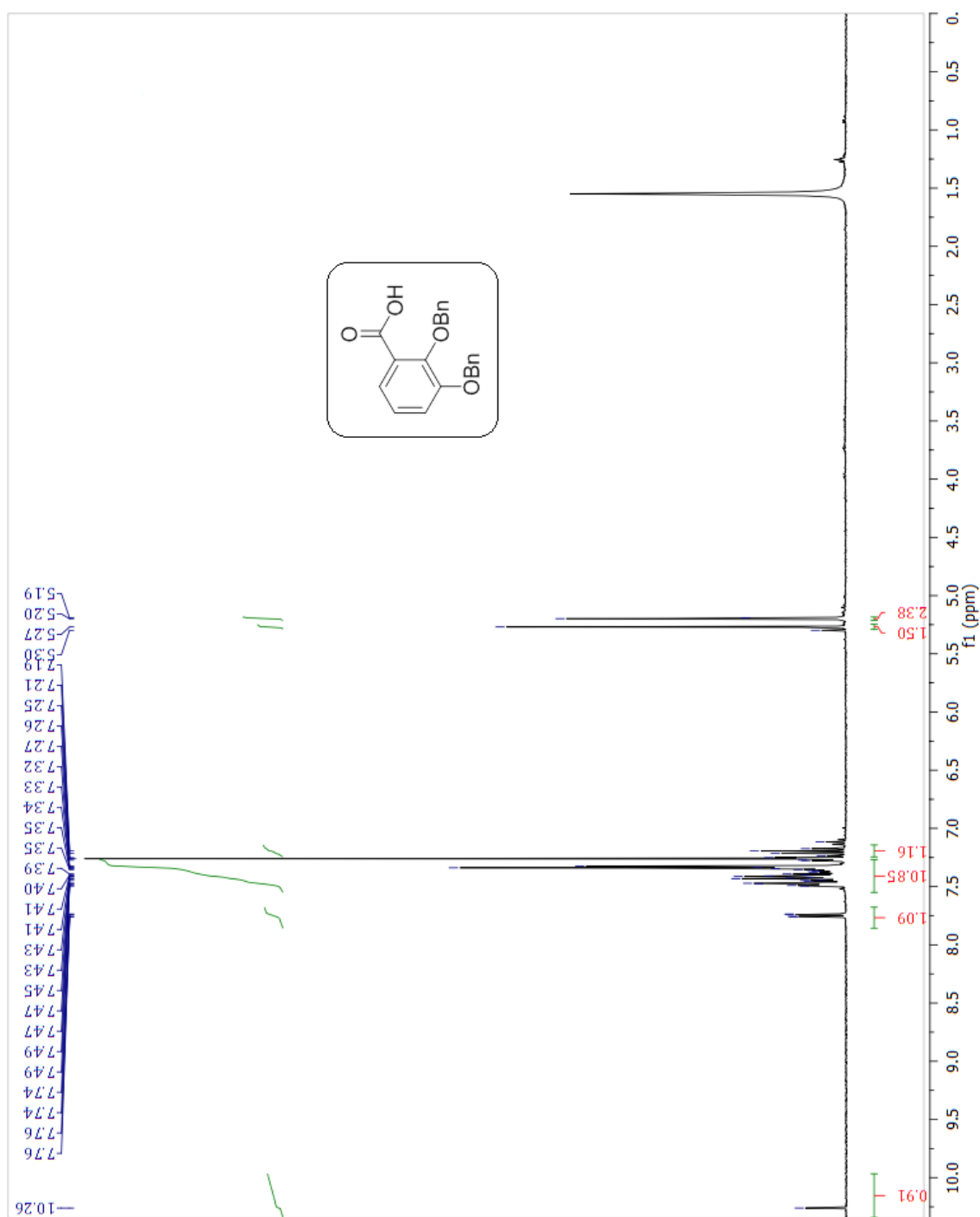


Figure A1.25: ¹H-NMR of 2, 3-Bis (benzyloxy) benzoic acid (17) in CDCl₃

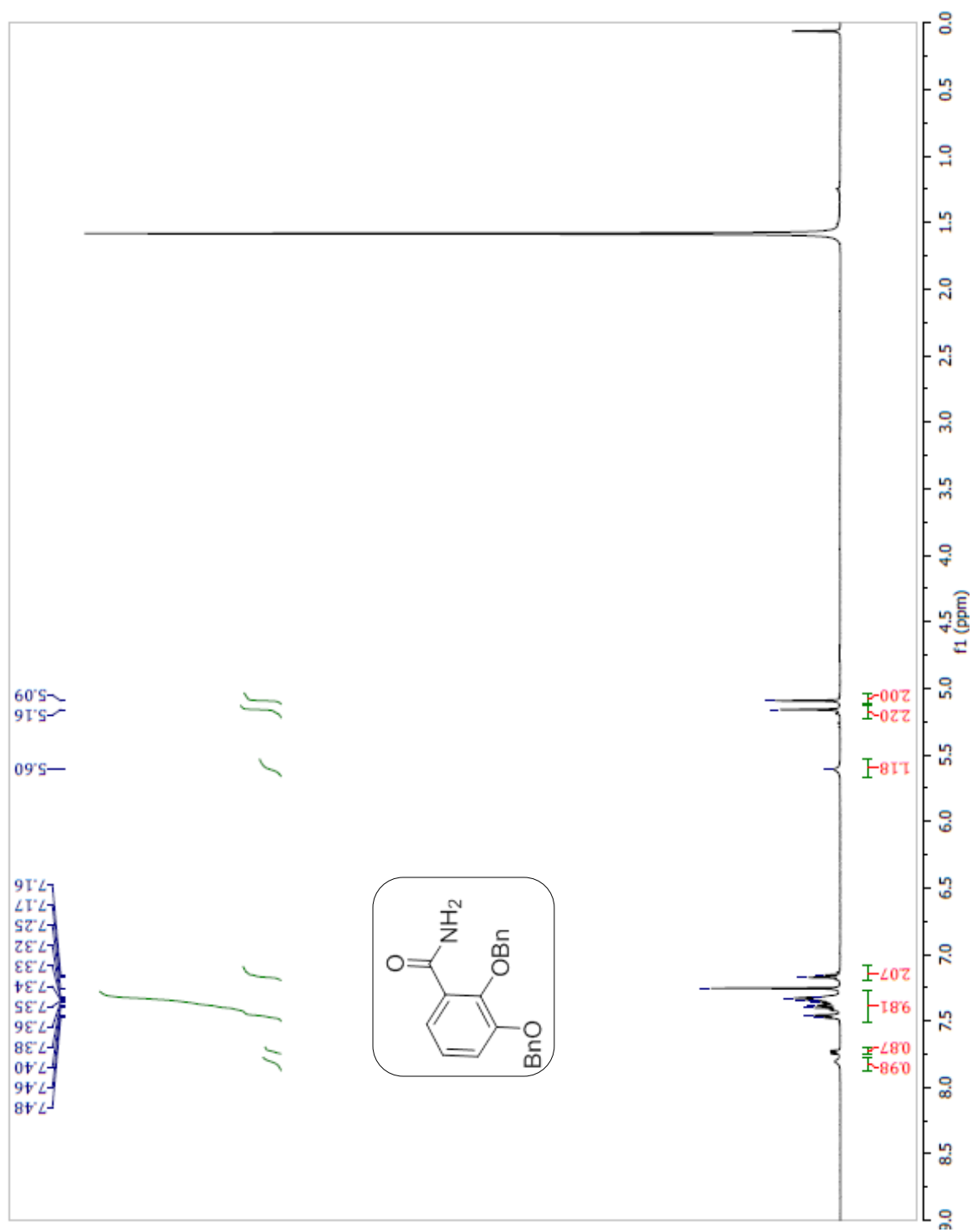


Figure A1.26: ¹H-NMR of 2,3-Bis(benzyloxy)benzamide (**18**) in CDCl₃

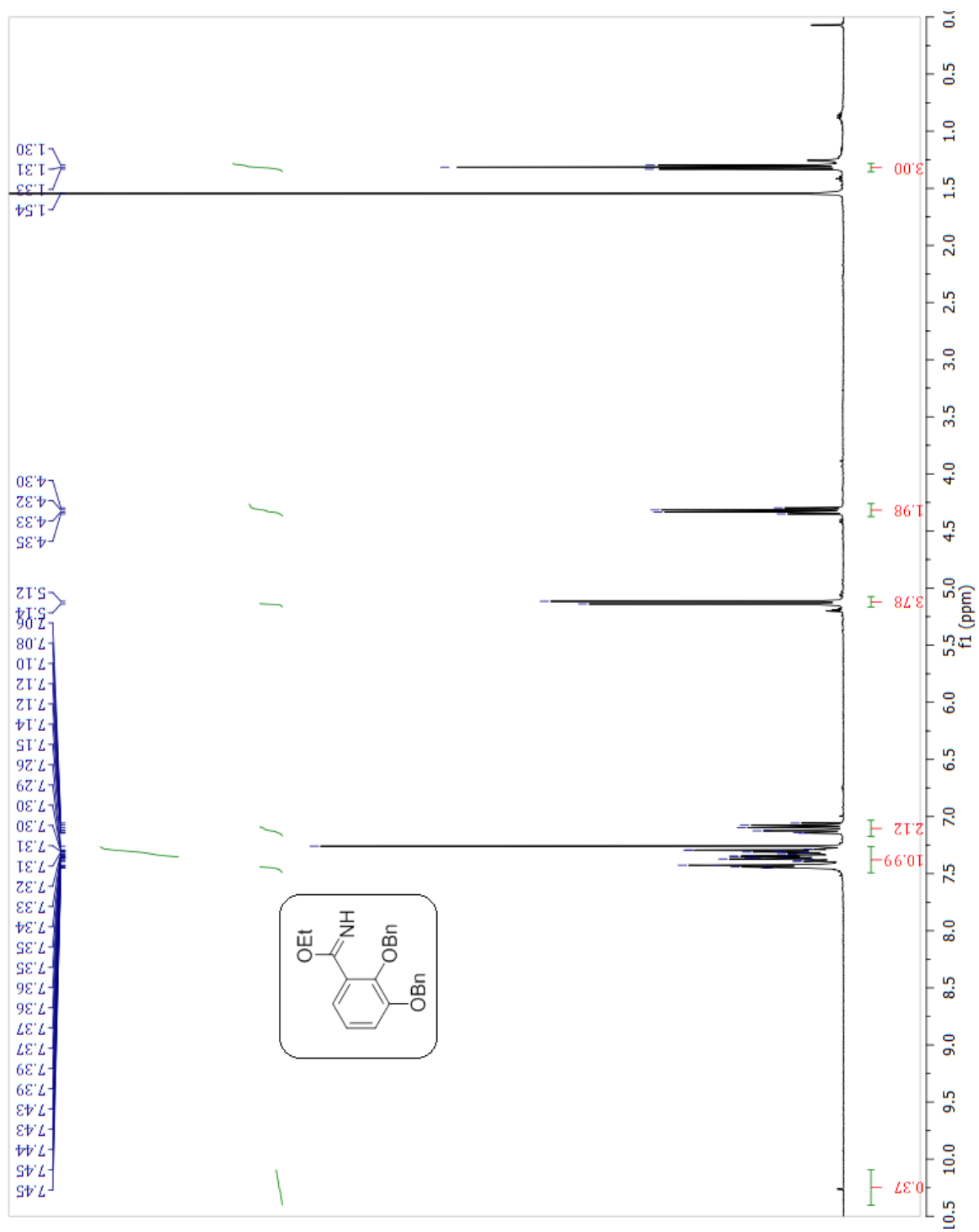


Figure A1.27: ¹H-NMR of Ethyl-2,3-Bis(benzyloxy)Benzimidate (**19**) in CDCl₃

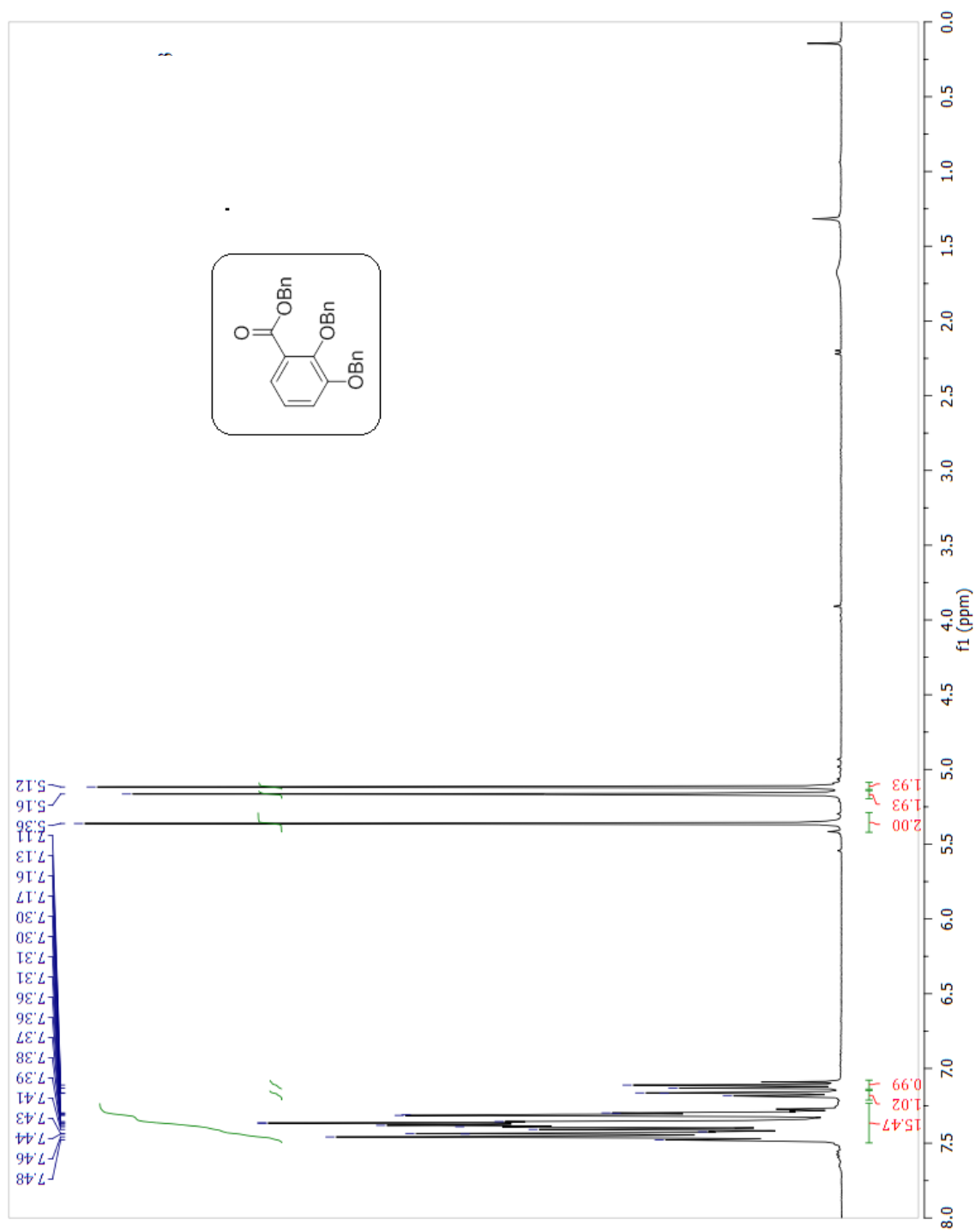


Figure A1.28: ¹H-NMR of Benzyl-2,3-Bis(Benzyloxy)Benzoate in CDCl₃

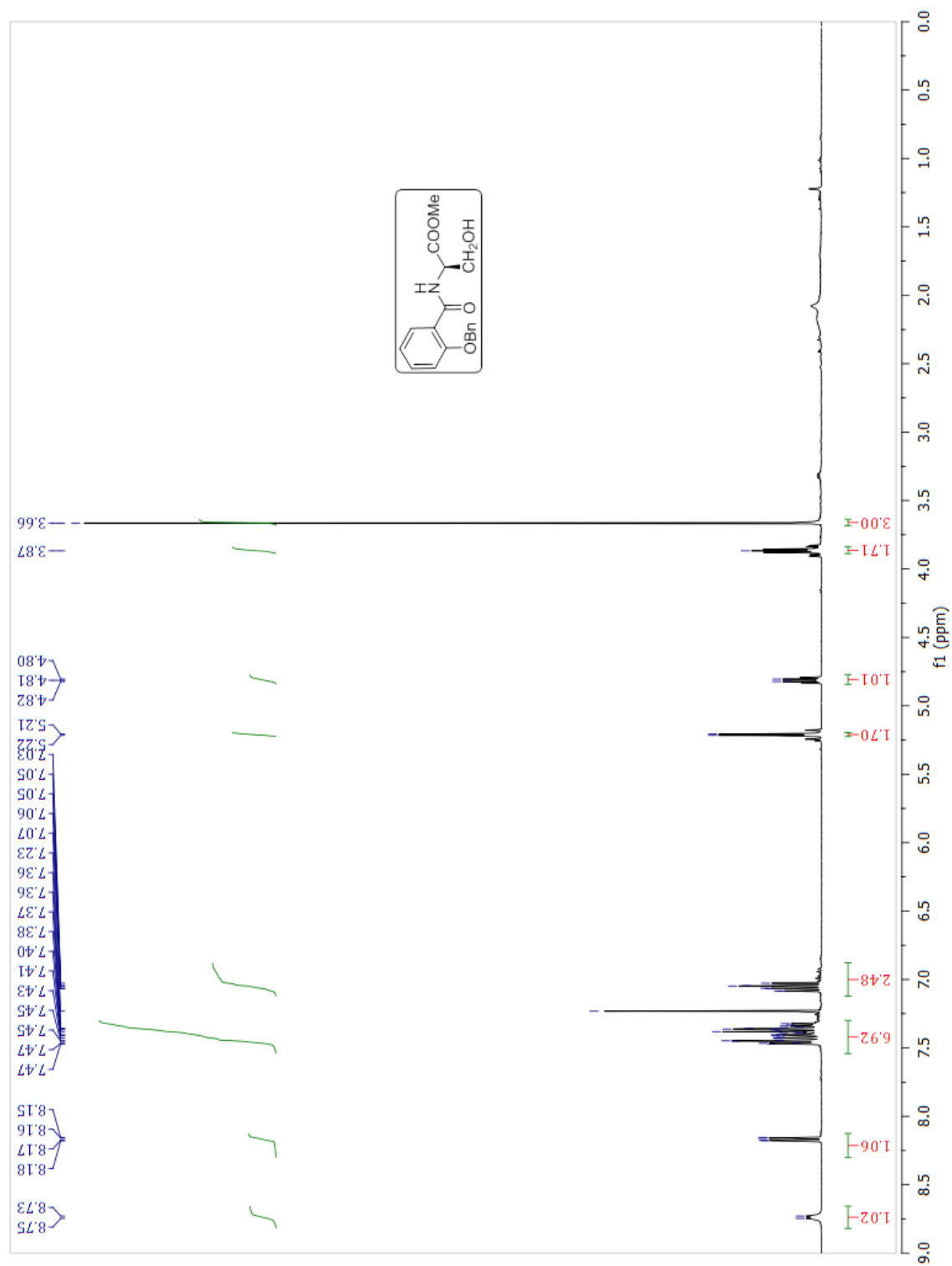


Figure A1.29: ^1H -NMR of *N*-[2-(benzyloxy)benzoyl]-L-serine methyl ester (**20**) in CDCl_3

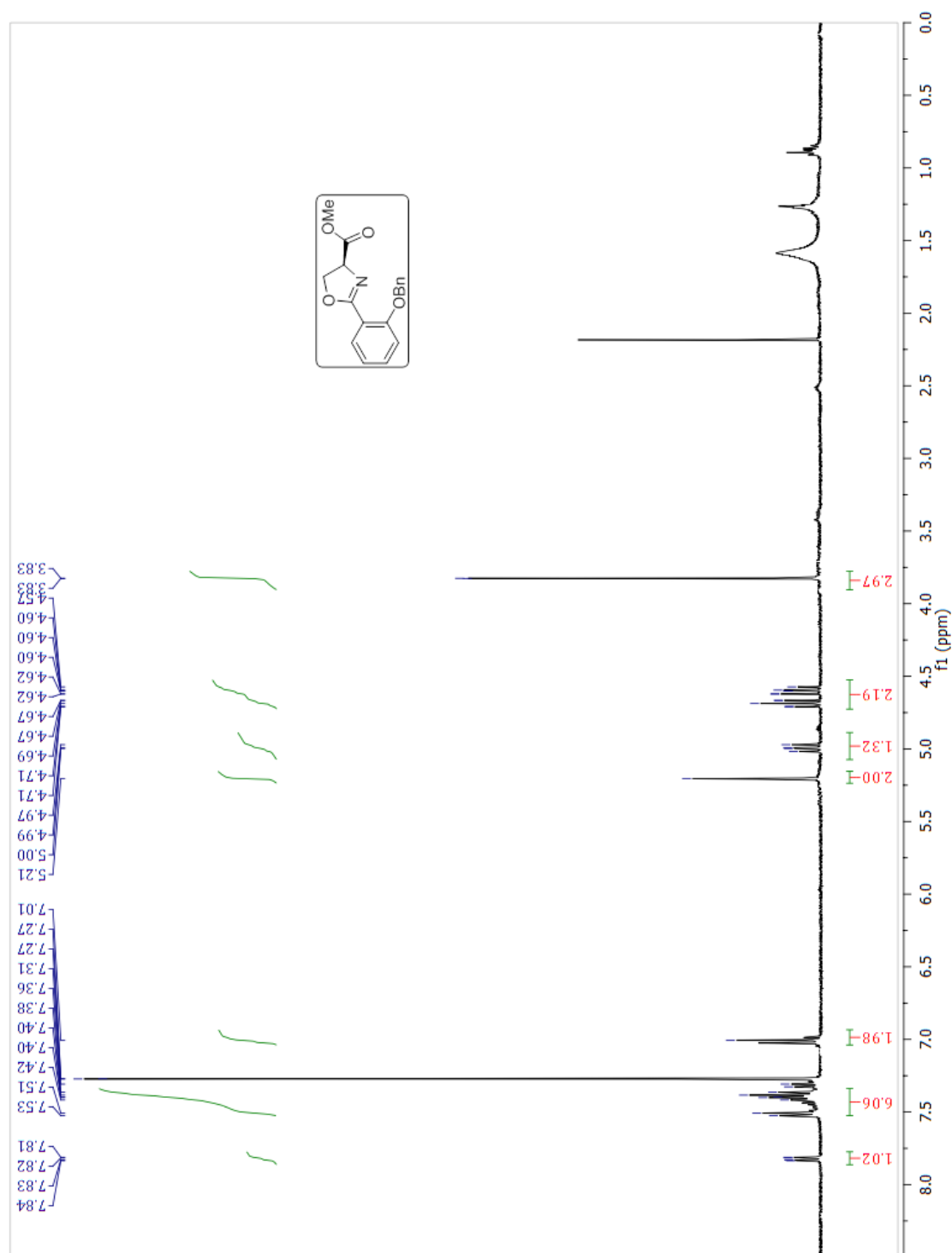


Figure A1.30: ¹H-NMR of (S)-Methyl-2-[2-Benzoyloxyphenyl]-1,3-oxazoline-4-carboxylate (**21**) in CDCl₃

A2

Figure A2.1: Absorption spectra of compound (**15**) in MeOH with and without Fe³⁺ 110

Figure A2.2: UV Spectrum of Photobactin using Spartan'10. 111

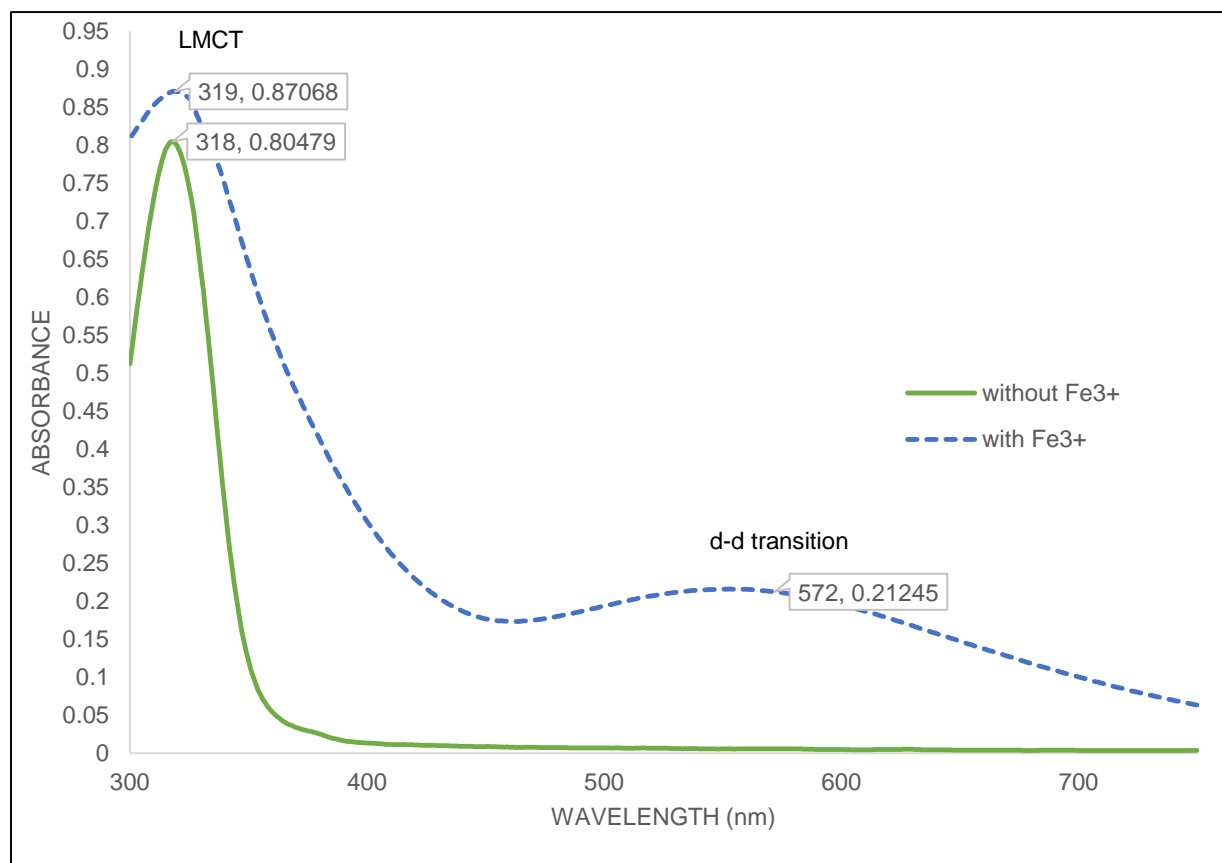


Figure A2.1: Absorption spectra of compound (15) in MeOH with and without Fe³⁺

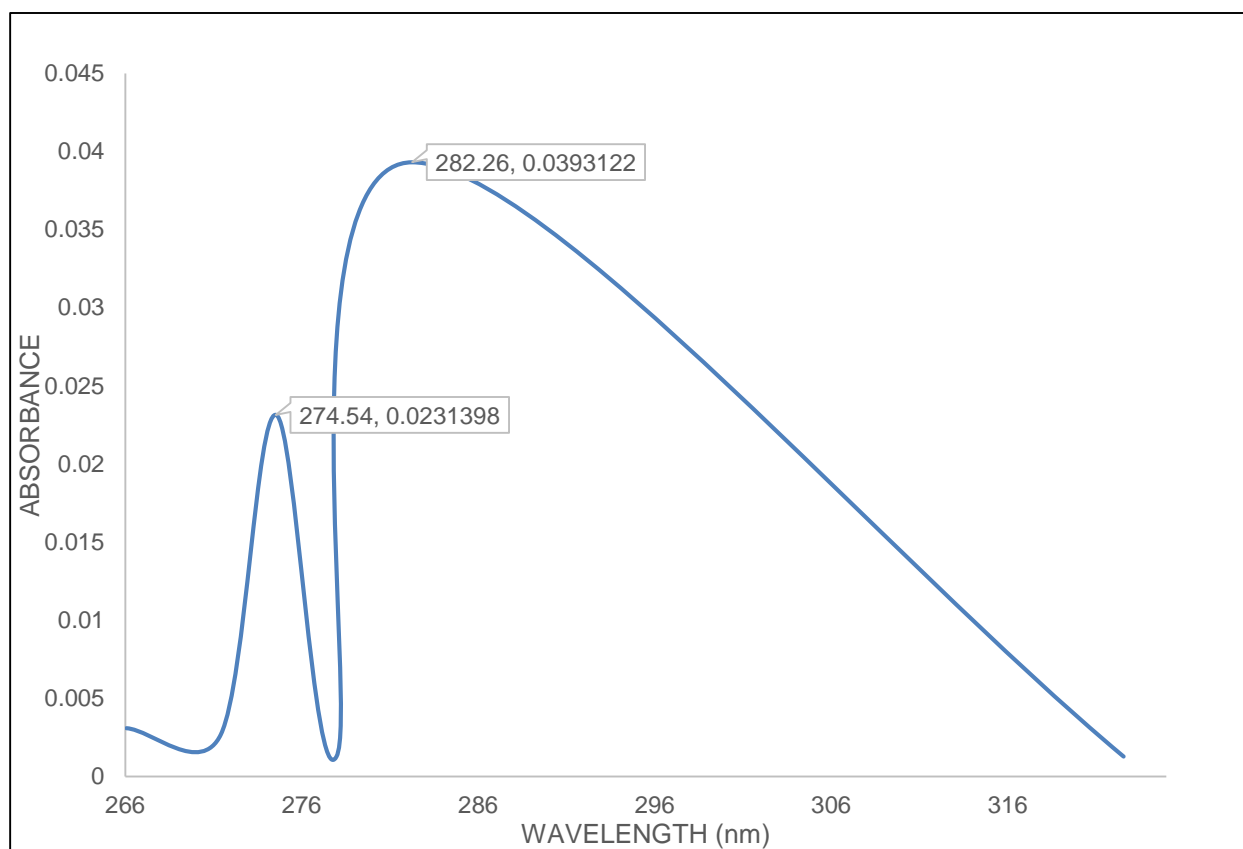


Figure A2.2: UV Spectrum of Photobactin using Spartan'10.

6. References

1. Witte, H., Seeliger, W. Simple Synthesis of 2-Substituted 2-Oxazolines and 5, 6-Dihydro-4H-1, 3-oxazines. *Angew. Chem. Int. Ed. Engl.*, **1972**, 11, 287.
2. Robinson, R. A new synthesis of oxazole derivatives. *J. Chem. Soc.*, **1909**, 95, 2167.
3. Wiley, R. H. The Chemistry of the Oxazoles. *Chem. Rev.*, **1945**, 37, 401.
4. Dewar, M. J. S., Turchi, I. J. Cornforth rearrangement. *J. Am. Chem. Soc.*, **1974**, 96, 6148.
5. Saha, R., Saha, N., Donofrio, R. S. Bestervelt, L. L. Microbial siderophores: a mini review. *J. Basic Microbiol.*, **2013**, 53, 303.
6. Miethke, M., Marahiel, M.A. Siderophore-based iron acquisition and pathogen control. *Microbiol. Mol. Biol. Rev.*, **2007**, 71, 413.
7. Griffiths, G. L., Sigel, S. P., Payne, S. M., Neilands, J. B. Vibriobactin, a siderophore from *Vibrio cholerae*. *J. Biol. Chem.*, **1984**, 259, 383.
8. Hider, R. C., Kong, X. Chemistry and biology of siderophores. *Nat. Prod. Rep.*, **2010**, 27, 637.
9. Seyedsayamdost, M. R., Cleto, S., Carr, G., Vlamakis, H., Vieira, M.J., Kolter, R., Clardy, J. Mixing and Matching Siderophore Clusters: Structure and Biosynthesis of Serratiochelins from *Serratia* sp. V4. *J. Am. Chem. Soc.*, **2012**, 134, 13550.
10. Li, N., Zhang, C., Li, B., Liu, X., Huang, Y., Xu, S., Gu, L. Unique iron coordination in iron-chelating molecule vibriobactin helps *Vibrio cholerae* evade mammalian siderocalin-mediated immune response. *J. Biol. Chem.*, **2012**, 287, 8912.
11. Mukai, A., Fukai, T., Matsumoto, Y., Ishikawa, J., Hoshino, Y., Yazawa, K., Harada, K., Mikami, Y. Transvalencin Z, a New Antimicrobial Compound with Salicylic Acid Residue from *Nocardia transvalensis* IFM 10065. *J. Antibiot.*, **2006**, 59, 366.
12. Ciche, T. A., Blackburn, M., Ensign, J.C. Photobactin: a Catechol Siderophore Produced by *Photobacterium luminescens*, an Entomopathogen Mutually Associated with *Heterorhabditis bacteriophora* NC1 Nematodes. *Appl. Environ. Microbiol.*, **2003**, 69, 4706.

13. Ong, S.A., Peterson, T., Neilands, J. B. Agrobactin, a siderophore from *Agrobacterium tumefaciens*. *J. Biol. Chem.*, **1979**, 254, 1860.
14. Peterson, T., Falk, K. E., Leong, S.A., Klevin, M. P., Neilands, J.B. Structure and behavior of spermidine siderophores. *J. Am. Chem.Soc.*, **1980**, 102, 7715.
15. Miller, M. J., Hu, J. Total Synthesis of a Mycobactin S, a Siderophore and Growth Promoter of *Mycobacterium Smegmatis*, and Determination of its Growth Inhibitory Activity against *Mycobacterium tuberculosis*. *J. Am. Chem. Soc.*, **1997**, 119, 3462.
16. Takeuchi, Y., Ozaki, S., Satoh, M., Mimura, K., Hara, S., Abe, H., Nishioka, H., Harayama, T. Synthesis of Acinetobactin. *Chem. Pharm. Bull.*, **2010**, 58, 1552.
17. Klein, D. R. *Organic Chemistry*. 1st ed. New York: Wiley, **2013**. pp. 407-408, 755, 800, 927, 1000-1003.
18. Pétursson, S; Baldwin, J. E. Synthesis of δ -(l- α -aminoadipoyl)-l-cysteiny-d-(O-methyl)-d-allothreonine a substrate for isopenicillin-N synthase and its O-methyl-d-threonine epimer. *Tetrahedron*, **1998**, 54, 6001.
19. Montalbetti, C.A.G.N., Falque, V. Amide bond formation and peptide coupling. *Tetrahedron*, **2005**, 61, 10827.
20. Sakakura, A., Umemuraa, S., Ishihara, K. Convergent total syntheses of fluvibactin and vibriobactin using molybdenum (VI) oxide-catalyzed dehydrative cyclization as a key step. *Chem. Commun.*, **2008**, 3561.
21. Atkins, G. M, Jr., Burgess, E. M. The reactions of an *N*-sulfonylamine inner salt. *J. Am. Chem. Soc.*, **1968**, 90, 4744.
22. Holerca, M. N., Percec, V. ¹H NMR Spectroscopic Investigation of the Mechanism of 2-Substituted-2-Oxazoline Ring Formation and of the Hydrolysis of the Corresponding Oxazolinium Salts. *Eur. J. Org. Chem.*, **2000**, 12, 2257.
23. Phillips, A. J., Uto, Y., Wipf, P., Reno, M. J., Williams, D. R. Synthesis of Functionalized Oxazolines and Oxazoles with DAST and Deoxo-Fluor. *Org. Lett.*, **2000**, 2, 1168.

24. Banala, S., Ensle, P., Süssmuth, R. D. Total Synthesis of the Ribosomally Synthesized Linear Azole-Containing Peptide Plantazolicin A from *Bacillus amyloliquefaciens*. *Angew. Chem. Int. Ed.*, **2013**, *52*, 9518.
25. Spectral Database of Organic Compounds. Retrieved October 20th 2013 from SDBS: <http://sdbb.db.aist.go.jp>
26. Zinelaabidine, C., Souad, O., Zoubir, J., Malika, B., Nour-Eddine, A. A Simple and Efficient Green Method for the Deprotection of *N*-Boc in Various Structurally Diverse Amines under Water-mediated Catalyst-free Conditions. *Int. J. Chem.*, **2012**, *4*, 73.
27. Routier, S., Saugé, L., Ayerbe, N., Coudert, G., Mérour, J. Y. A mild and selective method for *N*-Boc deprotection. *Tetrahedron Lett.*, **2002**, *43*, 589.
28. Blondelle, S. E; Houghten, R. A. Comparison of 55% TFA/dichloromethane and 100% TFA for Boc group removal during solid-phase peptide synthesis. *Int. J. Peptide Protein Res.*, **1993**, *41*, 522.
29. Kunishima, M., Kawachi, C., Monta, J., Terao, K., Iwasaki, F., Tani, S. 4-(4,6-dimethoxy-1,3,5-triazin-2-yl)-4-methyl-morpholinium chloride: an efficient condensing agent leading to the formation of amides and esters. *Tetrahedron*, **1999**, *55*, 13159.
30. Winstanley, K. J., Smith, D. K. Ortho-Substituted Catechol Derivatives: The Effect of Intramolecular Hydrogen-Bonding Pathways on Chloride Anion Recognition. *J. Org. Chem.*, **2007**, *72*, 2803.
31. McOmie, J. F. W., Watts, M. L., West, D. E. Demethylation of aryl methyl ethers by boron tribromide. *Tetrahedron*, **1968**, *24*, 2289.
32. Bergeron, R.J., Garlich, J. R., McManis, J. S. Total synthesis of vibriobactin. *Tetrahedron*, **1985**, *41*, 507.
33. Bergeron, R. J., McManis, J. S., Dionis, J., Garlich, J. R. An efficient total synthesis of agrobactin and its gallium (III) chelate. *J. Org. Chem.*, **1985**, *50*, 2782.

34. Rastetter, W. H., Erickson, T. J., Venuti, M.C. Synthesis of Iron Chelators. Enterobactin, Enantioenterobactin, and a Chiral Analogue. *J. Org. Chem.*, **1981**, *46*, 3579.
35. Housecroft, C. E., Sharpe, A. G. *Inorganic Chemistry*. 2nd ed. Harlow: Pearson Education, **2005**. 550-556.